arXiv:cond-mat/0607675v1 [cond-mat.stat-mech] 26 Jul 2006

MANY-BODY GREEN'S FUNCTION THEORY OF HEISENBERG FILMS

P. Fröbrich[1], P.J. Kuntz

Hahn-Meitner-Institut Berlin, Glienicker Straße 100, D-14109 Berlin, Germany,
[1]also: Institut für Theoretische Physik, Freie Universität Berlin
Arnimallee 14, D-14195 Berlin, Germany

Abstract:

The treatment of Heisenberg films with many-body Green's function theory (GFT) is reviewed. The basic equations of GFT are derived in sufficient detail so that the rest of the paper can be understood without having to consult further literature. The main part of the paper is concerned with applications of the formalism to ferromagnetic, antiferromagnetic and coupled ferromagnetic-antiferromagnetic Heisenberg films based on a generalized Tyablikov (RPA) decoupling of the exchange interaction and exchange anisotropy terms and an Anderson-Callen decoupling for a weak single-ion anisotropy. We not only give a consistent description of our own work but also refer extensively to related investigations. We discuss in particular the reorientation of the magnetization as a function of the temperature and film thickness. If the single-ion anisotropy is strong, it can be treated exactly by going to higher-order Green's functions. We also discuss the extension of the theory beyond RPA. Finally the limitations of GFT are pointed out.

Contents

1. Introduction and outline

Many-body GF theory is used in many fields in statistical mechanics (e.g. see the early reviews [1] or [2], or the more recent book [3]). Extensive applications of the formalism to the theory of magnetism can be found in the books [4] and [5]. In the sixties and seventies of the last century, emphasis was put on the properties of bulk magnets. Since then, the advance in experimental techniques has stimulated an increasing interest in magnetic systems with reduced dimension.

One main stream in current research is the attempt to describe 3D magnetic systems with strong electron-electron correlations in terms of electronic structures with the help of ab initio calculations: Density Functional Theory (DFT),which is successful by itself for systems with weak electron-electron correlations, must here be combined with many-body techniques, as in Dynamical Mean Field Theory (DMFT). For a recent review see e.g. Ref. [6].

The present paper is concerned with less ambitious models based on the Heisenberg Hamiltonian with the inclusion of anisotropies. It provides an overview of many-body Green's function (GF) techniques applied to the magnetic properties of layered two-dimensional structures; i.e. it is concerned essentially with quasi-two-dimensional Heisenberg films. The techniques developed in the present paper may also be useful for treating cases in which a Heisenberg kind of Hamiltonian is derived from a microscopic theory. Emphasis is put on the development of the formalism. For a paper that discusses the relevant experimental situation in more detail we refer to Ref. [7].

In Section 2, we derive the direct Heisenberg exchange interaction by plausibility arguments: an orthogonal basis leads to ferromagnetic exchange and a non-orthogonal basis in the Heitler-London framework allows antiferromagnetic exchange. In Section 3, we derive the basic equations of the formalism for the double-time Green's function in sufficient detail that it should not be necessary to consult any further literature to understand the rest of the paper. Section 4 deals with applications of the GF formalism to Heisenberg films. In the pedagogical Section 4.1 a ferromagnetic spin $S = 1/2$ Heisenberg monolayer in a magnetic field is treated. Section 4.2 deals with ferromagnetic Heisenberg films with anisotropies for general spin and Section 4.3 considers antiferromagnetic and coupled ferromagnetic-antiferromagnetic Heisenberg films. Section 5 extends the formalism beyond the RPA approach. Section 6 presents our conclusions and points out some open problems and limitations of Green's function theory (GFT).

2. The Heisenberg exchange interaction

The present article describes magnetic systems in terms of a Heisenberg Hamiltonian and anisotropy terms. This is a phenomenological approach, in which the strengths of the exchange interaction and anisotropies are considered as parameters which could be fitted to experiments. In this section, we discuss the origin of the Heisenberg exchange Hamiltonian.

The exchange interaction is a manifestation of the Coulomb interaction and quantum-mechanical indistinguishability (the Pauli principle). It is quite complicated to derive exchange Hamiltonians from first principles, but this is often possible by adopting adequate approximations. The form of the Heisenberg exchange Hamiltonian is a gross simplification that can, however, be made plausible for simple cases. The *ferromagnetic* direct exchange can be derived from a two-electron model by assuming orthogonal basis states. The direct *antiferromagnetic* exchange can be made plausible with the Heitler-London scheme.

2.1. Direct exchange with orthogonal basis states (ferromagnetism)

Consider two electrons (e.g. in a $3d^2$ configuration) and a Hamiltonian consisting of the sum of two single-electron Hamiltonians, $h_0(\mathbf{r}_1)$ and $h_0(\mathbf{r}_2)$ and the Coulomb interaction:

$$\mathcal{H} = h_0(\mathbf{r}_1) + h_0(\mathbf{r}_2) + \frac{e^2}{|\mathbf{r}_1 - \mathbf{r}_2|}, \tag{1}$$

where the single-electron problem is assumed to be solved:

$$\begin{aligned} h_0(\mathbf{r})\phi_a(\mathbf{r}) &= \epsilon_a \phi_a(\mathbf{r}), \\ \langle \phi_a(\mathbf{r}) | \phi_b(\mathbf{r}) \rangle &= \delta_{ab} \ . \end{aligned} \tag{2}$$

The electrons can couple to triplet ($S = 1$) or singlet ($S = 0$) states with wave functions characterized by $|S, S^z\rangle$:

$$\begin{aligned} |1,1\rangle = \psi_1 \ , \qquad |1,0\rangle &= \frac{1}{\sqrt{2}}(\psi_2 + \psi_3) \ , \qquad |1,-1\rangle = \psi_4 \ , \\ |0,0\rangle &= \frac{1}{\sqrt{2}}(\psi_2 - \psi_3) \ , \end{aligned} \tag{3}$$

and

$$\begin{aligned} \psi_1 &= \frac{1}{\sqrt{2}}\chi_\uparrow(s_1)\chi_\uparrow(s_2)[\phi_a(\mathbf{r}_1)\phi_b(\mathbf{r}_2) - \phi_a(\mathbf{r}_2)\phi_b(\mathbf{r}_1)] \ , \\ \psi_2 &= \frac{1}{\sqrt{2}}[\chi_\downarrow(s_1)\chi_\uparrow(s_2)\phi_a(\mathbf{r}_1)\phi_b(\mathbf{r}_2) - \chi_\uparrow(s_1)\chi_\downarrow(s_2)\phi_b(\mathbf{r}_1)\phi_a(\mathbf{r}_2)] \ , \\ \psi_3 &= \frac{1}{\sqrt{2}}[\chi_\uparrow(s_1)\chi_\downarrow(s_2)\phi_a(\mathbf{r}_1)\phi_b(\mathbf{r}_2) - \chi_\downarrow(s_1)\chi_\uparrow(s_2)\phi_b(\mathbf{r}_1)\phi_a(\mathbf{r}_2)] \ , \\ \psi_4 &= \frac{1}{\sqrt{2}}\chi_\downarrow(s_1)\chi_\downarrow(s_2)[\phi_a(\mathbf{r}_1)\phi_b(\mathbf{r}_2) - \phi_a(\mathbf{r}_2)\phi_b(\mathbf{r}_1)] \ . \end{aligned} \tag{4}$$

Here $\chi_{\uparrow(\downarrow)}$ are the spin wave functions with spins up or down.

Defining a Coulomb integal as

$$C_{ab} = e^2 \int d\mathbf{r}_1 \int d\mathbf{r}_2 \frac{|\phi_a(\mathbf{r}_1)|^2 |\phi_b(\mathbf{r}_2)|^2}{|\mathbf{r}_1 - \mathbf{r}_2|} \ , \tag{5}$$

and an exchange integral as

$$J_{ab} = e^2 \int d\mathbf{r}_1 \int d\mathbf{r}_2 \frac{\phi_a^*(\mathbf{r}_1)\phi_b(\mathbf{r}_1)\phi_b^*(\mathbf{r}_2)\phi_a(\mathbf{r}_2)}{|\mathbf{r}_1 - \mathbf{r}_2|} \ , \tag{6}$$

we may express the matrix elements of the Coulomb interaction as

$$\begin{aligned} \langle\psi_1|\frac{e^2}{|\mathbf{r}_1 - \mathbf{r}_2|}|\psi_1\rangle &= C_{ab} - J_{ab} \ , \\ \langle\psi_2|\frac{e^2}{|\mathbf{r}_1 - \mathbf{r}_2|}|\psi_2\rangle &= C_{ab} \ , \\ \langle\psi_2|\frac{e^2}{|\mathbf{r}_1 - \mathbf{r}_2|}|\psi_3\rangle &= -J_{ab} \ . \end{aligned} \tag{7}$$

We then find for the Hamiltonian matrix

$$(\epsilon_a + \epsilon_b) \begin{pmatrix} 1 & 0 & 0 & 0 \\ 0 & 1 & 0 & 0 \\ 0 & 0 & 1 & 0 \\ 0 & 0 & 0 & 1 \end{pmatrix} + \begin{pmatrix} C_{ab} - J_{ab} & 0 & 0 & 0 \\ 0 & C_{ab} & -J_{ab} & 0 \\ 0 & -J_{ab} & C_{ab} & 0 \\ 0 & 0 & 0 & C_{ab} - J_{ab} \end{pmatrix} \ . \tag{8}$$

There are three degenerate eigenvalues belonging to a triplet state,

$$\epsilon_t = \epsilon_a + \epsilon_b + C_{ab} - J_{ab}, \tag{9}$$

and one eigenvalue belonging to a singlet state,

$$\epsilon_s = \epsilon_a + \epsilon_b + C_{ab} + J_{ab} \ . \tag{10}$$

The exchange integral can be shown to be positive: if we take $f(\mathbf{r}) = \phi_a(\mathbf{r})\phi_b(\mathbf{r})$ and perform Fourier transforms, we have

$$\begin{aligned} J_{ab} &= \int d\mathbf{r}_1 f^*(\mathbf{r}_1) \int d\mathbf{r}_2 \frac{e^2}{|\mathbf{r}_1 - \mathbf{r}_2|} f(\mathbf{r}_2) \\ &= \int d\mathbf{r}_1 \frac{1}{(2\pi)^{3/2}} \int d\mathbf{k}' e^{-i\mathbf{k}'\mathbf{r}_1} f^*(\mathbf{k}') \\ &\quad \int d\mathbf{r}_2 \frac{4\pi e^2}{(2\pi)^3} \int d\mathbf{k}'' e^{i\mathbf{k}''(\mathbf{r}_1 - \mathbf{r}_2)} \frac{1}{k''^2} \frac{1}{(2\pi)^{3/2}} \int d\mathbf{k} e^{i\mathbf{k}\mathbf{r}_2} f(\mathbf{k}) \\ &= \int d\mathbf{k} |f(\mathbf{k})|^2 \frac{4\pi e^2}{k^2} \geq 0 \ . \end{aligned} \tag{11}$$

Because J_{ab} is greater than zero, the triplet is lower in energy than the singlet; i.e. in the lowest state the spins are parallel, which corresponds to a ferromagnetic situation.

The action of the Hamiltonian can be expressed by spin operators. We have

$$2\mathbf{S}_1\mathbf{S}_2 + 1/2 = (\mathbf{S}_1 + \mathbf{S}_2)^2 - 1 = \begin{cases} 1 & \text{for the triplet} \\ -1 & \text{for the singlet} \end{cases} . \tag{12}$$

The action of the triplet and singlet can then be expressed by a single Hamiltonian

$$\mathcal{H} = \frac{\epsilon_s + \epsilon_t}{2} - \frac{\epsilon_s - \epsilon_t}{2}(2\mathbf{S}_1\mathbf{S}_2 + \frac{1}{2}) = \text{const} - 2J_{ab}\mathbf{S}_1\mathbf{S}_2. \tag{13}$$

Generalizing the exchange interaction to a lattice, one may write

$$\mathcal{H} = -\frac{1}{2}\sum_{i\neq j} J_{ij}\mathbf{S}_i\mathbf{S}_j \ . \tag{14}$$

This is the most familiar form of the Heisenberg exchange, where i and j represent lattice site indices and the factor $\frac{1}{2}$ is introduced by convention.

2.2. Direct exchange with non-orthogonal states (antiferromagnetism)

Antiparallel spin alignment (antiferromagnetism) occurs in a two-center system like a hydrogen molecule in the Heitler-London approximation. Consider two hydrogen atoms centred at $\mathbf{R}_a$ and $\mathbf{R}_b$ respectively, with a Hamiltonian in which each electron feels both protons and the electron-electron and proton-proton interactions are included

$$\begin{aligned} \mathcal{H} &= H_{atom}(\mathbf{r}_1 - \mathbf{R}_a) + H_{atom}(\mathbf{r}_2 - \mathbf{R}_b) \\ &\quad - \frac{e^2}{|\mathbf{r}_1 - \mathbf{R}_b|} - \frac{e^2}{|\mathbf{r}_2 - \mathbf{R}_a|} + \frac{e^2}{|\mathbf{r}_1 - \mathbf{r}_2|} + \frac{e^2}{|\mathbf{R}_a - \mathbf{R}_b|} \ . \end{aligned} \tag{15}$$

Each electron occupies a separate 1s-orbital centred on one of the atoms. In the simplest approximation, the low-lying states are assumed to be described by four configurations with spins $\uparrow\uparrow, \uparrow\downarrow, \downarrow\uparrow, \downarrow\downarrow$. We denote the orbital basis functions at atoms a and b as $\phi_a(\mathbf{r})$ and $\phi_b(\mathbf{r})$. They are in general non-orthogonal:

$$\int \phi_a^*(\mathbf{r})\phi_b(\mathbf{r})d\mathbf{r} = l \neq 0 \ . \tag{16}$$

Each orbital function is associated with one of two spin functions, $\chi_\uparrow$ or $\chi_\downarrow$. The Hamiltonian is diagonalized in the subspace of the following four normalized spin-coupled functions corresponding to triplet and singlet states $\psi(S, S^z)$:

$$\begin{aligned} \psi(1,1) &= \frac{1}{\sqrt{2(1-l^2)}}\chi_\uparrow(s_1)\chi_\uparrow(s_2)[\phi_a(\mathbf{r}_1)\phi_b(\mathbf{r}_2) - \phi_a(\mathbf{r}_2)\phi_b(\mathbf{r}_1)] \ , \\ \psi(1,0) &= \frac{1}{\sqrt{2(1-l^2)}}[\chi_\uparrow(s_1)\chi_\downarrow(s_2) + \chi_\downarrow(s_1)\chi_\uparrow(s_2)][\phi_a(\mathbf{r}_1)\phi_b(\mathbf{r}_2) - \phi_a(\mathbf{r}_2)\phi_b(\mathbf{r}_1)] \ , \\ \psi(1,-1) &= \frac{1}{\sqrt{2(1-l^2)}}\chi_\downarrow(s_1)\chi_\downarrow(s_2)[\phi_a(\mathbf{r}_1)\phi_b(\mathbf{r}_2) - \phi_a(\mathbf{r}_2)\phi_b(\mathbf{r}_1)] \ , \\ \psi(0,0) &= \frac{1}{2\sqrt{(1+l^2)}}[\chi_\uparrow(s_1)\chi_\downarrow(s_2) - \chi_\downarrow(s_1)\chi_\uparrow(s_2)][\phi_a(\mathbf{r}_1)\phi_b(\mathbf{r}_2) + \phi_a(\mathbf{r}_2)\phi_b(\mathbf{r}_1)] \ . \end{aligned} \tag{17}$$

The triplet energy may again be written in terms of Coulomb and exchange integrals:

$$\epsilon_t = \langle\psi(1,1)|\mathcal{H}|\psi(1,1)\rangle = 2\epsilon_{atom} + \frac{C_{ab} - I_{ab}}{1 - l^2} \ . \tag{18}$$

Here, $2\epsilon_{atom}$ comes from the one-electron part of the Hamiltonian. The Coulomb integral (containing terms where the electron belonging to one nucleus feels the attraction of the other nucleus) is

$$\begin{aligned} C_{ab} &= \int d\mathbf{r}_1 \int d\mathbf{r}_2 |\phi_a(\mathbf{r}_1)|^2 \frac{e^2}{|\mathbf{r}_1 - \mathbf{r}_2|} |\phi_b(\mathbf{r}_2)|^2 \\ &\quad - \int d\mathbf{r}_1 \frac{e^2}{|\mathbf{r}_1 - \mathbf{R}_b|} |\phi_a(\mathbf{r}_1)|^2 - \int d\mathbf{r}_2 \frac{e^2}{|\mathbf{r}_2 - \mathbf{R}_a|} |\phi_b(\mathbf{r}_2)|^2 \ , \end{aligned} \tag{19}$$

and the exchange integral is

$$\begin{aligned} I_{ab} &= \int d\mathbf{r}_1 \int d\mathbf{r}_2 \phi_a^*(\mathbf{r}_1)\phi_b(\mathbf{r}_1) \frac{e^2}{|\mathbf{r}_1 - \mathbf{r}_2|} \phi_b^*(\mathbf{r}_2)\phi_a(\mathbf{r}_2) \\ &\quad - l \int d\mathbf{r}_1 \frac{e^2}{|\mathbf{r}_1 - \mathbf{R}_b|} \phi_a^*(\mathbf{r}_1)\phi_b(\mathbf{r}_1) - l \int d\mathbf{r}_2 \frac{e^2}{|\mathbf{r}_2 - \mathbf{R}_a|} \phi_b^*(\mathbf{r}_2)\phi_a(\mathbf{r}_2) \ . \end{aligned} \tag{20}$$

The singlet eigenenergy is

$$\epsilon_s = \langle\psi(0,0)|\mathcal{H}|\psi(0,0)\rangle = 2\epsilon_{atom} + \frac{C_{ab} + I_{ab}}{1 + l^2} \ . \tag{21}$$

The singlet-triplet splitting is

$$\epsilon_t - \epsilon_s = 2\frac{l^2 C_{ab} - I_{ab}}{1 - l^4} \ . \tag{22}$$

As in the previous subsection, an effective Hamiltonian may be defined as

$$\mathcal{H} = const + J_{12}\mathbf{S}_1\mathbf{S}_2 \ , \tag{23}$$

with

$$J_{12} = 2\frac{l^2 C_{ab} - I_{ab}}{1 - l^4}. \tag{24}$$

Without the Coulomb term, one has ferromagnetic coupling; with a sufficiently large overlap, the effective exchange coupling becomes antiferromagnetic ($J_{12} > 0$); the ground-state of the hydrogen molecule is a singlet state. Generalizing to a many-electron system, one has the Heisenberg model for an antiferromagnetic lattice.

Including ionic configurations where both electrons can sit on one or the other atom leads to a hopping mechanism for the electrons (kinetic exchange), which supports antiferromagnetic coupling, see e.g.([8], p.60).

An antiferromagnetic Heisenberg model is also obtained from the Hubbard model in the strong coupling limit, or from indirect exchange mechanisms like the RKKY scheme, leading to an effective Heisenberg model in second-order perturbation theory. Also, super-exchange or double exchange lead to Heisenberg like terms or even to biquadratic terms, see e.g. ([5]).

In the present article, we do not try to give a better justification of the Heisenberg model. Rather, we consider it a phenomenological model that proves to be successful in describing many experimental data when its parameters are fitted. A Heisenberg model is adequate when the spins are localized (e.g. in the rare earth elements). It should also be applicable to 3d-transition metal band magnets because the magnetic moments are quasi-localized when integrating over microscopically calculated spin densities. One also sees in experiments on bulk transition-metal ferromagnets that the magnetization follows the Bloch $T^{3/2}$ law at low temperatures. Above the Curie temperature, one observes a Curie-Weiss behaviour of the magnetic susceptibility. Both features follow from a Heisenberg type model.

3. Basic equations of the Green's function formalism

In this section we place together the essential definitions and derivations of the Green's function formalism which are necessary to understand the following article without frequent recourse to the literature. For further details of the basic features of the Green's function formalism as it is used in the present review, we recommend the article [1] and the books [3] and [5].

The double-time Green's functions (GF's), as they are exclusively used in the present article, are defined in Section 3.1 and their equations of motion are given in Section 3.2. In Section 3.3 we discuss the eigenvector method for determining the GF's. Once the GF's are known, the corresponding correlation functions (thermodynamic expectation values) are determined by the standard spectral theorem, where, in general, commutator and, in the case of zero eigenvalues of the equation-of-motion matrix, anti-commutator GF's have to be used. A proof of the standard spectral theorem is given in Section 3.4. In Section 3.5 we discuss the singular value decomposition of the equation-of-motion matrix and show how a transformation can be found to eliminate the null-space, obviating the need for the anti-commutator GF. This procedure is necessary whenever the quantities associated with the null-space are momentum-dependent because the standard spectral theorem fails in this case. In Section 3.6 we show that there is no advantage in starting the calculations with the anti-commutator GF instead of the commutator GF. In Section 3.7 we show how the intrinsic energy, the specific heat and the free energy can be calculated with Green's function theory (GFT).

3.1. Definition of the double-time Green's function

Because we deal later with multi-dimensional problems, we prefer to work with a vector of Green's functions having components characterised by the index α:

$$G^{\alpha}_{ij,\eta}(t-t') = \langle\langle A^{\alpha}_i(t); B_j(t')\rangle\rangle_\eta = -i\Theta(t-t')\langle[A^{\alpha}_i(t), B_j(t')]_\eta\rangle \ . \tag{25}$$

Throughout the paper we deal exclusively with such double-time GF's. In principle, either the commutator ($\eta = -1$) or anticommutator ($\eta = +1$) of the Heisenberg operators $A_i(t)^\alpha$ and $B_j(t')$ can be used (but see Section 3.6); i and j are lattice site indices.

The operators obey the Heisenberg equation of motion, e.g.

$$A^{\alpha}_i(t) = e^{iHt}A^{\alpha}_i e^{-iHt} \ , \quad \dot{A}^{\alpha}_i = -i[A^{\alpha}_i, H]_{-1} \ . \tag{26}$$

Here H is the Hamiltonian under consideration. We set $\hbar = 1$ throughout the paper.

For magnetic films, the A_i^α are spin operators obeying the usual commutator rules. One has, for instance (see Section 4.2.1),

$$\begin{aligned} A_i^\alpha &= (S_i^+, S_i^-, S_i^z), \\ B_j &= (S_j^z)^m (S_j^-)^n \quad \text{with } m+n \leq 2S+1 \ (m \geq 0, n \geq 1, \text{integer}). \end{aligned} \tag{27}$$

In eqn (25), i is the imaginary unit (when it is not an index) and the step function $\Theta(t-t')$ is defined as

$$\Theta(t-t') = \begin{cases} 1 & \text{for } t > t' \\ 0 & \text{for } t < t' \ . \end{cases} \tag{28}$$

The double brackets $\langle\langle A_i(t)^\alpha; B_j(t')\rangle\rangle_\eta$ are an alternative notation for the Green's functions $G^\alpha_{ij,\eta}(t-t')$. Single brackets denote correlation functions, e.g. $\langle [A_i^\alpha(t), B_j(t')]_\eta \rangle$, which are thermodynamic expectation values

$$\langle ... \rangle = \frac{1}{Z} \sum_n \langle n | e^{-\beta H} ... | n \rangle = \frac{1}{Z} Tr(e^{-\beta H} ...) \ , \tag{29}$$

where

$$Z = \sum_n \langle n | e^{-\beta H} | n \rangle = Tr(e^{-\beta H}) \tag{30}$$

is the partition function with $\beta = 1/(k_B T)$, T the temperature and k_B the Boltzmann constant.

Usually, it is more convenient to work with the Fourier transforms of the Green's functions in energy space,

$$\begin{aligned} G^\alpha_{ij}(\omega) &= \int_{-\infty}^{\infty} d(t-t') G^\alpha_{ij}(t-t') e^{i\omega(t-t')}, \\ G^\alpha_{ij}(t-t') &= \int_{-\infty}^{\infty} \frac{d\omega}{2\pi} G^\alpha_{ij}(\omega) e^{-i\omega(t-t')}, \end{aligned} \tag{31}$$

and in momentum space,

$$\begin{aligned} G^\alpha_{\mathbf{k}}(\omega) &= \frac{1}{N} \sum_{ij} G^\alpha_{ij}(\omega) e^{i\mathbf{k}(\mathbf{R}_i - \mathbf{R}_j)}, \\ G^\alpha_{ij}(\omega) &= \frac{1}{N} \sum_{\mathbf{k}} G^\alpha_{\mathbf{k}}(\omega) e^{-i\mathbf{k}(\mathbf{R}_i - \mathbf{R}_j)}, \\ \text{with} \quad \delta_{\text{ij}} &= \frac{1}{N} \sum_{\mathbf{k}} e^{i\mathbf{k}(\mathbf{R}_i - \mathbf{R}_j)}, \\ \text{and} \quad \delta_{\mathbf{k}\mathbf{k}'} &= \frac{1}{N} \sum_i e^{i(\mathbf{k}-\mathbf{k}')\mathbf{R}_i} \ . \end{aligned} \tag{32}$$

Here the $\mathbf{R}_i$ are the lattice site positions and N is the number of lattice sites.

3.2. The equations of motion

The Green's function vector has to be determined by its equation of motion. This is obtained by taking the time derivative of equation (25),

$$i\frac{\partial}{\partial t}G^{\alpha}_{ij,\eta}(t-t') = \delta(t-t')\langle[A^{\alpha}_i(t), B_j(t')]_{\eta}\rangle + \langle\langle[A^{\alpha}_i, H]_{-1}(t); B_j(t')\rangle\rangle_{\eta} \ , \qquad (33)$$

where the Heisenberg equation (26) has been used together with $\frac{\partial}{\partial t}\Theta(t-t') = \delta(t-t')$. Eqn (33) is a differential equation for determining the Green's functions. Because it is more convenient to work with algebraic equations, one usually performs a Fourier transform to energy space (31), characterized by the index ω:

$$\omega\langle\langle A^{\alpha}_i; B_j\rangle\rangle_{\eta,\omega} = \langle[A^{\alpha}_i, B_j]_{\eta}\rangle + \langle\langle[A^{\alpha}_i, H]_{-}; B_j\rangle\rangle_{\eta,\omega} \ . \qquad (34)$$

Observe that on the right-hand side a higher-order Green's function arises which leads to another equation of motion having even higher-order Green's functions and so on. In this way, an *exact* infinite hierarchy of equations of motion is generated. Only in rare cases does this hierarchy terminate automatically. Usually, one has to terminate the hierarchy somewhere in order to obtain a solvable closed system of equations: the Green's function of some specified order must be factored in such a way as to contain only Green's functions which already exist in the hierarchy up to the cut-off. This factorization is called the decoupling procedure and is the essential and most severe approximation in GF theory. Except for a few cases, it can be justified only by its success.

Very often one works with the lowest-order equation (34) only. The decoupling consists in this case in factoring the GF:

$$\langle\langle[A^{\alpha}_i, H]_{-}; B_j\rangle\rangle_{\eta,\omega} \simeq \sum_l \sum_{\beta} \Gamma^{\alpha\beta}_{il}\langle\langle A^{\beta}_l; B_j\rangle\rangle_{\eta,\omega} \ . \qquad (35)$$

The right-hand side now has only GF's which are of the same order as those already present. In this way one arrives at a closed system of equations of motion. The matrix $\Gamma^{\alpha\beta}_{il}$ is in general *unsymmetric*.

Inclusion of the second-order equation of motion would require a decoupling of the double-commutator GF $\langle\langle[[A^{\alpha}_i, H], H]; B_j\rangle\rangle$, etc.

For periodic lattice structures, the equations of motion are simplified by a Fourier transformation to momentum space (32), which eliminates the lattice site indices. The equations of motion in compact matrix notation are then

$$(\omega\mathbf{1} - \mathbf{\Gamma})\mathbf{G}_{\eta} = \mathbf{A}_{\eta} \ , \qquad (36)$$

where $\mathbf{A}_{\eta}$ is the inhomogeneity vector with components $A^{\alpha}_{\eta} = \langle[A^{\alpha}, B]_{\eta}\rangle$, and $\mathbf{1}$ is the unit matrix.

From Kramers rule one sees that the GF's have a pole structure with the eigenvalues of the matrix $\mathbf{\Gamma}$ as poles. In many applications, use is made only of these eigenvalues but we show in the next subsection that it is of great advantage to use the eigenvectors of this matrix as well, especially in treating multi-dimensional problems.

3.3. The eigenvector method and the standard spectral theorem

In this section, we show how to take advantage of the eigenvectors of the matrix $\mathbf{\Gamma}$ in transforming the GF's to a new set of GF's each having but a single pole. This is particularly important in treating degenerate eigenvalues of $\mathbf{\Gamma}$ because each eigenvalue can be associated with a definite (transformed) GF. Also, the extra cost of finding the eigenvectors is more than compensated by avoiding the effort of calculating determinants in a Kramers-like treatment and by the clarity gained in the formulation. We shall use the notation of reference [9].

The first step is to diagonalize the matrix $\mathbf{\Gamma}$

$$\mathbf{L\Gamma R} = \mathbf{\Omega}, \tag{37}$$

where $\mathbf{\Omega}$ is the diagonal matrix of N eigenvalues, ω_τ ($\tau = 1, ..., N$), N_0 of which are zero and $(N - N_0)$ are non-zero. The occurence of zero eigenvalues is not a rare case: they arise as a consequence of the spin algebra of certain of the GF's and are to be expected. The matrix $\mathbf{R}$ contains the right eigenvectors as columns and its inverse $\mathbf{L} = \mathbf{R}^{-1}$ contains the left eigenvectors as rows. $\mathbf{L}$ is constructed such that $\mathbf{LR} = \mathbf{1}$. We assume that the eigenvectors span the whole space so that it is also true that $\mathbf{RL} = \mathbf{1}$.

We now define new vectors by multiplying the original vectors with $\mathbf{L}$:

$$\mathcal{G}_\eta = \mathbf{LG}_\eta \quad \text{and} \quad \mathcal{A}_\eta = \mathbf{LA}_\eta \ . \tag{38}$$

Multiplying equation (36) from the left by $\mathbf{L}$ and inserting $\mathbf{1} = \mathbf{RL}$ leads to

$$(\omega\mathbf{1} - \mathbf{\Omega})\mathcal{G}_\eta = \mathcal{A}_\eta. \tag{39}$$

From this equation we see at once that each of the components τ of this Green's function vector has but a single pole (!)

$$(\mathcal{G}_\eta)_\tau = \frac{(\mathcal{A}_\eta)_\tau}{\omega - \omega_\tau} \ . \tag{40}$$

This allows a direct application of the standard spectral theorem (see e.g. [5, 3]; for its proof, see Section 3.4) to each component of the Greens's function vector *separately*. The spectral theorem relates the correlation vector

$$\mathcal{C} = \mathbf{LC}_\mathbf{k} = \mathbf{L}\langle BA\rangle_\mathbf{k} \tag{41}$$

to the Green's function vector. The index $\mathbf{k}$ indicates that we work in momentum space. Explicitly,

$$\mathcal{C}_\tau = \frac{i}{2\pi}\lim_{\delta\to 0}\int_{-\infty}^{\infty} d\omega \frac{\Big(\mathcal{G}_\eta(\omega+i\delta)-\mathcal{G}_\eta(\omega-i\delta)\Big)_\tau}{e^{\beta\omega}+\eta} = \frac{(\mathcal{A}_\eta)_\tau}{e^{\beta\omega_\tau}+\eta}, \tag{42}$$

where eqn (40) and $\frac{1}{\omega\pm i\delta} = \frac{P}{\omega} \mp i\pi\delta(\omega)$ have been used.

In general, we use the commutator GF's, in which case the inhomogeneities $\mathcal{A}_{\eta=-1}$ are independent of the momentum $\mathbf{k}$, whereas the $\mathcal{A}_{\eta=+1}$ are not. Using the anti-commutator GF's ($\eta=+1$) leads to problems connected with this $\mathbf{k}$-dependence (see Section 3.6). The commutator GF's, on the other hand, lead to problems with zero eigenvalues of the equation of motion matrix $\mathbf{\Gamma}$ because there are then zeroes in the denominator of eqn (42). In this case, the correlation vector must be split into two components $\mathcal{C}^1_\tau$ and $\mathcal{C}^0_{\tau_0}$ belonging to non-zero and zero eigenvalues respectively. We then have

$$(\mathcal{C}^1)_\tau = \frac{(\mathcal{A}_{-1})_\tau}{e^{\beta\omega_\tau}-1}, \tag{43}$$

where $\omega_\tau \neq 0$.

For the correlation vector belonging to zero eigenvalues, the anti-commutator GF is required (for a proof, see Section 3.4):

$$\begin{aligned}(\mathcal{C}^0)_{\tau_0} &= \lim_{\omega\to 0}\frac{1}{2}\omega(\mathcal{G}_{\eta=+1})_{\tau_0} \\ &= \frac{1}{2}\lim_{\omega\to 0}\frac{\omega(\mathcal{A}_{+1})_{\tau_0}}{\omega-(\omega_{\tau_0}=0)} = \frac{1}{2}(\mathcal{A}_{+1})_{\tau_0} \\ &= \frac{1}{2}(\mathbf{L}^0(\mathbf{A}_{-1}+2\mathbf{C}_\mathbf{k}))_{\tau_0} = (\mathbf{L}^0\mathbf{C}_\mathbf{k})_{\tau_0}\ .\end{aligned} \tag{44}$$

Here, the relation $\mathbf{A}_{+1} = \mathbf{A}_{-1} + 2\mathbf{C}_\mathbf{k}$ has been used together with the fact that the commutator GF is regular at the origin (see eqn (70)). By multiplying eqn (36) with $\mathbf{L}^0$, using $\mathbf{L}^0\mathbf{\Gamma}=0$ and taking the limit $\omega\to 0$ one obtains

$$\lim_{\omega\to 0}\mathbf{L}^0(\omega\mathbf{1}-\mathbf{\Gamma})\mathbf{G}_{-1} = \mathbf{L}^0\mathbf{A}_{-1} = 0\ . \tag{45}$$

We call this the regularity condition.

We now partition all quantities with respect to the non-zero and zero eigenvalue space

$$\mathbf{R} = (\mathbf{R}^1\mathbf{R}^0)\ , \qquad \mathbf{L} = \begin{pmatrix}\mathbf{L}^1\\ \mathbf{L}^0\end{pmatrix}\ , \qquad \mathcal{C} = \begin{pmatrix}\mathcal{C}^1 = \mathcal{E}^1\mathbf{L}^1\mathbf{A}_{-1}\\ \mathcal{C}^0 = \mathbf{L}^0\mathbf{C}_\mathbf{k}\end{pmatrix}\ , \tag{46}$$

where $\mathcal{E}^1$ is a diagonal $(N-N_0)\times(N-N_0)$ matrix with elements $1/(e^{\beta\omega_\tau}-1)$ on the diagonal ($\omega_\tau\neq 0$).

The original correlation vector in momentum space is then

$$\mathbf{C}_\mathbf{k} = \mathbf{R}\mathcal{C} = (\mathbf{R}^1\mathbf{R}^0)\begin{pmatrix}\mathcal{C}^1\\ \mathcal{C}^0\end{pmatrix} = \mathbf{R}^1\mathcal{E}^1\mathbf{L}^1\mathbf{A}_{-\mathbf{1}} + \mathbf{R}^0\mathbf{L}^0\mathbf{C}_\mathbf{k}\ . \tag{47}$$

We are interested in the diagonal correlations $\mathbf{C}$ (without the index $\mathbf{k}$) in configuration space

$$\mathbf{C} = \frac{1}{N}\sum_{\mathbf{k}} \mathbf{C}_{\mathbf{k}} = \int d\mathbf{k}\mathbf{C}_{\mathbf{k}}, \tag{48}$$

where the integration is over the first Brillouin zone. This leads to a set of integral equations for the components C_i (i=1,...,N) which have to be solved self-consistently. If the factor $\mathbf{R}^0\mathbf{L}^0$ is momentum independent, one can take it outside the integration in the second term of eqn (47) to get the C_i components explicitly:

$$C_i = \int d\mathbf{k}\Big(\sum_{j=1}^{N-N_0}\sum_{l=1}^{N} R^1_{ij}\mathcal{E}^1_{jj}L^1_{jl}(A_{-1})_l\Big) + \sum_{j=1}^{N_0}\sum_{l=1}^{N} R^0_{ij}L^0_{jl}C_l. \tag{49}$$

The components C_i are obtained by iterating on the C_i until Eqn (49) is satisfied.

If $\mathbf{R}^0\mathbf{L}^0$ is momentum-dependent, the standard procedure fails because one cannot take $\mathbf{R^0L^0}$ outside the integration. Instead, one needs a more complicated procedure that relies on the singular value decomposition of the $\mathbf{\Gamma}$-matrix (see Section 3.5). This leads to a formulation of the spectral theorem in which the null-space is eliminated and only the commutator GF is needed, obviating the use of the anticommutator GF.

◇◇

Equation (47) can also be derived without the anticommutator GF in the following simple way:

Start with the spectral theorem for the commutator GF (42) with $\eta = -1$

$$\mathbf{C}_{\mathbf{k}} = \mathbf{R}\mathcal{E}\mathbf{L}\mathbf{A}_{-1}, \tag{50}$$

and make use of the decomposition (46) and $\mathcal{E}_0 = 1/(e^{\beta 0} - 1) = \infty$. Then

$$\mathbf{C}_{\mathbf{k}} = (\mathbf{R}^1\mathbf{R}^0)\begin{pmatrix} \mathcal{E}^1 & 0 \\ 0 & \mathcal{E}^0 \end{pmatrix}\begin{pmatrix} \mathbf{L}^1 \\ \mathbf{L}^0 \end{pmatrix}\mathbf{A}_{-1} = \mathbf{R}^1\mathcal{E}^1\mathbf{L}^1\mathbf{A}_{-1} + \mathbf{R}^0\mathcal{E}^0\mathbf{L}^0\mathbf{A}_{-1}. \tag{51}$$

The second term is undetermined because $\mathcal{E}^0\mathbf{L}^0\mathbf{A}_{-1}$ has the indeterminate form $\infty \times 0$, see eqn(45). We get around this by multiplying the last equation from the left by $\mathbf{R}^0\mathbf{L}^0$:

$$\mathbf{R}^0\mathbf{L}^0\mathbf{C}_{\mathbf{k}} = \mathbf{R}^0\mathbf{L}^0\mathbf{R}^1\mathcal{E}^1\mathbf{L}^1\mathbf{A}_{-1} + \mathbf{R}^0\mathbf{L}^0\mathbf{R}^0\mathcal{E}^0\mathbf{L}^0\mathbf{A}_{-1} = \mathbf{R}^0\mathcal{E}^0\mathbf{L}^0\mathbf{A}_{-1}. \tag{52}$$

The last term is obtained because $\mathbf{L}^0\mathbf{R}^1 = 0$ and $\mathbf{R}^0\mathbf{L}^0\mathbf{R}^0\mathbf{L}^0 = \mathbf{R}^0\mathbf{L}^0$. Thus the term $\mathbf{R}^0\mathcal{E}^0\mathbf{L}^0\mathbf{A}_{-1}$ in eqn (51) can be replaced by $\mathbf{R}^0\mathbf{L}^0\mathbf{C}_{\mathbf{k}}$, which completes the proof of eqn (47).

◇◇

3.4. The proof of the standard spectral theorem

The spectral theorem is the relation of greatest importance for the Green's function formalism because it allows the calculation of the desired observables (or more

generally the correlation functions) from the corresponding Green's functions. Although its proof can be found in text books (e.g. [5, 3]), we reproduce it here for the convenience of the reader.

Considering one component of the GF vector (25) (for brevity we leave out the index α), we introduce the spectral function $S_{ij,\eta}(t-t')$ by

$$G_{ij,\eta}(t-t') = -i\Theta(t-t')2\pi S_{ij,\eta}(t-t'), \tag{53}$$

where, by comparing with eqn (25),

$$S_{ij,\eta}(t-t') = \frac{1}{2\pi}\langle [A_i(t), B_j(t')]_\eta \rangle = \frac{1}{2\pi}\langle A_i(t)B_j(t') + \eta B_j(t')A_i(t)\rangle \ . \tag{54}$$

Inserting a complete set of eigenstates ($H|m\rangle = \omega_m|m\rangle$) yields the following spectral representations for the correlations:

$$\langle A_i(t)B_j(t')\rangle = \frac{1}{Z}\sum_{nm}\langle n|B_j|m\rangle\langle m|A_i|n\rangle e^{-\beta\omega_n}e^{\beta(\omega_n-\omega_m)}e^{-i(\omega_n-\omega_m)(t-t')} \ , \tag{55}$$

$$\langle B_j(t')A_i(t)\rangle = \frac{1}{Z}\sum_{nm}\langle n|B_j|m\rangle\langle m|A_i|n\rangle e^{-\beta\omega_n}e^{-i(\omega_n-\omega_m)(t-t')} \ , \tag{56}$$

and the spectral function,

$$S_{ij,\eta}(t-t') = \frac{1}{2\pi}\frac{1}{Z}\sum_{nm}\langle n|B_j|m\rangle\langle m|A_i|n\rangle e^{-\beta\omega_n}(e^{\beta(\omega_n-\omega_m)}+\eta)e^{-i(\omega_n-\omega_m)(t-t')}, \tag{57}$$

whose Fourier transform to energy space is

$$S_{ij,\eta}(\omega) = \frac{1}{Z}\sum_{nm}\langle n|B_j|m\rangle\langle m|A_i|n\rangle e^{-\beta\omega_n}(e^{\beta\omega}+\eta)\delta(\omega-(\omega_n-\omega_m)). \tag{58}$$

A relation between the energy representations of $S_{ij,\eta}(\omega)$ and $G_{ij,\eta}(\omega)$ is derived by inserting in

$$G_{ij,\eta}(\omega) = -2\pi i\int_{-\infty}^{\infty} d(t-t')e^{i\omega(t-t')}\Theta(t-t')S_{ij,\eta}(t-t') \tag{59}$$

the following representation for the step function

$$\Theta(t-t') = \frac{i}{2\pi}\int_{-\infty}^{\infty} dx\frac{e^{-ix(t-t')}}{x+i\eta}, \tag{60}$$

and the Fourier transform of $S_{ij,\eta}(t-t')$:

$$\begin{aligned} G_{ij,\eta}(\omega) &= \int_{-\infty}^{\infty}d\omega'\int_{-\infty}^{\infty}dx\frac{1}{x+i\eta}\frac{1}{2\pi}\int_{-\infty}^{\infty}d(t-t')e^{i(\omega-\omega'-x)(t-t')}S_{ij,\eta}(\omega') \\ &= \int_{-\infty}^{\infty}d\omega'\frac{S_{ij,\eta}(\omega')}{\omega-\omega'+i\eta} \ . \end{aligned} \tag{61}$$

With

$$G_{ij,\eta}(\omega+i\delta) - G_{ij,\eta}(\omega-i\delta) = \int_{-\infty}^{\infty}d\omega' S_{ij,\eta}(\omega')(\frac{1}{\omega-\omega'+i\delta} - \frac{1}{\omega-\omega'-i\delta}) \tag{62}$$

and

$$\frac{1}{\omega - \omega' \pm i\delta} = P\frac{1}{\omega - \omega'} \mp i\pi\delta(\omega - \omega') \tag{63}$$

it follows that

$$S_{ij,\eta}(\omega) = \lim_{\delta\to 0}\frac{i}{2\pi}\Big(G_{ij,\eta}(\omega + i\delta) - G_{ij,\eta}(\omega - i\delta)\Big). \tag{64}$$

We can also see that

$$\langle B_j(t')A_i(t)\rangle = \int_{-\infty}^{\infty}\frac{d\omega}{e^{\beta\omega}+\eta}S_{ij,\eta}(\omega)e^{-i\omega(t-t')} \tag{65}$$

by inserting equation (58) in this equation and comparing with (56).

Together with equation (64) this yields

$$\langle B_j(t')A_i(t)\rangle = \lim_{\delta\to 0}\frac{i}{2\pi}\int_{-\infty}^{\infty}d\omega\frac{G_{ij,\eta}(\omega + i\delta) - G_{ij,\eta}(\omega - i\delta)}{e^{\beta\omega}+\eta}e^{-i\omega(t-t')}\ . \tag{66}$$

This is nothing else then equation (42) with $t = t'$ after a Fourier transformation to momentum space. It is valid for $\eta = \pm 1$.

For $\eta = -1$, this expression diverges in the limit $\omega \to 0$ and it is necessary to use eqn (44). This was first pointed out in reference [10], see also [11], and can be seen by decomposing the spectral function (58) into two terms referring to $\omega_n \neq \omega_m$ and $\omega_n = \omega_m$ respectively

$$S_{ij,\eta}(\omega) = \tilde{S}_{ij,\eta}|_{\omega_n\neq\omega_m} + (1+\eta)C^0_{ij}\delta(\omega). \tag{67}$$

Inserting this in eqn (61) and taking the limit $\omega \to 0$ of $\omega G_{ij,\eta}(\omega)$ one finds

$$\begin{aligned}\lim_{\omega\to 0}\omega G_{ij,\eta}(\omega) &= \lim_{\omega\to 0}\omega\int_{-\infty}^{\infty}d\omega'\Big(\frac{\tilde{S}_{ij,\eta}}{\omega-\omega'} + \frac{(1+\eta)C^0_{ij}\delta(\omega')}{\omega-\omega'}\Big)\\ &= 0 + (1+\eta)C^0_{ij}\ .\end{aligned} \tag{68}$$

From this expression, we see that the quantity C^0_{ij} is determined by the anti-commutator GF ($\eta = +1$)

$$C^0_{ij} = \frac{1}{2}\lim_{\omega\to 0}\omega G_{ij,\eta=+1}(\omega)\ , \tag{69}$$

whose Fourier transform to momentum space is equation (44). This completes the proof of the standard spectral theorem.

From equation (68) an important analytical property follows: the commutator Green's function ($\eta = -1$) is regular at the origin,

$$\lim_{\omega\to 0}\omega G_{ij,\eta=-1} = 0, \tag{70}$$

a fact which is necessary to derive the regularity condition (45). The anti-commutator Green's function has a first order pole at $\omega = 0$.

3.5. The singular value decomposition of Γ and its consequences

In this section we show that the singular value decomposition of the equation-of-motion matrix $\mathbf{\Gamma}$ obviates the need to use the anti-commutator GF when zero eigenvalues occur; the commutator GF suffices.

The standard spectral theorem is of practical use only if the quantity $\mathbf{R}^0\mathbf{L}^0$ in eqn (47) is momentum independent, because only then can one arrive at an equation that can be solved by iteration (see (49). If $\mathbf{R}^0\mathbf{L}^0$ depends on momentum, the standard procedure fails because equation (47) is of the form

$$(1 - \mathbf{R}^0\mathbf{L}^0)\mathbf{C_k} = \mathbf{R}^1\mathcal{E}^1\mathbf{L}^1\mathbf{A_{-1}}. \tag{71}$$

The term $(1 - \mathbf{R}^0\mathbf{L}^0)$ is idempotent and therefore has no inverse; hence, one cannot solve for $\mathbf{C_k}$. This arises for instance for the reorientation of the magnetization using exchange anisotropies, see Section 4.2.3.

$\diamond\diamond$

An idempotent operator P has no inverse.

Proof: assume the existence of an inverse: $P^{-1}P = 1$ and idempotence $P = P^2$,

then $P^{-1}P^2 = 1$, implying $P = 1$, which is a contradiction.

$\diamond\diamond$

The singular value decomposition (SVD) offers a way out of this situation by providing a transformation that eliminates the null-space; in effect, it defines a smaller number of Green's functions whose associated equation of motion matrix, γ, has no zero eigenvalues, thus dispensing with the anti-commutator GF as well as reducing the number of equations.

The singular value decomposition states that ... "any $M \times N$ matrix $\mathbf{A}$ whose number of rows M is greater or equal to its number of columns, can be written as the product of an $M \times N$ column-orthogonal matrix $\mathbf{U}$, an $N \times N$ diagonal matrix $\mathbf{W}$ with positive or zero elements and the transpose of an $N \times N$ orthogonal matrix V"..., [12]

The equation-of-motion matrix can therefore be decomposed as

$$\mathbf{\Gamma} = \mathbf{U}\mathbf{W}\tilde{\mathbf{V}} = \mathbf{u}\mathbf{w}\tilde{\mathbf{v}}. \tag{72}$$

where $\mathbf{U}$ and $\mathbf{V}$ are orthogonal matrices ($\tilde{\mathbf{U}}\mathbf{U} = \mathbf{1}, \tilde{\mathbf{V}}\mathbf{V} = \mathbf{1}$) and $\mathbf{W}$ is a diagonal matrix with singular values on the diagonal. $\mathbf{U}, \mathbf{V}$ and $\mathbf{W}$ can be determined very efficiently numerically [12]. The matrices $\mathbf{U}$ and $\mathbf{V}$ can also be obtained by diagonalising $\tilde{\mathbf{\Gamma}}\mathbf{\Gamma}$ or $\mathbf{\Gamma}\tilde{\mathbf{\Gamma}}$ respectively. The singular values are the positive square roots of the eigenvalues of these matrices:

$$\begin{aligned} \tilde{\mathbf{V}}\tilde{\mathbf{\Gamma}}\mathbf{\Gamma}\mathbf{V} &= \tilde{\mathbf{V}}\mathbf{V}\mathbf{W}\tilde{\mathbf{U}}\mathbf{U}\mathbf{W}\tilde{\mathbf{V}}\mathbf{V} = \mathbf{W}^2, \\ \tilde{\mathbf{U}}\mathbf{\Gamma}\tilde{\mathbf{\Gamma}}\mathbf{U} &= \tilde{\mathbf{U}}\mathbf{U}\mathbf{W}\tilde{\mathbf{V}}\mathbf{V}\mathbf{W}\tilde{\mathbf{U}}\mathbf{U} = \mathbf{W}^2. \end{aligned} \tag{73}$$

If $\mathbf{\Gamma}$ has zero eigenvalues, it has the same number of zero singular values. The matrix $\mathbf{\Gamma}$ is also given by $\mathbf{uw\tilde{v}}$, where $\mathbf{u}$ and $\mathbf{v}$ are obtained from $\mathbf{U}$ and $\mathbf{V}$ by omitting columns corresponding to singular values zero. $\mathbf{u}$ and $\mathbf{v}$ are again orthogonal matrices ($\mathbf{\tilde{u}u} = \mathbf{1}, \mathbf{\tilde{v}v} = \mathbf{1}$). Note that $\mathbf{v\tilde{v}}$ is a projector onto the non-null-space and $\mathbf{v_0\tilde{v}_0}$ a projector onto the null-space ($\mathbf{v\tilde{v}} + \mathbf{v_0\tilde{v}_0} = \mathbf{1}$). The matrix $\mathbf{w}$ is diagonal having positive singular values on the diagonal.

To eliminate the null-space, it suffices to use the following transformations:

$$\begin{aligned} \gamma &= \mathbf{\tilde{v}\Gamma v}, \\ \mathbf{g} &= \mathbf{\tilde{v}G}, \\ \mathbf{a} &= \mathbf{\tilde{v}A}, \\ \mathbf{c} &= \mathbf{\tilde{v}C_k}. \end{aligned} \tag{74}$$

Multiplying eqn (36) by $\mathbf{\tilde{v}v} = 1$ and $\mathbf{\Gamma} = \mathbf{uw}(\mathbf{\tilde{v}v})\mathbf{\tilde{v}} = (\mathbf{uw\tilde{v}})\mathbf{v\tilde{v}} = \mathbf{\Gamma v\tilde{v}}$ one obtains

$$\begin{aligned} \mathbf{\tilde{v}}(\omega\mathbf{1} - \mathbf{\Gamma v\tilde{v}})\mathbf{G} &= \mathbf{\tilde{v}A_{-1}}, \\ (\omega\mathbf{1} - \mathbf{\tilde{v}\Gamma v})\mathbf{\tilde{v}G} &= \mathbf{\tilde{v}A_{-1}}, \\ (\omega\mathbf{1} - \gamma)\mathbf{g} &= \mathbf{a}. \end{aligned}$$

Now we diagonalize γ

$$\mathbf{l}\gamma\mathbf{r} = \omega^1, \quad \text{where} \quad \mathbf{l} = \mathbf{L^1 v} \text{ and } \mathbf{r} = \mathbf{\tilde{v}R^1}. \tag{75}$$

γ is a reduced matrix with the same non-zero eigenvalues ω^1 as the original matrix $\mathbf{\Gamma}$. Since there are now no zero eigenvalues, we can apply the spectral theorem with respect to the non-null-space:

$$\mathbf{c} = \mathbf{r}\mathcal{E}^1\mathbf{la}, \tag{76}$$

where $\mathcal{E}^1$ is the matrix occurring in eqn (47). A Fourier transformation to configuration space yields the self-consistency equations (analogous to eqn (49):

$$0 = \int d\mathbf{k}(\mathbf{r}\mathcal{E}^1\mathbf{l\tilde{v}A_{-1}} - \mathbf{\tilde{v}C_k}). \tag{77}$$

Again, this can be solved for the correlations in configuration space $\mathbf{C}$ if one can find a row-vector $\mathbf{\tilde{v}}_j$ which is $\mathbf{k}$-independent, i. e.

$$\int d\mathbf{k}\ \mathbf{\tilde{v}}_j\mathbf{C_k} = \mathbf{\tilde{v}}_j \int d\mathbf{k}\ \mathbf{C_k} = \mathbf{\tilde{v}}_j\mathbf{C}. \tag{78}$$

This equation may be supplemented by the regularity condition

$$\lim_{\omega\to 0} \mathbf{\tilde{u}}_0(\omega\mathbf{1} - \mathbf{uw\tilde{v}})\mathbf{G} = \mathbf{\tilde{u}}_0\mathbf{A_{-1}} = 0. \tag{79}$$

This is because $\mathbf{\tilde{u}}_0\mathbf{u} = 0$ and because the commutator GF is regular at the origin.

One may be tempted to object that eqn (78) is no improvement over eqn (49) because, in both cases, it is the $\mathbf{k}$ dependence of a term containing $\mathbf{C_k}$ that creates a problem. In practice, however, it is much better to use SVD because diagonalization of the full matrix $\mathbf{\Gamma}$ to get $\mathbf{R}^0$ and $\mathbf{L}^0$ is fraught with numerical difficulties when there are non-zero eigenvalues which are very small. Furthermore, the vectors $\mathbf{R}^0$ and $\mathbf{L}^0$ are non-orthogonal, whereas the projector $\mathbf{v}\tilde{\mathbf{v}}$ onto the non-null-space is built from orthogonal vectors – this makes it easier in practice to find a row vector $\tilde{\mathbf{v}}_\mathbf{i}$ that is independent of the momentum $\mathbf{k}$. This search is technically complicated, and for a more detailed description, we refer the reader to Ref. [13]. Here, we give a recipe for seeking for appropriate $\tilde{\mathbf{v}}_j$.

The row vectors in $\tilde{\mathbf{v}}$ are determined numerically and are unique up to a sign change or, for degenerate singular values, up to an orthogonal transformation of the degenerate vectors. In order to distinguish among the row vectors of $\tilde{\mathbf{v}}$, it is very helpful if they are suitably labelled; e.g. they can often be characterized by a layer index or a sublattice index. The following procedure is useful: decompose the $\mathbf{\Gamma}$-matrix into a reference matrix and the rest,

$$\mathbf{\Gamma} = \mathbf{\Gamma}_{ref} + \mathbf{\Gamma}_{rest}, \tag{80}$$

where $\mathbf{\Gamma}_{ref}$ has a block structure determined by the chosen labels. With a singular value decomposition,

$$\mathbf{\Gamma}_{ref} = \mathbf{U}_{ref}\mathbf{W}_{ref}\tilde{\mathbf{V}}_{ref}, \tag{81}$$

one can define a block-label operator

$$\mathbf{P}_{op} := \sum_{i=1}^{N_B} \mathbf{V}_{ref}(i)L(i)\tilde{\mathbf{V}}_{ref}(i), \tag{82}$$

with $L(i) = N_B - i + 1$. In the basis of the singular vectors $\mathbf{v}$ (and analogously for $\mathbf{v}_0$), we define a matrix

$$\mathbf{P} = \tilde{\mathbf{v}}\mathbf{P}_{op}\mathbf{v} = \sum_{i=1}^{N_B} \tilde{\mathbf{v}}\mathbf{V}_{ref}(i)\sqrt{L(i)}\sqrt{L(i)}\tilde{\mathbf{V}}_{ref}(i)\mathbf{v} = \tilde{\mathbf{S}}\mathbf{S} \tag{83}$$

with

$$\mathbf{S} = [\sqrt{L(1)}\tilde{\mathbf{V}}_{ref}(1) \oplus ... \oplus \sqrt{L(N_B)}\tilde{\mathbf{V}}_{ref}(N_B)]\mathbf{v}, \tag{84}$$

where $\oplus$ defines the direct sum.

Now the singular value decomposition of $\mathbf{S}$,

$$\mathbf{S} = \mathbf{L}\mathbf{y}\tilde{\mathbf{Z}}, \tag{85}$$

furnishes a matrix $\tilde{\mathbf{Z}}$ that diagonalizes $\tilde{\mathbf{S}}\mathbf{S}$:

$$\tilde{\mathbf{S}}\mathbf{S} = \mathbf{Z}\mathbf{y}\tilde{\mathbf{L}}\mathbf{L}\mathbf{y}\tilde{\mathbf{Z}} = \mathbf{Z}\mathbf{y}^\mathbf{2}\tilde{\mathbf{Z}}, \tag{86}$$

where $\mathbf{y}^2 \approx L(i)$, which labels the blocks. To each block-label belongs a labelled vector

$$\tilde{\mathbf{v}}_L = \tilde{\mathbf{Z}}\tilde{\mathbf{v}}, \quad (\mathrm{L} = \text{labelling}) \tag{87}$$

which is the desired result.

A further difficulty is connected with the fact that the computed $\tilde{\mathbf{v}}$ will not necessarily be continuous, even if the elements of the $\mathbf{\Gamma}$-matrix are changed continuously (e.g. by varying the momentum $\mathbf{k}$ on which they depend); i.e. vectors at neighbouring values of $\mathbf{k}$ can have arbitrary phases. This difficulty is overcome by a smoothing procedure, which consists of the following steps:

(1) Create well-behaved reference vectors $\mathbf{V}_{ref}(r = 1, .., N_r)$ in the momentum range of the first Brillouin zone for the vectors $\mathbf{V}^0$ at k_0 and $\mathbf{V}^1$ at k_1, etc. by overlaps as in the labelling procedure.

(2) Interpolate the reference vectors at each k

$$\tilde{\bar{\mathbf{V}}}_{ref}(k) = w_l \tilde{\mathbf{V}}_{ref}(k_l) + w_h \tilde{\mathbf{V}}_{ref}(k_h) \tag{88}$$

with

$$w_l = \cos^2\left(\frac{\pi}{2}(\frac{k - k_l}{k_h - k_l})\right) \quad \text{and} \quad w_h = 1 - w_l \ . \tag{89}$$

(3) Orthonormalize the reference vectors

$$\begin{aligned} \mathcal{Y} &= \tilde{\bar{\mathbf{V}}}_{ref}\bar{\mathbf{V}}_{ref}, \\ \lambda &= \tilde{\mathbf{T}}\mathcal{Y}\mathbf{T}, \\ \mathcal{Y}^{-1/2} &= \mathbf{T}\lambda^{-1/2}\tilde{\mathbf{T}}, \\ \tilde{\mathbf{V}}_{ref} &= \mathcal{Y}^{-1/2}\tilde{\bar{\mathbf{V}}}_{ref} \ . \end{aligned} \tag{90}$$

We now have reference vectors for the non-null and the null-space: $\mathbf{V}_{ref} = (\mathbf{v}_{ref}, \mathbf{v}_{0,ref})$.

(4) Match the untreated (or, if necessary, labelled) vectors $\tilde{\mathbf{v}}$ to the orthonormalized reference vectors $\tilde{\mathbf{v}}_{ref}$. This is done by seeking a transformation $\mathbf{Q}$ that rotates the target (original) vectors among themselves to achieve the best match

$$\tilde{\mathbf{v}}_S = \mathbf{Q}\tilde{\mathbf{v}}. \quad (\mathrm{S} = \text{smoothed}) \tag{91}$$

$\mathbf{Q}$ is found by a SVD of the overlap matrix of the reference vectors with the target vectors

$$\mathcal{S} = \tilde{\mathbf{v}}_{ref}\mathbf{v} = \mathcal{L}\mathbf{x}\tilde{\mathcal{Z}}. \tag{92}$$

Here $\mathbf{x}$ is a diagonal matrix of the singular values of the overlap matrix which are close to 1 by construction ($\mathbf{x} \simeq \mathbf{1}$). The desired transformation matrix is

$$\mathbf{Q} = \mathcal{L}\tilde{\mathcal{Z}}, \tag{93}$$

which is a rotation matrix because

$$\tilde{\mathbf{Q}}\mathbf{Q} = \mathcal{Z}\tilde{\mathcal{L}}\mathcal{L}\tilde{\mathcal{Z}} = \mathcal{Z}\tilde{\mathcal{Z}} = \mathbf{1}. \tag{94}$$

The overlap matrix of the reference vectors with the smoothed vectors is close to the unit matrix because the phases of the new vectors have been fixed by $\tilde{\mathbf{Q}}$:

$$\tilde{\mathbf{v}}_{ref}\mathbf{v}_S = \tilde{\mathbf{v}}_{ref}\mathbf{v}\tilde{\mathbf{Q}} = \mathbf{S}\mathcal{Z}\tilde{\mathcal{L}} = \mathcal{L}\mathbf{x}\tilde{\mathcal{Z}}\mathcal{Z}\tilde{\mathcal{L}} = \mathcal{L}\mathbf{x}\tilde{\mathcal{L}} \simeq \mathbf{1}. \tag{95}$$

To summarize, the untreated vectors $\tilde{\mathbf{v}}$ of the original problem can be labelled and smoothed by the tranformation

$$\tilde{\mathbf{v}}_{LS} = \mathbf{Q}\tilde{\mathbf{v}}_L = \mathcal{L}\tilde{\mathcal{Z}}\tilde{\mathbf{Z}}\tilde{\mathbf{v}}. \tag{96}$$

In practice, some of the row vectors of this transformation matrix turn out to be momentum-independent and can be used in solving equation (77).

The procedure described above was successfully applied to Heisenberg multilayers with exchange anisotropies, see Section 4.2.3 and to coupled ferro- and antiferromagnetic layers, see Section 4.3.2. We stress once more that the standard spectral theorem fails in these cases.

3.6. No advantage to using the anti-commutator instead of the commutator Green's function

We begin with the simplest case of a Green's function G_η which has but a single pole and an inhomogeneity A_η:

$$\begin{aligned} G_\eta &= \langle\langle A; B\rangle\rangle, \\ A_\eta &= \langle [A, B]_\eta \rangle, \end{aligned} \tag{97}$$

i.e.

$$G_\eta^\alpha = \frac{A_\eta^\alpha}{(\omega - \omega_{\mathbf{k}})}. \tag{98}$$

The corresponding correlations in momentum and configuration space are

$$\begin{aligned} C_{\mathbf{k}} &= \langle BA \rangle, \\ C &= \frac{1}{N}\sum_{\mathbf{k}} C_{\mathbf{k}}. \end{aligned} \tag{99}$$

Applying the spectral theorem gives

$$C_{\mathbf{k}} = \frac{A_\eta}{e^{\beta\omega_{\mathbf{k}}} + \eta}\ . \tag{100}$$

Note that $\mathbf{A}_{+1}(\mathbf{k}) = \mathbf{A}_{-1} + 2\mathbf{C}_{\mathbf{k}}$ and $\mathbf{A}_{+1}(\mathbf{k})$ depends on $\mathbf{k}$, whereas $\mathbf{A}_{-1}$ does not.

The commutator ($\eta = -1$) GF yields the correlation in configuration space

$$C = \frac{1}{N} \sum_{\mathbf{k}} \frac{A_{-1}}{e^{\beta\omega_{\mathbf{k}}} - 1}, \tag{101}$$

whereas the anti-commutator ($\eta = +1$) GF leads to

$$C = \frac{1}{N} \sum_{\mathbf{k}} \frac{A_{+1}(\mathbf{k})}{e^{\beta\omega_{\mathbf{k}}} + 1} = \frac{1}{N} \sum_{\mathbf{k}} \frac{A_{-1} + 2C_{\mathbf{k}}}{e^{\beta\omega_{\mathbf{k}}} + 1} \ , \tag{102}$$

which cannot be solved because $C_{\mathbf{k}}$ is unknown. Putting eqn (100) with $\eta = -1$ into eqn (102) leads again to equation (101),

$$C = \frac{1}{N} \sum_{\mathbf{k}} \frac{A_{-1} + 2\frac{A_{-1}}{e^{\beta\omega_{\mathbf{k}}} - 1}}{e^{\beta\omega_{\mathbf{k}}} + 1} = \frac{1}{N} \sum_{\mathbf{k}} \frac{A_{-1}}{e^{\beta\omega_{\mathbf{k}}} - 1} \ , \tag{103}$$

which can be solved self-consistently. This shows that there is no advantage in starting the calculation with the anti-commutator GF.

One can show this more generally with the eigenvector method of Section 3.3, see [37]: starting with the anti-commutator formulation, the spectral theorem yields

$$\mathbf{C_k} = \mathbf{R}\mathcal{E}\mathbf{L}\mathbf{A}_{\eta=+1}, \tag{104}$$

where $\mathcal{E}$ is a diagonal matrix with elements $\mathcal{E}_{ij} = \delta_{ij}(e^{\beta\omega_i} + 1)^{-1}$ and $\mathbf{A}_{\eta=+1}$ depends on the momentum $\mathbf{k}$, preventing a direct use of this equation.

Because $\mathbf{A}_{\eta=+1}$=$\mathbf{A}_{-1} + 2\mathbf{C_k}$,

$$\mathbf{C_k} = \mathbf{R}\mathcal{E}\mathbf{L}(\mathbf{A}_{-1} + 2\mathbf{C_k}) \tag{105}$$

or

$$\mathbf{C_k} = (1 - 2\mathbf{R}\mathcal{E}\mathbf{L})^{-1}\mathbf{R}\mathcal{E}\mathbf{L}\mathbf{A}_{-1} \ . \tag{106}$$

Introducing

$$(\mathbf{R}\mathcal{E}\mathbf{L})^{-1} = \mathbf{L}^{-1}\mathcal{E}^{-1}\mathbf{R}^{-1} = \mathbf{R}\mathcal{E}^{-1}\mathbf{L} \tag{107}$$

in (106),

$$\mathbf{C_k} = (\mathbf{R}(\mathbf{1} - \mathbf{2}\mathcal{E})\mathbf{L})^{-1}\mathbf{R}\mathcal{E}\mathbf{L}\mathbf{A}_{-1} = \mathbf{R}(\mathbf{1} - \mathbf{2}\mathcal{E})^{-1}\mathcal{E}\mathbf{L}\mathbf{A}_{-1} = \mathbf{R}\tilde{\mathcal{E}}\mathbf{L}\mathbf{A}_{-1}, \tag{108}$$

where $\tilde{\mathcal{E}}_{ij} = \delta_{ij}\mathcal{E}_{ii}/(1 - 2\mathcal{E}_{ii}) = \delta_{ij}(e^{\beta\omega_i} - 1)^{-1}$. This is still of no use because of the zero eigenvalues. But we have shown in Section 3.3 that the term $\mathbf{R}^0\mathbf{L}^0$ remedies this:

$$\mathbf{C_k} = \mathbf{R}^1\mathcal{E}^1\mathbf{L}^1\mathbf{A}_{-1} + \mathbf{R}^0\mathbf{L}^0\mathbf{C_k} \tag{109}$$

which is equation (47), where $\mathcal{E}^1$ is the matrix $\tilde{\mathcal{E}}$ leaving out the diverging terms.

3.7. The intrinsic energy, the specific heat and the free energy

The intrinsic energy is the thermodynamic expectation value of the underlying Hamiltonian

$$E = \langle H \rangle = N E_i \ , \tag{110}$$

where E_i is the intrinsic energy per lattice site and N is the number of lattice sites. The specific heat at constant volume is obtained by differentiating the intrinsic energy with respect to the temperature

$$c_V = \frac{dE}{dT} = -\beta^2 \frac{dE}{d\beta} \ . \tag{111}$$

The free energy is obtained by integrating over the intrinsic energy

$$F(T) = E(0) - T \int_0^T dT' \frac{E(T') - E(0)}{T'} \ . \tag{112}$$

$\diamond\diamond$

Proof of this formula:

From $F = E - TS$ and $S = -\frac{dF}{dT}|_V$ one has

$$E(T) = -T^2 \frac{d}{dT} \frac{F(T)}{T} \tag{113}$$

from which one obtains eqn (112) by integration. Differentiating (112) gives (113).

$\diamond\diamond$

In order to see how the intrinsic energy per lattice site can be calculated explicitly, consider the quantity

$$B_i^{C,A} = \langle A_i [C_i, H]_- \rangle, \tag{114}$$

where A_i and C_i are the spin operators necessary for constructing equations of motion for those Green's functions from which the moments $\langle (S^z)^n \rangle$ $(n = 1, ..., 2S)$ are calculated. S is the spin quantum number. The quantity (114) can on one hand be related to the relevant Green's functions and on the other hand be calculated explicitly by evaluating the commutator. This leads to a set of equations from which, together with equation (110), the intrinsic energy can be calculated.

The connection to the Green's function results from the spectral theorem:

$$\begin{aligned} B_i^{C,A} &= \langle A_i [C_i, H]_- \rangle = i \frac{d}{dt} \langle A_i(t') C_i(t) \rangle |_{t=t'} \\ &= i \frac{d}{dt} \lim_{\delta \to 0} \frac{1}{N} \sum_{\mathbf{k}} \frac{i}{2\pi} \int \frac{d\omega}{e^{\beta\omega} - 1} (G_{\mathbf{k}}^{C,A}(\omega + i\delta) - G_{\mathbf{k}}^{C,A}(\omega - i\delta)) e^{-i\omega(t-t')} |_{t=t'} \\ &= \lim_{\delta \to 0} \frac{1}{N} \sum_{\mathbf{k}} \frac{i}{2\pi} \int \frac{\omega d\omega}{e^{\beta\omega} - 1} \Big(G_{\mathbf{k}}^{C,A}(\omega + i\delta) - G_{\mathbf{k}}^{C,A}(\omega - i\delta) \Big) \ . \end{aligned} \tag{115}$$

In Appendix 7.1, we treat explicitly the cases for spin $S = 1/2$ and $S = 1$ for a Heisenberg Hamiltonian with an external field and a single-ion anisotropy. For S=1/2, one needs $A_i = S_i^-$ and $C_i = S_i^+$; for S=1, one needs a) $A_i = S_i^-$ and $C_i = S_i^+$ and b) $A_i = S_i^-$ and $C_i = (2S_i^z - 1)S_i^+$.

4. The GF formalism for Heisenberg films

This chapter starts in Section 4.1 with the example of a spin $S = 1/2$ ferromagnetic Heisenberg monolayer in a magnetic field [14]. This is an exercise in applying the GF formalism in a simple case. The Tyablicov (RPA) and Callen decouplings are introduced, the limit of mean field theory (MFT) is discussed, the Mermin-Wagner theorem is proved for this case, and the effective (temperature-dependent) single-ion anisotropy is calculated by thermodynamic perturbation theory.

In Section 4.2, ferromagnetic Heisenberg films with anisotropies and general spin S are treated. For the single-ion anisotropy, the Anderson-Callen decoupling is used. The exchange anisotropy is treated by a generalized Tyablikov decoupling. Susceptibilities are calculated. It is also shown how the single-ion anisotropy can be treated exactly. As a further application, it is shown that spin waves are very important for treating a trilayer in which two ferromagnets are separated by a non-magnetic layer. Finally, the temperature dependence of the interlayer coupling is discussed.

Section 4.3 deals with a unified treatment of ferromagnetic (FM), antiferromagnetic (AFM) and coupled ferromagnetic-antiferromagnetic (FM-AFM) Heisenberg films.

4.1. The ferromagnetic Heisenberg monolayer in a magnetic field

We choose this example because it illustrates the GF formalism in a simple case and allows the validity of the different approximations within the formalism to be checked against 'exact' Quantum Monte Carlo (QMC) calculations [15].

The Heisenberg Hamiltonian for a ferromagnetic monolayer in a magnetic field is

$$\begin{aligned} H &= -\frac{1}{2}\sum_{<kl>} J_{kl}\mathbf{S}_k\mathbf{S}_l - B\sum_l S_l^z \\ &= -\frac{1}{2}\sum_{<kl>} J_{kl}(S_k^- S_l^+ + S_k^z S_l^z) - B\sum_l S_l^z. \end{aligned} \tag{116}$$

Here J_{kl} is the exchange interaction strength, k and l are lattice site indices, and $< kl >$ means summation over nearest neighbours only. The magnetic field B is assumed to be in the z-direction perpendicular to the film xy-plane . The second line of eqn (116) is obtained with the usual definition $S_k^{\pm} = S_k^x \pm iS_k^y$ in terms of the components of the spin operators.

For spin $S = 1/2$, the magnetization is obtained from the relation

$$\langle S_i^z\rangle = 1/2 - \langle S_i^- S_i^+\rangle, \tag{117}$$

and the correlation $\langle S_i^- S_i^+ \rangle$ is determined via the spectral theorem from the commutator GF

$$G_{ij,\eta=-1}(\omega) = \langle\langle S_i^+; S_j^- \rangle\rangle. \tag{118}$$

The GF is determined from the equation of motion in energy space

$$\omega \langle\langle S_i^+; S_j^- \rangle\rangle = \langle [S_i^+, S_j^-] \rangle + \langle\langle [S_i^+, H]_-; S_j^- \rangle\rangle \ . \tag{119}$$

Using spin commutator relations, one obtains

$$[S_i^+, H]_- = B S_i^+ - \sum_i J_{il} (S_i^z S_l^+ - S_l^z S_i^+). \tag{120}$$

The equation of motion is then

$$(\omega - B) \langle\langle S_i^+; S_j^- \rangle\rangle = 2 \langle S_i^z \rangle \delta_{ij} - \sum_l J_{il} \Big(\langle\langle S_i^z S_l^+; S_j^- \rangle\rangle - \langle\langle S_l^z S_i^+; S_j^- \rangle\rangle \Big) \ , \tag{121}$$

which is exact as it stands but, in order to use the equation, the higher-order Green's functions on the right hand side must be decoupled.

4.1.1. The Tyablikov (RPA)-decoupling

This decoupling, introduced by Tyablikov [16], is often called the random phase approximation (RPA) because it is equivalent to that approximation in other areas of physics. It consists in factoring the higher-order Green's functions:

$$\begin{aligned} \langle\langle S_i^z S_l^+; S_j^- \rangle\rangle &\simeq \langle S_i^z \rangle \langle\langle S_l^+; S_j^- \rangle\rangle = \langle S_i^z \rangle G_{lj}, \\ \langle\langle S_l^z S_i^+; S_j^- \rangle\rangle &\simeq \langle S_l^z \rangle \langle\langle S_i^+; S_j^- \rangle\rangle = \langle S_l^z \rangle G_{ij}. \end{aligned} \tag{122}$$

There is no a priori justification for this factorization but it has turned out to be successful, also in other areas of physics where the resulting equations can be derived with methods different from Green's function theory. In the present context, the quality of this approximation can be checked against 'exact' QMC results [15], see Section 4.1.5.

For a ferromagnet, there is translational invariance for the magnetization at different lattice sites: $\langle S_i^z \rangle = \langle S_l^z \rangle = \langle S^z \rangle$. After the decoupling, the equation of motion is

$$(\omega - B - \langle S^z \rangle \sum_l J_{il}) G_{ij}(\omega) + \langle S^z \rangle \sum_l J_{il} G_{lj}(\omega) = 2 \langle S^z \rangle \delta_{ij}. \tag{123}$$

A Fourier transform to momentum space (32) yields

$$\Big(\omega - B - \langle S^z \rangle (J_0 - J_{\mathbf{k}})\Big) G_{\mathbf{k}}(\omega) = 2 \langle S^z \rangle, \tag{124}$$

and the Green's has the pole structure

$$G_{\mathbf{k}}(\omega) = \frac{2\langle S^z\rangle}{\omega - \omega_{\mathbf{k}}^{RPA}}, \tag{125}$$

with the dispersion relation

$$\omega_{\mathbf{k}}^{RPA} = B + \langle S^z\rangle(J_0 - J_{\mathbf{k}}). \tag{126}$$

For a square lattice with the number of nearest neighbours $z = 4$ and a lattice constant unity, one has

$$\begin{aligned} J_0 &= \frac{1}{N}\sum_{ij} J_{ij} e^{i(\mathbf{k}=0)(\mathbf{R}_i - \mathbf{R}_j)} = zJ = 4J, \\ J_{\mathbf{k}} &= \frac{1}{N}\sum_{ij} J_{ij} e^{i\mathbf{k}(\mathbf{R}_i - \mathbf{R}_j)} = 2J(\cos k_x + \cos k_y). \end{aligned} \tag{127}$$

Applying the spectral theorem (42) – there is no zero eigenvalue – and performing the ω-integration with the relation

$$\frac{1}{\omega - \omega_{\mathbf{k}} \pm i\eta} = P\frac{1}{\omega - \omega_{\mathbf{k}}} \mp i\pi\delta(\omega - \omega_{\mathbf{k}}) \tag{128}$$

yields for the magnetization $\langle S^z\rangle$ of the spin $S = 1/2$ monolayer

$$\begin{aligned} \langle S_i^z\rangle &= \frac{1}{2} - \langle S_i^- S_i^+\rangle \\ &= \frac{1}{2} - \lim_{\delta\to 0}\frac{1}{N}\sum_{\mathbf{k}}\frac{i}{2\pi}\int_{-\infty}^{\infty}\frac{G_{\mathbf{k}}(\omega + i\delta) - G_{\mathbf{k}}(\omega - i\delta)}{e^{\beta\omega} - 1} \\ &= \frac{1}{2} - \frac{1}{N}\sum_{\mathbf{k}}\frac{2\langle S^z\rangle}{e^{\beta\omega_{\mathbf{k}}^{RPA}} - 1} \\ &= \frac{1}{2} - \frac{1}{\pi^2}\int_0^{\pi} dk_x \int_0^{\pi} dk_y \frac{2\langle S^z\rangle}{e^{\beta\omega_{\mathbf{k}}^{RPA}} - 1}, \end{aligned} \tag{129}$$

where the sum over the momenta has been replaced by an integration over the first Brillouin zone of the square lattice.

With the relation $\frac{2}{e^x - 1} = \coth(x/2) - 1$, one obtains the following expression for the magnetization

$$\langle S^z\rangle = [\frac{2}{\pi^2}\int_0^{\pi} dk_x \int_0^{\pi} dk_y \coth(\frac{\beta\omega_{\mathbf{k}}^{RPA}}{2})]^{-1}. \tag{130}$$

This equation must be iterated to self-consistency in $\langle S^z\rangle$, which can then be compared with QMC (see Section 4.1.5).

4.1.2. The Callen decoupling

In this section, we discuss an attempt of Callen [17] to improve the RPA. We do this because it is the basis of an approximate decoupling of the terms stemming from

the single-ion anisotropy (see Section 4.2.1). This generalisation of the Tyablikov (RPA) decoupling results from the ansatz

$$\langle\langle S_i^z S_l^+; S_j^-\rangle\rangle \simeq \langle S_i^z\rangle\langle\langle S_l^+; S_j^-\rangle\rangle - \alpha\langle S_i^- S_l^+\rangle\langle\langle S_i^+; S_j^-\rangle\rangle, \tag{131}$$

with $\alpha = \frac{\langle S^z\rangle}{2S^2}$; $\alpha \to 0$ corresponds to the Tyablikov (RPA) decoupling. Inserting this expression into the equation of motion and applying the spectral theorem leads again to a single-pole expression for the Green's function with a modified dispersion relation. The spectral theorem yields

$$\langle S^z\rangle = \Big[\frac{2}{\pi^2}\int_0^\pi dk_x \int_0^\pi dk_y \coth(\frac{\beta\omega_{\mathbf{k}}^{Callen}}{2})\Big]^{-1}, \tag{132}$$

with

$$\omega_{\mathbf{k}}^{Callen} = B + \langle S^z\rangle\Big(J_0 - J_{\mathbf{k}}\Big)\Big(1 + \frac{\alpha}{\pi^2}\int_0^\pi dk_x \int_0^\pi dk_y \frac{J_{\mathbf{k}}}{J_0}\coth(\frac{\beta\omega_{\mathbf{k}}^{Callen}}{2})\Big). \tag{133}$$

Again, eqn (132) must be iterated to self-consistency in $\langle S^z\rangle$. Although it takes some higher-order correlations are into account, the Callen approach is worse than RPA for the present case but still much better than a mean field (MFT) result (see Section 4.1.5).

$\diamond\diamond$

Derivation of the Callen dispersion relation (133).

In order to make the Callen decoupling plausible, consider two equivalent formulas for spin $S = 1/2$

$$\begin{aligned} S_i^z &= S - S_i^- S_i^+, \\ S_i^z &= \frac{1}{2}(S_i^+ S_i^- - S_i^- S_i^+). \end{aligned} \tag{134}$$

Multiplying the first equation by α and the second by $(1-\alpha)$, one can write the Green's function $\langle\langle S_i^z S_l^+; S_j^-\rangle\rangle$in the following form:

$$\langle\langle S_i^z S_l^+; S_j^-\rangle\rangle = \alpha S\langle\langle S_l^+; S_j^-\rangle\rangle + \frac{1}{2}(1-\alpha)\langle\langle S_i^+ S_i^- S_l^+; S_j^-\rangle\rangle - \frac{1}{2}(1+\alpha)\langle\langle S_i^- S_i^+ S_l^+; S_j^-\rangle\rangle. \tag{135}$$

Now factorize the Green's functions on the right hand side as follows:

$$\begin{aligned} \langle\langle S_i^+ S_i^- S_l^+; S_j^-\rangle\rangle &\simeq \langle S_i^+ S_i^-\rangle\langle\langle S_l^+; S_j^-\rangle\rangle + \langle S_i^+ S_l^+\rangle\langle\langle S_i^-; S_j^-\rangle\rangle + \langle S_i^- S_l^+\rangle\langle\langle S_i^+; S_j^-\rangle\rangle, \\ \langle\langle S_i^- S_i^+ S_l^+; S_j^-\rangle\rangle &\simeq \langle S_i^- S_i^+\rangle\langle\langle S_l^+; S_j^-\rangle\rangle + \langle S_i^- S_l^+\rangle\langle\langle S_i^+; S_j^-\rangle\rangle + \langle S_i^+ S_l^+\rangle\langle\langle S_i^-; S_j^-\rangle\rangle. \end{aligned} \tag{136}$$

Approximating the terms non-diagonal in the z-component of the spin by $\langle S_i^+ S_l^+\rangle \simeq 0$ and using the relation $\langle S_i^+ S_i^-\rangle = 2\langle S_i^z\rangle + \langle S_i^- S_i^+\rangle$, we obtain

$$\langle\langle S_i^z S_l^+; S_j^-\rangle\rangle \simeq \langle S_i^z\rangle\langle\langle S_l^+; S_j^-\rangle\rangle - \alpha\langle S_i^- S_l^+\rangle\langle\langle S_i^+; S_j^-\rangle\rangle, \tag{137}$$

which is expression (131). Taking $\alpha = \frac{\langle S^z \rangle}{S}$ interpolates between the case $\alpha = 1$, where the first of the equations (134) should be used for the decoupling at low temperatures ($\langle S^z \rangle \simeq S$), and $\alpha = 0$, where the second formula should be used ($\langle S^z \rangle \simeq 0$). For arbitrary spins, arguments in favor of $\alpha = \frac{\langle S^z \rangle}{2S^2}$ (which includes the spin $S = 1/2$ case) are given in [17].

Introducing the decoupling (137) into the equation of motion (121) yields

$$\Big(\omega - B - \langle S^z \rangle \sum_l J_{il} - \alpha \sum_l J_{il} \langle S_i^- S_l^+ \rangle\Big) G_{ij}(\omega)$$
$$+\Big(\langle S^z \rangle \sum_l J_{il} + \alpha \sum_l J_{il} \langle S_l^- S_i^+ \rangle\Big) G_{lj}(\omega) = 2\delta_{ij} \langle S^z \rangle. \tag{138}$$

A Fourier transform to momentum space leads to

$$\Big[\omega - B - \langle S^z \rangle (J_0 - J_{\mathbf{k}}) - \alpha \frac{1}{N} \sum_{\mathbf{q}} (J_{\mathbf{q}} - J_{\mathbf{q}+\mathbf{k}}) \langle S^- S^+ \rangle_{\mathbf{q}}\Big] G_{\mathbf{k}}(\omega) = 2\langle S^z \rangle, \tag{139}$$

where the Green's function is given by

$$G_{\mathbf{k}}(\omega) = \frac{2\langle S^z \rangle}{\omega - \omega_{\mathbf{k}}^{Callen}} \tag{140}$$

with

$$\omega_{\mathbf{k}}^{Callen} = B + \langle S^z \rangle (J_0 - J_{\mathbf{k}}) + \alpha \frac{1}{N} \sum_{\mathbf{q}} (J_{\mathbf{q}} - J_{\mathbf{q}+\mathbf{k}}) \langle S^- S^+ \rangle_{\mathbf{q}}. \tag{141}$$

The spectral theorem then determines

$$\langle S^- S^+ \rangle_{\mathbf{k}} = \frac{i}{2\pi} \lim_{\delta \to 0} \int_{-\infty}^{\infty} \frac{d\omega}{e^{\beta\omega} - 1} (G_{\mathbf{k}}(\omega + i\delta) - G_{\mathbf{k}}(\omega - i\delta) = 2\langle S^z \rangle \Phi_{\mathbf{k}}. \tag{142}$$

with

$$\Phi_{\mathbf{k}} = \frac{1}{e^{\beta\omega_{\mathbf{k}}^{Callen}} - 1} = \tfrac{1}{2}\Big(\coth(\tfrac{\beta\omega_{\mathbf{k}}^{Callen}}{2}) - 1\Big). \tag{143}$$

It remains to simplify the term proportional to α in the dispersion relation:

$$\begin{aligned} & 2\alpha \langle S^z \rangle \frac{1}{N} \sum_{\mathbf{q}} (J_{\mathbf{q}} - J_{\mathbf{q}+\mathbf{k}}) \Phi_{\mathbf{q}} \\ = \;& 2\alpha \langle S^z \rangle \frac{1}{N} \sum_{ij} J_{ij} (1 - e^{i\mathbf{k}(\mathbf{R}_i - \mathbf{R}_j)}) \frac{1}{N} \sum_{\mathbf{q}} e^{i\mathbf{q}(\mathbf{R}_i - \mathbf{R}_j)} \Phi_{\mathbf{q}} \\ = \;& 2\alpha \langle S^z \rangle (J_0 - J_{\mathbf{k}}) \frac{1}{N} \sum_{\mathbf{q}} \frac{J_{\mathbf{q}}}{J_0} \Phi_{\mathbf{q}}, \end{aligned} \tag{144}$$

where we have made use of

$$\frac{1}{N} \sum_{\mathbf{q}} e^{i\mathbf{q}(\mathbf{R}_i - \mathbf{R}_j)} \Phi_{\mathbf{q}} = \frac{1}{N} \sum_{\mathbf{q}} \frac{J}{zJ} \sum_{<ij>} e^{i\mathbf{q}(\mathbf{R}_i - \mathbf{R}_j)} \Phi_{\mathbf{q}} = \frac{1}{N} \sum_{\mathbf{q}} \frac{J_{\mathbf{q}}}{J_0} \Phi_{\mathbf{q}} \;, \tag{145}$$

and z is the number of nearest neighbours. This completes the proof for the Callen dispersion relation.

$\diamond\diamond$

In Ref. [17], Callen also derives a closed form expression for the magnetization for general spin S from the solution of a differential equation. The result is

$$\langle S^z \rangle = \frac{(S - \Phi_{\mathbf{k}})(1 + \Phi_{\mathbf{k}})^{(2S+1)} + (S + 1 + \Phi_{\mathbf{k}})\Phi_{\mathbf{k}}^{(2S+1)}}{(1 + \Phi_{\mathbf{k}})^{(2S+1)} - \Phi_{\mathbf{k}}^{(2S+1)}} \ , \tag{146}$$

a formula which was also found by Pravecki [18]. For the treatment of general spin S, see also Refs. [19].

4.1.3. Mean field theory (MFT)

In mean field theory (MFT), which is frequently used as the simplest approximation, one neglects correlations which lead to collective excitations (magnons). The essential approximation consists in writing operator products as

$$\begin{aligned} S_i^\alpha S_j^\beta &= (S_i^\alpha - \langle S_i^\alpha \rangle)(S_j^\beta - \langle S_j^\beta \rangle) + S_i^\alpha \langle S_j^\beta \rangle + \langle S_i^\alpha \rangle S_j^\beta - \langle S_i^\alpha \rangle \langle S_j^\beta \rangle \\ &\simeq S_i^\alpha \langle S_j^\beta \rangle + \langle S_i^\alpha \rangle S_j^\beta - \langle S_i^\alpha \rangle \langle S_j^\beta \rangle, \end{aligned} \tag{147}$$

where the mean field assumptions $S_i^\alpha \simeq \langle S_i^\alpha \rangle$ and $S_j^\beta \simeq \langle S_j^\beta \rangle$ have been made. Neglecting transverse expectation values ($\langle S_j^\pm \rangle = 0$) as well leads to the mean field Hamiltonian

$$H^{MFT} = -\sum_{kl} J_{kl} \langle S_k^z \rangle S_l^z - B \sum_l S_l^z + \frac{1}{2} \sum_{kl} \langle S_k^z \rangle \langle S_l^z \rangle, \tag{148}$$

where the last term, being a constant, does not influence the equations of motion but has to be taken into account when calculating the intrinsic energy.

In Green's function theory, the Hamiltonian H^{MFT} leads without further approximations to the equations of motion

$$(\omega - B - \langle S^z \rangle \sum_k J_{ik}) G_{ij} = 2 \langle S^z \rangle \delta_{ij} \ , \tag{149}$$

whose Fourier transform to momentum space is

$$(\omega - B - \langle S^z \rangle J_0) G_{\mathbf{k}}(\omega) = 2 \langle S^z \rangle, \tag{150}$$

where $J_0 = zJ$ (z is the number of nearest neighbours; $z = 4$ for a square lattice) and

$$G_{\mathbf{k}}(\omega) = \frac{2 \langle S^z \rangle}{\omega - \omega^{MFT}} \ , \tag{151}$$

with a momentum-independent dispersion relation

$$\omega^{MFT} = B + \langle S^z \rangle J_0. \tag{152}$$

Because there is no momentum dependence in this relation, the k-integration in the spectral theorem is trivial, so that

$$\langle S^z \rangle = \frac{1}{2} - \langle S^- S^+ \rangle = \frac{1}{2} - \frac{1}{N} \sum_{\mathbf{k}} \frac{2\langle S^z \rangle}{e^{\beta\omega^{MFT}} - 1} = \frac{1}{2} - \frac{2\langle S^z \rangle}{e^{\beta\omega^{MFT}} - 1} \ , \tag{153}$$

from which

$$\langle S^z \rangle = \frac{1}{2} \tanh(\frac{\beta\omega^{MFT}}{2}). \tag{154}$$

This result is obtained from the RPA result by setting $J_{\mathbf{k}}$ to zero in eqn (126), thereby neglecting the **k**-dependence of the lattice. In MFT, it is only the number of nearest neighbours z that count. This is also true for the more complicated cases discussed later. The neglect of the **k**-dependence (this corresponds to the neglect of magnons) makes MFT much worse than RPA, as seen in Fig. 1 of Section 4.1.5 .

Because MFT is easily applied, often with qualitatively reasonable results, we quote a few papers where MFT is extensively used: in Refs. [20] and [21] and references therein, the spin reorientation transition is treated and effective (temperature-dependent) lattice anisotropy coeefficients are calculated; in Ref. [78], coupled ferro-antiferromagnetic layers are treated.

4.1.4. The Mermin-Wagner theorem

Mermin and Wagner [22] have shown quite generally that the pure Heisenberg model (without magnetic field and anisotropies) in less than 3 dimensions does not exhibit collective order at finite temperatures (for $\langle S^z \rangle \to 0$ the Curie temperature goes to 0: $T_{\text{Curie}} \to 0$).

From the expressions derived above, we can see that RPA obeys the theorem whereas MFT violates it. Expanding the RPA expression for the magnetization (130) for small $\langle S^z \rangle$ and $B = 0$, one obtains an expression for the Curie temperature

$$T_{\text{Curie}}^{RPA} = \frac{1}{\sum_{\mathbf{k}} \frac{2}{J_0 - J_{\mathbf{k}}}} \simeq \frac{1}{\frac{2}{2\pi^2} \int_0^\pi dk_x \int_0^\pi dk_y \frac{2}{J_0 - J_{\mathbf{k}}}} \propto \frac{1}{\int_0^\pi dk_x \int_0^\pi \frac{1}{k_x^2 + k_y^2}} \to 0 \ . \tag{155}$$

This is so because the integral diverges at the lower boundary, which can be seen by expanding the square lattice dependence of $J_{\mathbf{k}}$, eqn (127), for small momenta. This means that the Mermin-Wagner theorem is obeyed in RPA. In three dimensions, the RPA expression gives a finite value for the Curie temperature and is used in ab initio calculations of the Heisenberg exchange interaction to determine the Curie temperature, see e.g. [23].

Calculating the Curie temperature from the MFT result (154) for $B = 0$ by expanding for small $\langle S^z \rangle$ gives a finite Curie temperature

$$T_{\text{Curie}}^{MFT} = \frac{1}{4} J_0 = \frac{1}{4} z J = J \ , \tag{156}$$

where we have taken $z = 4$, the number of nearest neighbours for a square lattice. This is in clear violation of the theorem.

4.1.5. Comparing with Quantum Monte Carlo calculations

In this section, we compare the temperature dependence of the magnetization of a ferromagnetic spin $S = 1/2$ Heisenberg monolayer on a square lattice obtained with the approximations just described with quantum Monte Carlo (QMC) calculations [15], which are 'exact' within their statistical errors. The results are shown in Fig.1. The RPA of Section 4.1.1 is the best and is a fairly good approximation. Before QMC calculations were available, it was not possible to check the quality of RPA. Although there are additional correlations taken into account in the Callen approach of Section 4.1.2, its results for spin $S = 1/2$ are not as good as those from simple RPA. In Ref. [17], Callen argues that his decoupling should give better results for larger spin values, but there are no QMC calculations available to support his statements. The mean field theory (MFT) of Section 4.1.3 yields by far the worst results. This results from not taking collective excitations (magnons) into account, which is also the reason for the violation of the Mermin-Wagner theorem.

We mention that RPA gives still better results for the magnetization when higher-order Green's functions with vertex corrections for their decoupling are included [85]. For quantities with transverse correlations, like the intrinsic energy or the specific heat, one has to go beyond RPA. See Section 5, in particular Ref. [85].

4.1.6. The effective (temperature dependent) single-ion lattice anisotropy

Lattice anisotropy coefficients are defined in an expansion of the free energy in powers of $\cos\theta$ [24], where θ is the polar angle between the magnetization $\langle \mathbf{S} \rangle$ and the normal to the film plane

$$F(T,\theta) = F_0(T) - K_2(T)\cos\theta - K_4(T)\cos^4\theta - \mathbf{B}\cdot\langle\mathbf{S}\rangle \ . \tag{157}$$

The anisotropy coefficients can be calculated by thermodynamic perturbation theory, where the Hamiltonian $H = H_0 + V$ is separated into an unperturbed part H_0 consisting of the exchange coupling and the magnetic field and a perturbation $V_n = -K_n \sum_l (S_l^z)^n$ (n=2,4). Within first order perturbation theory, effective anisotropy coefficients can be defined as

$$\mathcal{K}_n(T) = K_n f_n(T) \ , \tag{158}$$

where the temperature dependence is introduced by the functions $f_n(T)$ which are expressed in terms of expectation values $\langle (S^z)^n \rangle_0$ for the unperturbed Hamiltonian

$$f_2(T) \ = \ \tfrac{1}{2}\Big(3\langle (S^z)^2\rangle_0 - S(S+1)\Big) \ , \tag{159}$$

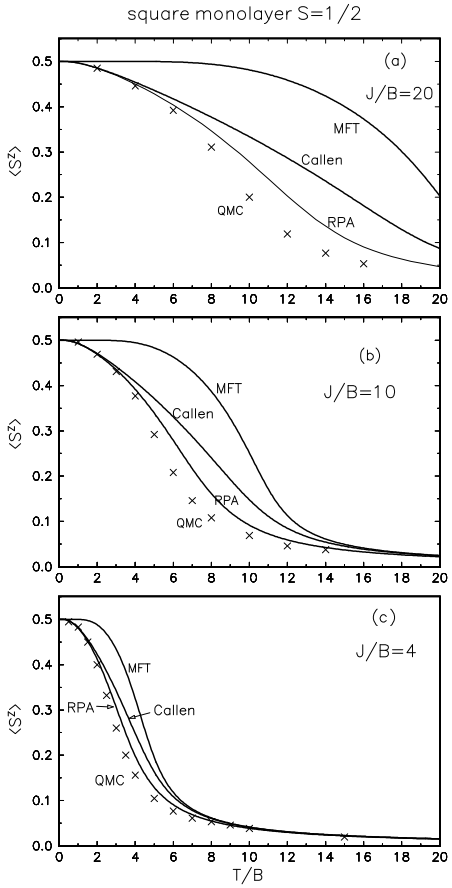

Figure 1: The temperature dependence of the magnetization of a ferromagnetic Heisenberg monolayer for a square lattice with spin $S = 1/2$. Comparison between the 'exact' quantum Monte Carlo (QMC) result [15] and the results obtained with MFT, RPA and Callen decoupling. We have used (a) J/B=20, (b) J/B=10 and (c) J/B=4 (from reference [14]).

$$f_4(T) \;=\; \tfrac{1}{8}[35\langle(S^z)^4\rangle_0 - (30S(S+1)-25)\langle(S^z)^2\rangle_0 + 3S(S+1)(S(S+1)-2)] \; .$$

The moments are calculated with RPA and MFT in Ref. [14] and the resulting temperature dependent coefficients are shown in Fig. (2) for $S = 2$ and $S = 10$, where $K_n = 1$ and a scaling $J \to J/S(S+1)$ and $B \to B/S$ has been used. The resulting behaviour of the $\mathcal{K}_n(T)$ calculated by RPA differs markedly from that obtained by MFT particularly at low temperatures: whereas the $\mathcal{K}_n(T)$ obtained with MFT show an exponential decay in this temperature range, those calculated from RPA decrease more rapidly and exhibit a nearly linear behaviour. The $\mathcal{K}(T)$ calculated with RPA exhibit a much weaker dependence on the spin S than those calculated with MFT.

In Section 4.2.2 we show that it is better to calculate the effective anisotropy

coefficients *non-perturbatively* by minimizing the free energy with repect to the re-orientation angle.

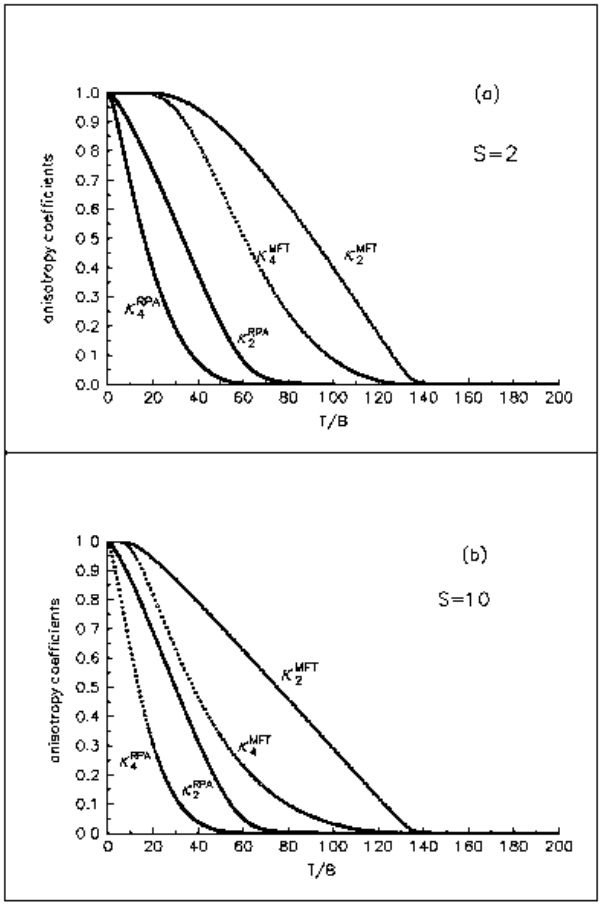

Figure 2: The temperature dependence of the effective lattice anisotropy coefficients $\mathcal{K}_2(T)$ and $\mathcal{K}_4(T)$ of a square Heisenberg monolayer calculated with thermodynamic perturbation theory for MFT and RPA. We have used $J/B = 100$ and (a) $S = 2$ and (b) $S = 10$. To allow for comparison between different spin values, we used the scaling $J \to J/S(S+1)$ and $B \to B/S$.

4.2. Ferromagnetic Heisenberg films with anisotropies for general spin S

An isotropic Heisenberg model in less than three dimensions does not show spontaneous magnetization at finite temperature, as explained by the Mermin-Wagner theorem [22]. Such an idealized system does not, however, exist in nature, since even the smallest anisotropy leads to a finite magnetization. This can be caused by an external magnetic field (as shown in the previous chapter), single-ion anisotropies, exchange anisotropies, or the magnetic dipole-dipole interaction.

Many applications of GF-theory deal only with the magnetization in one direction of space. They treat multi-layers but not all use the full power of the eigenvector method outlined in Section 3.3. We mention only a few. Diep-The-Huang et al. [25] treat ferro- and antiferromagnetic multilayers but, instead of the eigenvector method, they use Kramers rule for calculating the GF's. Schiller and Nolting [26] treat sc(100) and fcc(100) ferromagnetic Heisenberg spins with $S = 7/2$ using RPA for the exchange interaction and the Lines decoupling [29] for the single-ion anisotropy. C. Cucci et al. [27] consider fcc (100), (110) and (111) ferromagnetic Heisenberg films using RPA, the Lines decoupling and the eigenvector method.

In the following, we do not restrict the magnetization to be in one direction of space because we are interested in the reorientation of the magnetization as a function of the temperature and film thickness. Therefore, we deal from the outset with a multi-dimensional case; the orientation of the magnetization in one direction and the monolayer then occur naturally as special cases. An essential complication connected with the reorientation problem is the occurrence of zero eigenvalues of the equation-of-motion matrix, which can be handled with the techniques developed in Section 3.

We do not discuss papers dealing with the magnetic reorientation on the basis of a boson expansion, as e.g. Refs. [30, 31] who start with a Holstein-Primakoff transformation in lowest order, because the validitity of a linearized spin wave theory is limited to low temperatures only.

4.2.1. The Hamiltonian and the decoupling procedures

We consider a spin Hamiltonian consisting of an isotropic Heisenberg exchange interaction with strength J_{kl} between nearest neighbour lattice sites, an exchange anisotropy with strength D_{kl}, a second-order single-ion lattice anisotropy with strength $K_{2,k}$, a magnetic dipole coupling with strength g_{kl} and an external magnetic field

$\mathbf{B} = (B^x, B^y, B^z)$:

$$\begin{aligned}\mathcal{H} = & - \frac{1}{2}\sum_{<kl>} J_{kl}(S_k^- S_l^+ + S_k^z S_l^z) - \frac{1}{2}\sum_{<kl>} D_{kl} S_k^z S_l^z - \sum_k K_{2,k}(S_k^z)^2 \\ & - \sum_k \Big(\frac{1}{2}B^- S_k^+ + \frac{1}{2}B^+ S_k^- + B^z S_k^z\Big) \\ & + \frac{1}{2}\sum_{kl}\frac{g_{kl}}{r_{kl}^5}\Big(r_{kl}^2(S_k^- S_l^+ + S_k^z S_l^z) - 3(\mathbf{S}_k\mathbf{r}_{kl})(\mathbf{S}_l\mathbf{r}_{kl})\Big). \end{aligned} \tag{160}$$

Here the notation $S_k^{\pm} = S_k^x \pm iS_k^y$ and $B^{\pm} = B^x \pm iB^y$ is introduced, where k and l are lattice site indices and $< kl >$ indicates summation over nearest neighbours only.

In order to treat the spin reorientation transition for general spin S, we need the following Green's functions:

$$G_{ij,\eta}^{\alpha,mn}(\omega) = \langle\langle S_i^{\alpha}; (S_j^z)^m (S_j^-)^n\rangle\rangle_{\omega,\eta} \ , \tag{161}$$

where $\alpha = (+,-,z)$ takes care of all directions in space, $\eta = \pm 1$ refers to the anti-commutator or commutator Green's functions respectively, and $n \geq 1$, $m \geq 0$ ($m + n \leq 2S + 1$) are positive integers. We follow the formalism of Section 3 by evaluating all formulas for the Hamiltonian (160).

The exact equations of motion

$$\omega G_{ij,\eta}^{\alpha,mn}(\omega) = A_{ij,\eta}^{\alpha,mn} + \langle\langle [S_i^{\alpha}, \mathcal{H}]_-; (S_j^z)^m (S_j^-)^n\rangle\rangle_{\omega,\eta} \tag{162}$$

with the inhomogeneities

$$A_{ij,\eta}^{\alpha,mn} = \langle [S_i^{\alpha}, (S_j^z)^m (S_j^-)^n]_{\eta}\rangle \tag{163}$$

are given explicitly by

$$\begin{aligned}\omega G_{ij,\eta}^{\pm,mn} &= A_{ij,\eta}^{\pm,mn} \\ &\quad \mp \sum_k J_{ik}\Big(\langle\langle S_i^z S_k^{\pm}; (S_j^z)^m (S_j^-)^n\rangle\rangle - \langle\langle S_k^z S_i^{\pm}; (S_j^z)^m (S_j^-)^n\rangle\rangle\Big) \\ &\quad \pm \sum_k D_{ik}\langle\langle S_k^z S_i^{\pm}; (S_j^z)^m (S_j^-)^n\rangle\rangle \\ &\quad \pm K_{2,i}\langle\langle (S_i^{\pm} S_i^z + S_i^z S_i^{\pm}); (S_j^z)^m (S_j^-)^n\rangle\rangle \\ &\quad \mp B^{\pm} G_{ij,\eta}^{z,mn} \pm B^z G_{ij,\eta}^{\pm,mn} \ , \\ \omega G_{ij,\eta}^{z,mn} &= A_{ij(\eta)}^{z,mn} \\ &\quad + \frac{1}{2}\sum_k J_{ik}\langle\langle (S_i^- S_k^+ - S_k^- S_i^+); (S_j^z)^m (S_j^-)^n\rangle\rangle \\ &\quad - \frac{1}{2}B^- G_{ij,\eta}^{+,mn} + \frac{1}{2}B^+ G_{ij,\eta}^{-,mn}. \end{aligned} \tag{164}$$

For the moment, we leave out the terms due to the dipole-dipole interaction, which we include later.

Once these equations are solved, the components of the magnetization can be determined from the Green's functions via the spectral theorem. A closed system of equations results from decoupling the higher-order Green's functions on the right-hand sides. For the exchange interaction and exchange anisotropy terms, we use a generalized Tyablikov- (or RPA-) decoupling:

$$\langle\langle S_i^\alpha S_k^\beta; (S_j^z)^m (S_j^-)^n \rangle\rangle_\eta \simeq \langle S_i^\alpha \rangle G_{kj,\eta}^{\beta,mn} + \langle S_k^\beta \rangle G_{ij,\eta}^{\alpha,mn}. \tag{165}$$

The terms stemming from the single-ion anisotropy have to be decoupled differently, because RPA decoupling leads to unphysical results; e.g. for spin $S = 1/2$, the terms due to the single-ion anisotropy do not vanish in RPA as they should do because, in this case, $\sum_i K_{2,i} \langle (S_i^z)^2 \rangle$ is a constant and does not influence the equations of motion. In the appendix of Ref. [28], we investigate different decoupling schemes proposed in the literature, e.g. those of Lines [29] or that of Anderson and Callen [32]. These should be reasonable for single-ion anisotropies small compared to the exchange interaction. We found the Anderson-Callen decoupling to be most adequate in our context. It treats the diagonal terms as they occur from the single-ion anisotropy in the same way that Callen [17] used in his attempt to improve the RPA. Consider eqn (131) for $i = l$: add the term for $\langle\langle S_i^z S_i^+; ... \rangle\rangle$ and do the same for the corresponding expressions for $G^{-,mn}$. Using $S_i^\mp S_i^\pm = S(S+1) \mp S_i^z - S_i^z S_i^z$, one obtains

$$\begin{aligned} &\langle\langle (S_i^\pm S_i^z + S_i^z S_i^\pm); (S_j^z)^m (S_j^-)^n \rangle\rangle_\eta \\ &\simeq 2\langle S_i^z \rangle \Big(1 - \frac{1}{2S^2}[S(S+1) - \langle S_i^z S_i^z \rangle]\Big) G_{ij,\eta}^{\pm,mn}. \end{aligned} \tag{166}$$

This term vanishes for $S = 1/2$ as it should.

In Section 4.2.5, we shall demonstrate a procedure for treating the single-ion anisotropy exactly by going to higher-order Green's functions. With this, single-ion anisotropies with arbitrary strength can be treated. This procedure is, however, tedious to apply for spins $S > 1$, whereas there is no problem when staying at the level of the lowest-order Green's function as discussed in the present section.

Applying the decouplings (165) and (166) and a Fourier transform to momentum space, one obtains, for a ferromagnetic film with N layers, $3N$ equations of motion which can be written in compact matrix notation as

$$(\omega \mathbf{1} - \mathbf{\Gamma}) \mathbf{G}^{mn} = \mathbf{A}^{mn} \ . \tag{167}$$

$\mathbf{G}^{mn}$ is a $3N$-dimensional Green's function vector and $\mathbf{1}$ is the $3N \times 3N$ unit matrix. The Green's functions and the inhomogeneity vectors each consist of N three-dimensional subvectors which are characterized by the indices i and j, which are

now layer indices:

$$\mathbf{G}_{ij}^{mn}(\mathbf{k},\omega) \;=\; \begin{pmatrix} G_{ij}^{+,mn}(\mathbf{k},\omega) \\ G_{ij}^{-,mn}(\mathbf{k},\omega) \\ G_{ij}^{z,mn}(\mathbf{k},\omega) \end{pmatrix}, \qquad \mathbf{A}_{ij}^{mn}= \begin{pmatrix} A_{ij}^{+,mn} \\ A_{ij}^{-,mn} \\ A_{ij}^{z,mn} \end{pmatrix} \; . \tag{168}$$

The equations of motion are then expressed in terms of these layer vectors and 3×3 submatrices $\mathbf{\Gamma}_{ij}$ of the $3N \times 3N$ matrix $\mathbf{\Gamma}$

$$\left[\omega\mathbf{1} - \begin{pmatrix} \mathbf{\Gamma}_{11} & \mathbf{\Gamma}_{12} & \dots & \mathbf{\Gamma}_{1N} \\ \mathbf{\Gamma}_{21} & \mathbf{\Gamma}_{22} & \dots & \mathbf{\Gamma}_{2N} \\ \dots & \dots & \dots & \dots \\ \mathbf{\Gamma}_{N1} & \mathbf{\Gamma}_{N2} & \dots & \mathbf{\Gamma}_{NN} \end{pmatrix}\right] \begin{bmatrix} \mathbf{G}_{1j} \\ \mathbf{G}_{2j} \\ \dots \\ \mathbf{G}_{Nj} \end{bmatrix} = \begin{bmatrix} \mathbf{A}_{1j}\delta_{1j} \\ \mathbf{A}_{2j}\delta_{2j} \\ \dots \\ \mathbf{A}_{Nj}\delta_{Nj} \end{bmatrix}, \quad j = 1, ..., N \; . \tag{169}$$

The $\mathbf{\Gamma}$ matrix reduces to a band matrix with zeros in the $\mathbf{\Gamma}_{ij}$ sub-matrices, when $j > i+1$ and $j < i-1$. The diagonal sub-matrices $\mathbf{\Gamma}_{ii}$ are of size 3×3 and have the form

$$\mathbf{\Gamma}_{ii} = \begin{pmatrix} H_i^z & 0 & -H_i^+ \\ 0 & -H_i^z & H_i^- \\ -\frac{1}{2}\tilde{H}_i^- & \frac{1}{2}\tilde{H}_i^+ & 0 \end{pmatrix} \; . \tag{170}$$

where

$$\begin{aligned} H_i^z &= B_i^z + \langle S_i^z\rangle\Big(J_{ii}(q-\gamma_{\mathbf{k}}) + D_{ii}q\Big) + (J_{i,i+1}+D_{i,i+1})\langle S_{i+1}^z\rangle + (J_{i,i-1}+D_{i,i-1})\langle S_{i-1}^z\rangle \\ &\quad + K_{2,i}2\langle S_i^z\rangle\Big(1 - \frac{1}{2S^2}[S(S+1) - \langle S_i^z S_i^z\rangle]\Big) \; , \\ \tilde{H}_i^{\pm} &= B_i^{\pm} + \langle S_i^{\pm}\rangle J_{ii}(q-\gamma_{\mathbf{k}}) + J_{i,i+1}\langle S_{i+1}^{\pm}\rangle + J_{i,i-1}\langle S_{i-1}^{\pm}\rangle \; , \\ H_i^{\pm} &= \tilde{H}_i^{\pm} - \langle S_i^{\pm}\rangle D_{ii}\gamma_{\mathbf{k}} \; . \end{aligned} \tag{171}$$

For a square lattice and a lattice constant taken to be unity, $\gamma_{\mathbf{k}} = 2(\cos k_x + \cos k_y)$ and $q = 4$ is the number of nearest neighbours.

If the dipole-dipole coupling is small compared to the exchange interaction, it can be treated in the mean field approximation (see e.g. the appendix of [9] and Section 7.4 of this review). In this case, the dipole coupling leads to a renormalization of the magnetic field and one finds

$$\begin{aligned} B_i^{\pm} &= B^{\pm} + \sum_{j=1}^{N} g_{ij}\langle S_j^{\pm}\rangle T^{|i-j|}, \\ B_i^z &= B^z - 2\sum_{j=1}^{N} g_{ij}\langle S_j^z\rangle T^{|i-j|} \; ; \end{aligned} \tag{172}$$

i.e. there is an enhancement of the transverse fields and a reduction of the field perpendicular to the film plane.

The lattice sums for a two-dimensional square lattice are given by ($n = |i - j|$)

$$T^n = \sum_{lm} \frac{l^2 - n^2}{(l^2 + m^2 + n^2)^{5/2}}. \tag{173}$$

The indices lm run over all sites of the j^{th} layer excluding terms with $l^2+m^2+n^2 = 0$.

The 3×3 non-diagonal sub-matrices $\mathbf{\Gamma}_{ij}$ for $j = i \pm 1$ are of the form

$$\mathbf{\Gamma}_{ij} = \begin{pmatrix} -J_{ij}\langle S_i^z\rangle & 0 & (J_{ij} + D_{ij})\langle S_i^+\rangle \\ 0 & J_{ij}\langle S_i^z\rangle & -(J_{ij} + D_{ij)}\langle S_i^-\rangle \\ \frac{1}{2}J_{ij}\langle S_i^-\rangle & -\frac{1}{2}J_{ij}\langle S_i^+\rangle & 0 \end{pmatrix}. \tag{174}$$

Now the system of equations of motion is completely specified.

The case ($K_{ij} \neq 0, D_{ij} = 0$) has been treated in Ref. [28] for a monolayer and in Ref. [9] for the multilayer by the eigenvector method. In this case $\tilde{H}_i^{\pm} = H_i^{\pm}$. In the case (($K_{ij} = 0, D_{ij} \neq 0$), treated in [37], one has $\tilde{H}_i^{\pm} \neq H_i^{\pm}$, which leads to additional dependencies on the momentum vector $\mathbf{k}$, requiring a refinement of the treatment. We discuss these cases separately in the following subsections.

4.2.2. Approximate treatment of the single-ion anisotropy

For the single-ion anisotropy, one can use eqn (49) directly because the term $\mathbf{R}^0\mathbf{L}^0$ turns out to be independent of the momentum $\mathbf{k}$. The $+, -, z$ components of the vector $\mathbf{C}_{\mathbf{k}}^{mn}$ are, however, not independent, i.e. there are not enough equations to solve for the unknowns. The remedy is to supplement eqn (49) with the regularity conditions (45).

For illustration, consider the monolayer. For $D_{ij} = 0$ and $K_2 \neq 0$ and $\tilde{H}^{\pm} = H^{\pm}$, the eigenvalues of the equation-of-motion matrix $\mathbf{\Gamma}$ (170) and eigenvector matrices $\mathbf{R}$ and $\mathbf{L}$ can be determined analytically. The eigenvalues are $\omega_0 = 0$, $\omega_{\pm} = \pm E_{\mathbf{k}} = \pm\sqrt{H^+H^- + H^zH^z}$. The right eigenvectors are arranged so that the columns 1,2 and 3 correspond to the eigenvalues 0, $+E_{\mathbf{k}}$ and $-E_{\mathbf{k}}$ respectively:

$$\mathbf{R} = \begin{pmatrix} \frac{H^+}{H^z} & \frac{-(E_{\mathbf{k}}+H^z)}{H^-} & \frac{(E_{\mathbf{k}}-H^z)}{H^-} \\ \frac{H^-}{H^z} & \frac{(E_{\mathbf{k}}-H^z)}{H^+} & \frac{-(E_{\mathbf{k}}+H^z)}{H^+} \\ 1 & 1 & 1 \end{pmatrix}, \tag{175}$$

and the left eigenvectors are arranged in rows 1,2,3 corresponding to the eigenvalues $0, +E_{\mathbf{k}}, -E_{\mathbf{k}}$:

$$\mathbf{L} = \frac{1}{4E_{\mathbf{k}}^2} \begin{pmatrix} 2H^-H^z & 2H^+H^z & 4H^zH^z \\ -(E_{\mathbf{k}} + H^z)H^- & (E_{\mathbf{k}} - H^z)H^+ & 2H^-H^+ \\ (E_{\mathbf{k}} - H^z)H^- & -(E_{\mathbf{k}} + H^z)H^+ & 2H^-H^+ \end{pmatrix}. \tag{176}$$

With the knowledge of $\mathbf{L^0}$ the regularity conditions (45) are

$$\mathbf{L^0 A_{-1}} = 0 = (H^- H^z, H^+ H^z, 2H^z H^z) \begin{pmatrix} A_{-1}^{+,mn} \\ A_{-1}^{-,mn} \\ A_{-1}^{z,mn} \end{pmatrix}. \tag{177}$$

For $m = 0,\ n = 1$, with $A_{-1}^{+,01} = 2\langle S^z \rangle$, $A_{-1}^{-,01} = 0$ and $A_{-1}^{z,01} = -\langle S^- \rangle$,

$$\langle S^- \rangle = \frac{H^-}{H^z}\langle S^z \rangle = \frac{\Big(\langle S^- \rangle J(q-\gamma_{\mathbf{k}}) + B^-\Big)\langle S^z \rangle}{B^z + \langle S^z \rangle J(q-\gamma_{\mathbf{k}}) + K_2 2\langle S^z \rangle \Big(1 - \frac{1}{2S^2}[S(S+1) - \langle S^z S^z \rangle]\Big)}\ . \tag{178}$$

Solving for $\langle S^- \rangle$ and taking the complex conjugate,

$$\langle S^\pm \rangle = \frac{B^\pm}{B^z + K_2 2\langle S^z \rangle \Big(1 - \frac{1}{2S^2}[S(S+1) - \langle S^z S^z \rangle]\Big)} \langle S^z \rangle. \tag{179}$$

Thus, once $\langle S^z \rangle$ and $\langle S^z S^z \rangle$ have been calculated, the transverse correlations follow from the rgularity condition. Note that the prefactor $\frac{H^-}{H^z}$ does not depend on the momentum vector $\mathbf{k}$.

The lowest spin for which the single-ion anisotropy has an effect is $S = 1$ (for $S = 1/2$ the anisotropy term is a constant and does not contribute to the equations of motion). In this case, only equations of motion with $(m = 0, n = 1)$ and $(m = 1, n = 1)$ are needed to determine the correlations $\langle S^z \rangle$ and $\langle S^z S^z \rangle$. The regularity conditions with $m + n \leq 2S + 1 = 3$ suffice to express all remaining correlations as functions of $\langle S^z \rangle$ and $\langle S^z S^z \rangle$ (for more details see Appendix B of Ref. [28]).

For the monolayer with general spin S, comparison of (178) with (179) shows that

$$\frac{H^\pm}{H^z} = \frac{B^\pm}{Z}, \tag{180}$$

with $Z = B^z + K_2 2\langle S^z \rangle \Big(1 - \frac{1}{2S^2}(S(S+1) - \langle S^z S^z \rangle)\Big)$. The regularity conditions (177) can therefore be written for general m, n in the form

$$-2Z A_{-1}^{z,mn} = A_{-1}^{+,mn} B^- + A_{-1}^{-,mn} B^+\ . \tag{181}$$

Using the z-component of equation (47) for the monolayer, one obtains a relation between the correlations in momentum space

$$\begin{aligned} &2\frac{B^+ B^-}{Z^2}\langle (S^z)^m (S^-)^n S^z \rangle - \frac{B^-}{Z}\langle (S^z)^m (S^-)^n S^+ \rangle - \frac{B^+}{Z}\langle (S^z)^m (S^-)^n S^- \rangle \\ &= \frac{1}{2} A_{-1}^{+,mn} \frac{E_{\mathbf{k}}}{H^z}\frac{B^-}{Z}\Big[\frac{E_{\mathbf{k}}}{H^z} - \coth(\frac{\beta E_{\mathbf{k}}}{2})\Big] + \frac{1}{2} A_{-1}^{-,mn} \frac{E_{\mathbf{k}}}{H^z}\frac{B^+}{Z}\Big[\frac{E_{\mathbf{k}}}{H^z} + \coth(\frac{\beta E_{\mathbf{k}}}{2})\Big]. \end{aligned} \tag{182}$$

Note that all correlation functions in this equation are written in a standard form where powers of S^z are written to the left of the powers of S^-:

$$C(m,n) = \langle (S^z)^m (S^-)^n \rangle. \tag{183}$$

The relations $[S^z,(S^-)^n]_- = -n(S^-)^n$ and $S^-S^+ = S(S+1) - S^z - (S^z)^2$ allow us to express all correlations in terms of the $C(m,n)$:

$$\begin{aligned}
\langle (S^z)^m (S^-)^n S^z\rangle &= nC(m,n) + C(m+1,n)\ ,\\
\langle (S^z)^m (S^-)^n S^+\rangle &= \Big(S(S+1) - n(n-1)\Big)C(m,n-1) - (2n-1)C(m+1,n-1)\\
&\quad -C(m+2,n-1)\ ,\\
\langle (S^z)^m (S^-)^n S^-\rangle &= C(m,n+1)\ .
\end{aligned} \tag{184}$$

The inhomogeneities can also be expressed in terms of the $C(m,n)$ using binomial series:

$$\begin{aligned}
A_{-1}^{z,mn} &= -nC(m,n)\ ,\\
A_{-1}^{+,mn} &= \langle\Big[\Big((S^z-1)^m - (S^z)^m\Big)S^-S^+ + 2S^z(S^z-1)^m + (n-1)(n+2S^z)(S^z)^m\Big](S^-)^{n-1}\rangle\\
&= S(S+1)\sum_{i=1}^{m}\left(\begin{array}{c} m\\ i\end{array}\right)(-1)^i C(m-i,n-1) + (2n+m)C(m+1,n-1)\\
&\quad + \sum_{i=2}^{m+1}\left(\begin{array}{c} m+1\\ i\end{array}\right)(-1)^{i+1}C(m+2-i,n-1) + n(n-1)C(m,n-1)\ ,\\
A_{-1}^{-,mn} &= \langle[(S^z+1)^m - (S^z)^m](S^-)^{n+1}\rangle = \sum_{i=1}^{m}\left(\begin{array}{c} m\\ i\end{array}\right)C(m-i,n+1)\ .
\end{aligned} \tag{185}$$

The regularity conditions for all m and n can be written in terms of correlations defined in the standard form by inserting equation (185) into equation (181):

$$\begin{aligned}
2ZnC(m,n) &= B^-\Big[S(S+1)\sum_{i=1}^{m}\left(\begin{array}{c} m\\ i\end{array}\right)(-1)^i C(m-i,n-1)\\
&+(2n+m)C(m+1,n-1) + \sum_{i=2}^{m+1}\left(\begin{array}{c} m+1\\ i\end{array}\right)(-1)^{i+1}C(m+2-i,n-1)\\
&+n(n-1)C(m,n-1)\Big] + B^+\sum_{i=1}^{m}\left(\begin{array}{c} m\\ i\end{array}\right)C(m-i,n+1)\ .
\end{aligned} \tag{186}$$

For a given spin S and given values of $C(m,0)$ for $m \le 2S+1$ this set of linear equations is solved for $C(m,n>0)$ for all $m+n \le 2S+1$. The resulting values are then checked for consistency by insertion into the $2S$ equations (182) using equations (184) and (185). The solution consists of moments $\langle (S^z)^p\rangle$ (p=1,...,2S) for which eqns (182) are self-consistently fulfilled. Note that the highest moment $\langle (S^z)^{2S+1}\rangle$ has been eliminated in favour of the lower ones through the relation $\prod_{M_S}(S^z - M_S) = 0$.

Multilayers are treated simply by adorning the correlations and the quantity Z with a layer index i:

$$Z_i = B_i^z + J_{i,i+1}\langle S_{i+1}^z\rangle + J_{i,i-1}\langle S_{i-1}^z\rangle$$

$$+K_{2,i}2\langle S_i^z\rangle\Big(1-\frac{1}{2S^2}[S(S+1)-\langle S_i^z S_i^z\rangle]\Big)\ . \tag{187}$$

An alternative method of solution of the present problem is first to eliminate the null-space by a singular value decomposition (SVD) of the equation-of- motion matrix $\mathbf{\Gamma}$ (170) and then using equation (77) directly. The advantage is to reduce the dimension of the problem by the number of zero eigenvalues.

The monolayer for $S = 1$ is suitable [38] for demonstrating the procedure because the SVD of $\mathbf{\Gamma}$ and the vector $\tilde{\mathbf{v}}$ of eqn (77) can be obtained analytically. In order to consider a reorientation of the magnetization in the xz-plane, we put $B^y = 0$, so that $H^{\pm} = H^x$. The $\mathbf{\Gamma}$-matrix can be expressed as a product of three matrices:

$$\mathbf{\Gamma} = \mathbf{U}\mathbf{W}\tilde{\mathbf{V}} = \mathbf{u}\mathbf{w}\tilde{\mathbf{v}}. \tag{188}$$

Proceeding as in Section 3.5, it is a simple exercise to obtain the three factors:

$$\mathbf{W} = \begin{pmatrix} \epsilon_1 & 0 & 0 \\ 0 & \epsilon_2 & 0 \\ 0 & 0 & 0 \end{pmatrix}; \qquad \mathbf{w} = \begin{pmatrix} \epsilon_1 & 0 \\ 0 & \epsilon_2 \end{pmatrix}, \tag{189}$$

with $\epsilon_1 = \sqrt{H^z H^z + 2H^x H^x}$ and $\epsilon_2 = \sqrt{H^z H^z + \frac{1}{2}H^x H^x}$. We also find

$$\mathbf{U} = \begin{pmatrix} \frac{-\sqrt{2}}{2} & \frac{-H^z}{\sqrt{2}\epsilon_2} & \frac{H^x}{2\epsilon_2} \\ \frac{\sqrt{2}}{2} & \frac{-H^z}{\sqrt{2}\epsilon_2} & \frac{H^x}{2\epsilon_2} \\ 0 & \frac{H^x}{\sqrt{2}\epsilon_2} & \frac{H^z}{\epsilon_2} \end{pmatrix}; \qquad \mathbf{u} = \begin{pmatrix} \frac{-\sqrt{2}}{2} & \frac{-H^z}{\sqrt{2}\epsilon_2} \\ \frac{\sqrt{2}}{2} & \frac{-H^z}{\sqrt{2}\epsilon_2} \\ 0 & \frac{H^x}{\sqrt{2}\epsilon_2} \end{pmatrix}, \tag{190}$$

and

$$\tilde{\mathbf{V}} = \begin{pmatrix} \frac{-H^z}{\sqrt{2}\epsilon_1} & \frac{-H^z}{\sqrt{2}\epsilon_1} & \frac{\sqrt{2}H^x}{\epsilon_1} \\ \frac{-\sqrt{2}}{2} & \frac{\sqrt{2}}{2} & 0 \\ \frac{H^x}{\epsilon_1} & \frac{H^x}{\epsilon_1} & \frac{H^z}{\epsilon_1} \end{pmatrix}; \qquad \tilde{\mathbf{v}} = \begin{pmatrix} \frac{-H^z}{\sqrt{2}\epsilon_1} & \frac{-H^z}{\sqrt{2}\epsilon_1} & \frac{\sqrt{2}H^x}{\epsilon_1} \\ \frac{-\sqrt{2}}{2} & \frac{\sqrt{2}}{2} & 0 \end{pmatrix}, \tag{191}$$

Now everything is specified and one can solve equation (77). There is the technical problem that the vectors at neighbouring k-values in general have arbitrary phases but this can be overcome with the help of the smoothing procedure described in Section 3.5.

In Fig. 3 we show as an example the results for the spin $S = 1$ Heisenberg monolayer. It does not matter whether one uses eqn (49) or eqn (77); the results are the same, as they should be.

This is not the case in later examples (see Sections 4.2.3 and 4.3.2) where it is necessary to use the singular value decomposition to deal with a momentum-dependent factor $\mathbf{R}^0\mathbf{L}^0$.

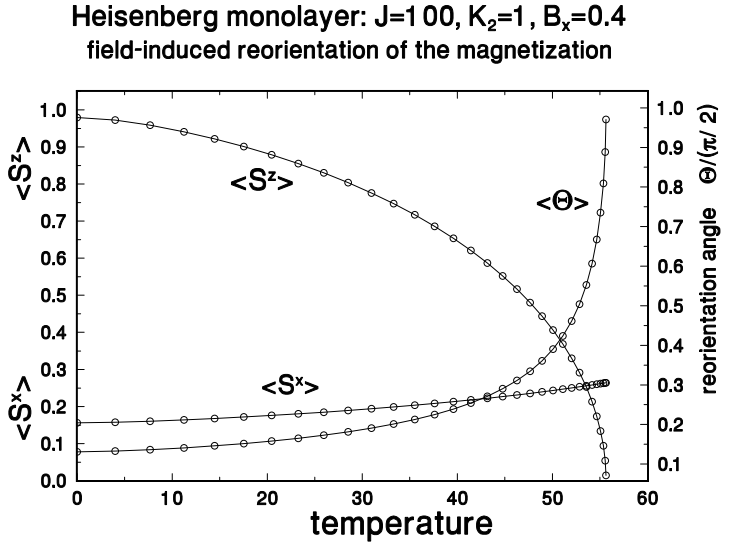

Figure 3: Magnetizations $\langle S^z \rangle$ and $\langle S^x \rangle$ and the reorientation angle Θ for a spin S=1 Heisenberg monolayer as function of the temperature.

For spin $S > 1$ and multilayer systems, one can use both methods as long as $\mathbf{R}^0\mathbf{L}^0$ is independent of the momentum, but the singular value decomposition and the matrix $\tilde{\mathbf{v}}$ now have to be determined numerically.

In the next figures, we show further examples from Ref. [9]. Fig. 4 shows normalized magnetizations $\langle S^z \rangle / S$ and $\langle S^x \rangle / S$ for a monolayer as functions of the temperature for all integral and half-integral spin values between $S = 1$ and $S = 6$ calculated with Green's function theory. The reorientation temperature T_R^S depends slightly on S. The inset shows the corresponding results in mean field theory for spins $S = 1, 2, 7/2$, and $11/2$. In this case, the reorientation temperature does not depend on S. Note the very different temperature scale, which is due to the missing magnon correlations in MFT.

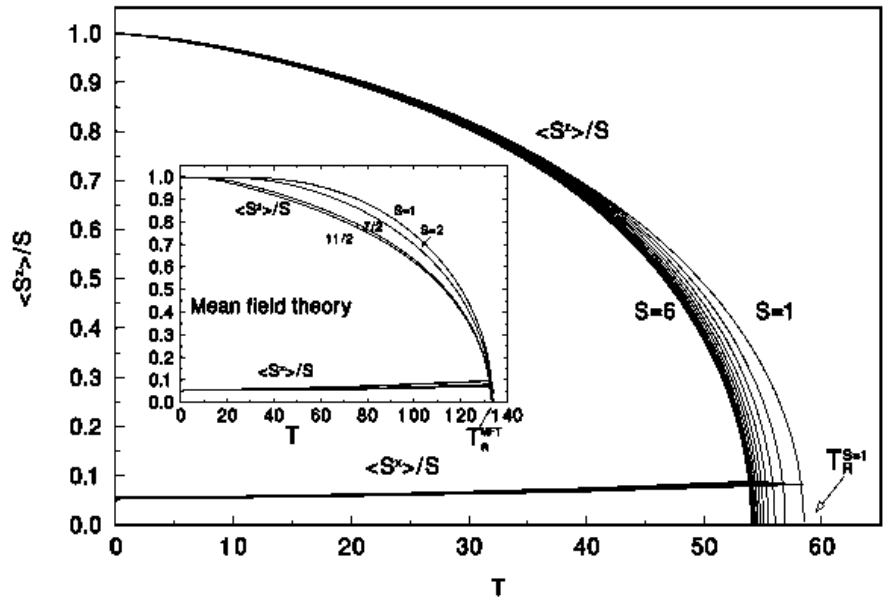

Figure 4: Normalized magnetizations $\langle S^z\rangle/S$ and $\langle S^x\rangle/S$ for a monolayer as functions of the temperature for all integral and half-integral spin values between $S = 1$ and $S = 6$ calculated with Green's function theory. The reorientation temperature T_R^S depends slightly on S. The inset shows the corresponding results in mean field theory for spins $S = 1, 2, 7/2$, and $11/2$. The reorientation temperature for MFT does not depend on S.

Fig. 5 shows the equilibrium reorientation angle as a function of the temperature for the systems of Fig. 4 calculated with GFT. The inset shows the corresponding results for MFT.

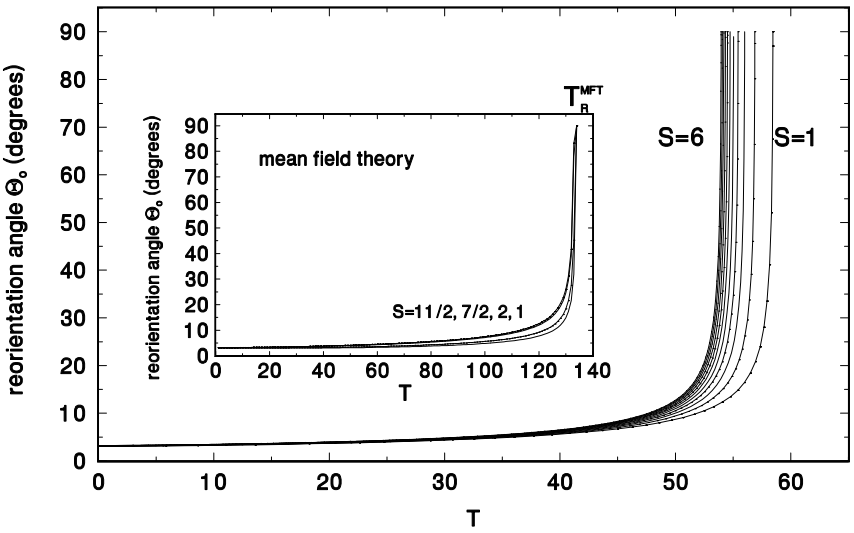

Figure 5: Equilibrium reorientation angle as a function of the temperature for the systems of Fig. 4 calculated with GFT. The inset shows the corresponding results for MFT.

Fig. 6 shows the sublayer magnetizations $\langle S_i^z \rangle$ as functions of the temperature for thin ferromagnetic films with N layers and spin $S = 1$. The reorientation temperature T_R^N for the different films can be read off from the curve in the $N - T$ plane, where $\langle S_i^z \rangle = 0$.

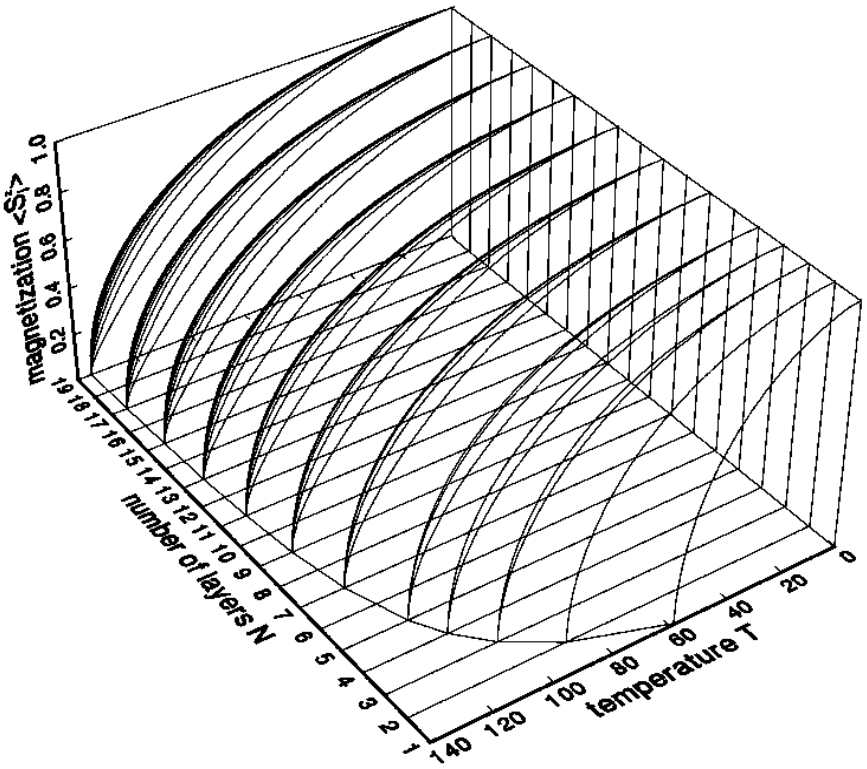

Figure 6: Sublayer magnetizations $\langle S_i^z \rangle$ as functions of the temperature for thin ferromagnetic films with N layers and spin $S = 1$. The reorientation temperature T_R^N for the different films can be read off from the curve in the $N - T$ plane, where $\langle S_i^z \rangle = 0$.

In Fig. 7, the average equilibrium reorientation angle Θ_0 is shown as a function of the temperature for different film thicknesses. N is the number of layers in each film and T_R^N are the reorientation temperatures at $\Theta_0 = 90^o$.

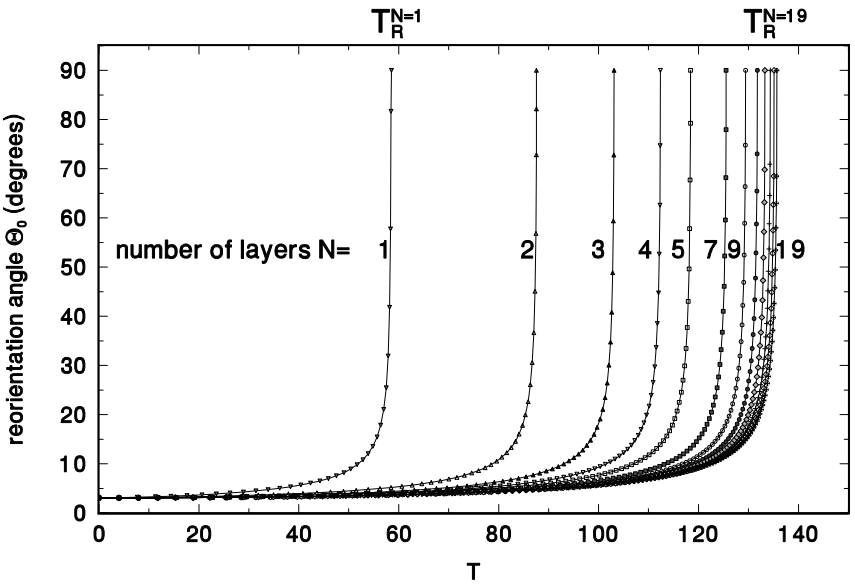

Figure 7: The average equilibrium reorientation angle Θ_0 as a function of the temperature for different film thicknesses. N is the number of layers in each film and T_R^N are the reorientation temperatures at $\Theta_0 = 90^o$.

If one is interested in the effective (temperature-dependent) lattice anisotropy coefficient $\mathcal{K}_2(T)$, one should not use the thermodynamic perturbation theory discussed in Section 4.1.6, but rather a non-perturbative approach in which the free energy is minimized with respect to the layer-dependent reorientation angles θ_i: $\partial F_i(T)/\partial\theta_i|_{\theta_{i0}} = 0$, where θ_{i0} are the equilibrium reorientation angles. The effective anisotropy of a film consisting of N layers is

$$\mathcal{K}_2(T) = \sum_{i=1}^{N} \mathcal{K}_{2,i}(T) \tag{192}$$

with

$$\begin{aligned} \mathcal{K}_{2,i}(T) \;=\; & \frac{M_i(T)}{2\sin\theta_{0,i}\cos\theta_{0,i}} \\ & \Big[\cos\theta_{0,i}(B^x + J_{i,i+1}M_{i+1}(T)\sin\theta_{0,i+1} + J_{i,i-1}M_{i,i-1}\sin\theta_{0,i-1} + T_i^{\sin}) \\ & - \sin\theta_{0,i}(B^z + J_{i,i+1}M_{i+1}(T)\cos\theta_{0,i+1} + J_{i,i-1}M_{i,i-1}\cos\theta_{0,i-1} - 2T_i^{\cos})\Big] \end{aligned} \tag{193}$$

Here $M_i(T) = \sqrt{\langle S_i^x\rangle^2 + \langle S_i^z\rangle^2}$ and $\theta_{0,i} = \arctan(\langle S_i^x\rangle/\langle S_i^z\rangle)$ are determined from

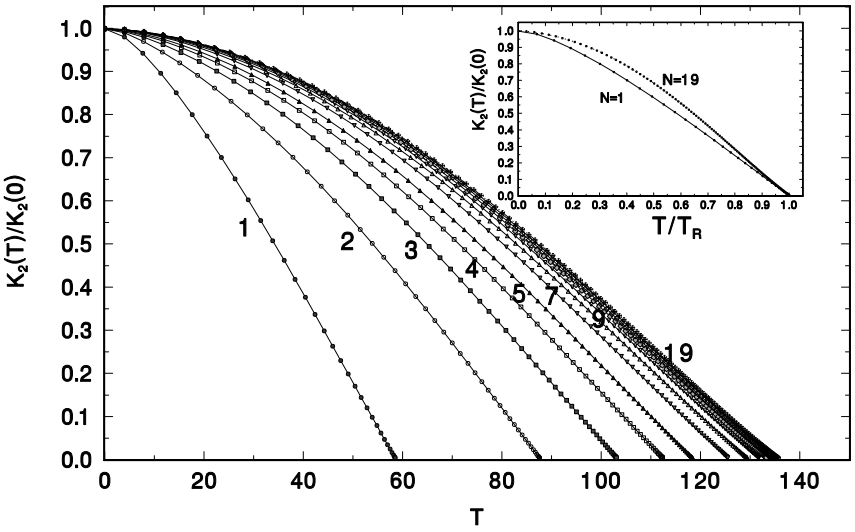

Figure 8: Average effective anisotropy $\mathcal{K}_2(T)/\mathcal{K}_2(0)$ as a function of the temperature and film thickness N. The inset demonstrates the different functional dependence on T for layers with N=1 and N=19 if the temperature is scaled with the reorientation temperature.

the magnetization components and

$$T_i^{\sin} = \sum_{j=1}^{N} g_{ij} M_j \sin\theta_{0,j} T^{|i-j|} \ ,$$
$$T_i^{\cos} = \sum_{j=1}^{N} g_{ij} M_j \cos\theta_{0,j} T^{|i-j|} \ , \qquad (194)$$

where $T^{|i-j|}$ are dipole lattice sums, see (173).

In Fig. 8, average effective anisotropies $\mathcal{K}_2(N,T)/\mathcal{K}_2(N,0)$ of films with different thicknesses N are shown as functions of the temperature.

Up to now, we have used S^+, S^-, S^z as the basic operators to define the Green's functions suitable for treating the reorientation of the magnetization in the case of uniaxial anisotropies. When there are anisotropies in all directions of space, it is more natural to start with the operators S^x, S^y, S^z, because this treats the three directions of space on an equal footing. This is done in Ref. [33], where the Anderson-Callen decoupling of the single-ion anisotropy terms is invoked for all directions of space. A formal advantage is that the equation-of-motion matrix turns out to be hermitean. Generalising a formula due to Callen [17] leads to analytical expressions for the first and second moments of the spin operators. Reorientation transitions and effective (temperature-dependent) anisotropies are calculated for

various 3D and 2D cases.

The GF theory is used in Ref. [34] to investigate the interplay between a single-ion easy-plane anisotropy and the dipole-dipole interaction for a Heisenberg monolayer with the Hamiltonian ($K_2 > 0$)

$$H = -J \sum_{<ij>} \mathbf{S}_i \mathbf{S}_j + K_2 \sum_i (S_i^x)^2 - B \sum_i S_i^z + H^{dipole}$$

.

The Tyablikov decoupling is used for the exchange and the dipole-dipole interactions and the Anderson-Callen decoupling for the single-ion anisotropy. An interesting result is that the easy-plane anisotropy alone cannot stabilize the long-range ferromagnetic order at finite temperatures, one needs the dipole-dipole interaction in addition in order to do so.

The spin reorientation problem is also investigated in Refs. [35, 36]. In these papers, a single-ion anisotropy is used and the dipole-dipole interaction is approximated by the dipole demagnetization energy. The exchange interaction and demagnetization energy terms are treated by the Tyablikov (RPA) decoupling and a decoupling due to Lines [29] is applied to the single-ion anisotropy terms. However, instead of calculating the longitudinal and transverse components of the magnetization vector, only the z-component of the magnetization is calculated as a function of the temperature. For the multi-layer case, the vanishing of the gap in the corresponding spin-wave spectrum at a particular temperature is interpreted as the onset of the reorientation transition. Effective (temperature-dependent) anisotropies are also calculated within this approximation.

4.2.3. Treating the exchange anisotropy

Although the formalism described in Section 4.2.1 looks very similar for the single-ion and exchange anisotropy, the direct application of the standard spectral theorem is not possible because the term $\mathbf{R^0L^0}$ in eqn (47) turns out to be momentum dependent owing to the fact that for the exchange anisotropy $\tilde{H}_i^{\pm} \neq H_i^{\pm}$ in eqn (171). Thus the Fourier transform in the second term of eqn (47) cannot be performed.

In Ref. [37] we found by intuition a transformation which eliminates one of the rows of $\mathbf{R^0L^0}$ in the equation

$$\mathbf{C} = \mathbf{R^1}\mathcal{E}^{\mathbf{1}}\mathbf{L^1A_{-1}} + \mathbf{R^0L^0C}\ , \tag{195}$$

thus allowing the corresponding row to serve as an integral equation of the eigenvector method.

The transformation is found to be

$$\mathbf{T}^{-1} = \frac{1}{2}\begin{pmatrix} 1 & 1 & 0 \\ -1 & 1 & 0 \\ 0 & 0 & 2 \end{pmatrix} \qquad \mathbf{T} = \begin{pmatrix} 1 & -1 & 0 \\ 1 & 1 & 0 \\ 0 & 0 & 1 \end{pmatrix} \tag{196}$$

with $\mathbf{T}^{-1}\mathbf{T} = \mathbf{1}$.

Applying this transformation to equation (195)

$$\mathbf{T}^{-1}\mathbf{C} = \mathbf{T}^{-1}\mathbf{R^1}\mathcal{E}^{\mathbf{1}}\mathbf{L^1}\mathbf{T}\mathbf{T}^{-1}\mathbf{A_{-1}} + \mathbf{T}^{-1}\mathbf{R}_0\mathbf{L}_0\mathbf{T}\mathbf{T}^{-1}\mathbf{C} \tag{197}$$

and inserting the analytical eigenvectors $\mathbf{R}$ and $\mathbf{L}$ for the monolayer

$$\mathbf{R} = \begin{pmatrix} \frac{H^x}{H^z} & \frac{-(\epsilon_{\mathbf{k}}+H^z)}{\tilde{H}^x} & \frac{(\epsilon_{\mathbf{k}}-H^z)}{\tilde{H}^x} \\ \frac{H^x}{H^z} & \frac{(\epsilon_{\mathbf{k}}-H^z)}{\tilde{H}^x} & \frac{-(\epsilon_{\mathbf{k}}+H^z)}{\tilde{H}^x} \\ 1 & 1 & 1 \end{pmatrix}\ , \tag{198}$$

and

$$\mathbf{L} = \frac{1}{4\epsilon_{\mathbf{k}}^2}\begin{pmatrix} 2\tilde{H}^x H^z & 2\tilde{H}^x H^z & 4H^z H^z \\ -(\epsilon_{\mathbf{k}}+H^z)\tilde{H}^x & (\epsilon_{\mathbf{k}}-H^z)\tilde{H}^x & 2H^x\tilde{H}^x \\ (\epsilon_{\mathbf{k}}-H^z)\tilde{H}^x & -(\epsilon_{\mathbf{k}}+H^z)\tilde{H}^x & 2H^x\tilde{H}^x \end{pmatrix}\ , \tag{199}$$

the second component of the vector $\mathbf{T}^{-1}\mathbf{R}_0\mathbf{L}_0\mathbf{T}\mathbf{T}^{-1}\mathbf{C}$ transforms to zero and one obtains, together with the regularity conditions (45), the integral equations for the correlations for each (m, n) pair.

The eigenvector method immediately generalizes to the case of N layers if the transformation T is extended to $3N$ dimensions by constructing $3N \times 3N$-matrices with sub-matrices (196) on the diagonal.

The intuited transformation (196) can also be found systematically enlisting the help of the singular value decomposition of the $\mathbf{\Gamma}$-matrix as described in Sections

3.5 and 4.2.2. This automatically yields some momentum-independent components of a row vector $\tilde{\mathbf{v}}_j$ which enables the Fourier transformation (78).

This procedure also works for the case of coupled ferro- and antiferromagnetic layers described in Section 4.3.2.

Some typical results for systems with exchange anisotropy are shown in Figs. 9 and 10. In Fig. 9 the magnetization $\langle S^z \rangle$ and its second moment $\langle S^z S^z \rangle$ are plotted as functions of the temperature for a ferromagnetic spin $S = 1$ Heisenberg monolayer for a square lattice with an exchange interaction strength of $J = 100$ and an exchange anisotropy strength of $D = 0.7$. It is interesting to note that there is practically no difference in the magnetization curves when using an Anderson-Callen decoupled single-ion anisotropy, once its strength is fitted to an appropriate value, $K_2 = 1.0$. This makes it difficult to decide which kind of anisotropy is acting in an actual film.

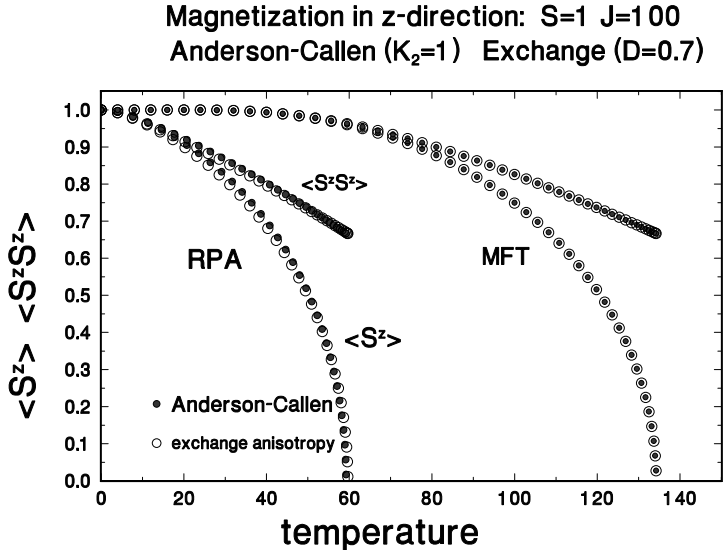

Figure 9: The magnetization $\langle S^z \rangle$ and its second moment $\langle S^z S^z \rangle$ of a ferromagnetic spin $S = 1$ Heisenberg monolayer for a square lattice as functions of the temperature, comparing a GFT calculation using an exchange anisotropy ($D = 0$, open circles) with a single-ion anisotropy ($K_2 = 1.0$, solid dots). The corresponding MFT results are also shown. Note the different Curie temperatures.

A novel feature occurs with the introduction of the magnetic dipole coupling: the eigenvalues and eigenvectors of the $\mathbf{\Gamma}$-matrix become complex above a certain temperature, i.e. below a certain value of $\langle S^z \rangle$. This behaviour occurs quite naturally in the theory. It has nothing to do with a damping mechanism and has to be taken seriously in order to obtain the results of Fig. 10. Because the $\mathbf{\Gamma}$-matrix is real, its eigenvalues and eigenvectors, if complex, occur pairwise as complex conjugates, and the integral equations to be solved must be real.

In Fig. 10, the components of the magnetization $\langle S^z \rangle$ and $\langle S^x \rangle$ and the absolute value S for a fixed magnetic field $B^x = 0.3$ are shown as functions of the temperature for a ferromagnetic spin $S = 1$ Heisenberg monolayer for a square lattice. Also shown are the equilibrium reorientation angle, Θ_0 and the critical reorientation temperature, T_R, at which the in-plane orientation is reached. The small horizontal arrow indicates the value of $\langle S^z \rangle$ below which complex eigenvalues occur. The results

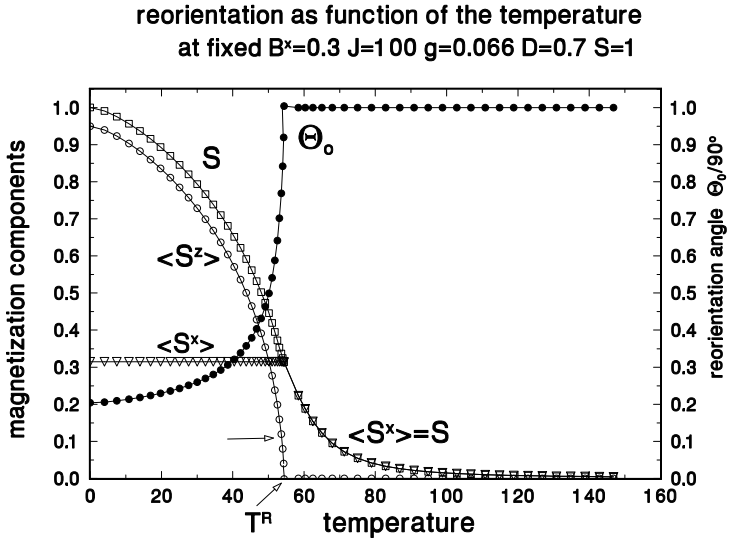

Figure 10: The components of the magnetization $\langle S^z \rangle$ and $\langle S^x \rangle$ and its absolute value S for a fixed magnetic field $B^x = 0.3$ as functions of the temperature for a ferromagnetic spin $S = 1$ Heisenberg monolayer for a square lattice. The exchange interaction strength is $J = 100$, the exchange anisotropy strength is $D = 0.7$ and the strength of the magnetic dipole coupling is $g = 0.066$, a value corresponding to Co. Also shown are the equilibrium reorientation angle, Θ_0, and the critical reorientation temperature, T_R, at which the in-plane orientation is reached. The small horizontal arrow indicates the value of $\langle S^z \rangle$ below which complex eigenvalues occur.

for the exchange anisotropy and the single-ion anisotropy for spins $S > 1$ and multilayers look very similar, as seen by comparing references [9] with [37]. We therefore do not show the corresponding figures here.

Similar results for general spin S using the exchange interaction together with the dipole coupling in the mean field approximation are found in Ref. [39], but for the monolayer only. We also mention Ref. [40], where the competition of the exchange anisotropy with the single-ion anisotropy is investigated for a ferromagnetic S=1 Heisenberg monolayer, and Ref. [41], where the formalism is applied to multilayers and higher spin values with parameters that are different at the surface and the interior of the film. In Ref. [42] the spin reorientation transition for a ferromagnetic Heisenberg monolayer with exchange interaction, exchange anisotropy and dipole dipole interaction is treated with the RPA, where, however, a somewhat artificial temperature dependence of the exchange interaction had to be used in order to obtain a favorable comparison with experiment.

4.2.4. Susceptibilities

In reference [75] Jensen et al. report measurements of the parallel and transverse susceptibilities of a bi-layer Cobalt film having an *in-plane* uniaxial anisotropy. They analyse their results with the help of a many-body Green's function theory assuming an *exchange* anisotropy and a value for the spin of $S = 1/2$. Here, we generalize their theoretical model, extending it to multilayers and arbitrary spin. We discuss not only the exchange exchange anisotropy but also the *single-ion* anisotropy. A comparison of the two cases allows an evaluation of the robustness of the theoretical conclusions as well as possibly identifying any qualitative differences which might enable an experiment to discern which type of anisotropy is acting in a real film. Accordingly, we investigate the parallel and transverse susceptibilities for arbitrary spin in multilayer systems. In keeping with the earlier work [75], we use the Green's function formalism and neglect the dipole-dipole interaction, since it is nearly isotropic for the in-plane case. The theory is formulated in complete analogy to Sections 4.2.2 and 4.2.3 (where an *out-of-plane* magnetization was discussed), the only difference being that the applied magnetic fields allow only an *in-plane* magnetization. For a detailed description, refer to references [76] and [77].

The adequate decouplings for the in-plane situation are the same as for the out-of-plane case: whereas a RPA decoupling is reasonable for the terms coming from the exchange interaction and the exchange anisotropy, it leads to incorrect expressions for the single-ion anisotropy terms. For the latter we therefore use the method proposed by Anderson and Callen [32] at the level of lowest order in the Green's function hierarchy. This is certainly an adequate approximation for small anisotropies, as we have shown in Ref. [48] for the case of an out-of-plane single-ion anisotropy of a monolayer by comparing with 'exact' Quantum Monte Carlo calculations. In addition to Sections 4.2.2 and 4.2.3, we refer the reader to the literature for a discussion of the roles of the single-ion- [9, 28, 44] and exchange[37]-anisotropies with respect to *reorientation* of the magnetization of a ferromagnetic film with an *out-of-plane* anisotropy as a function of temperature and film thickness.

The susceptibilities with respect to the easy (χ_{zz}) and hard (χ_{xx}) axes are calculated as differential quotients

$$\begin{aligned} \chi_{zz} &= \Big(\langle S^z(B^z)\rangle - \langle S^z(0)\rangle\Big)/B^z \\ \chi_{xx} &= \Big(\langle S^x(B^x)\rangle - \langle S^x(0)\rangle\Big)/B^x, \end{aligned} \tag{200}$$

where a value $B^{z(x)} = 0.01/S$ turns out to be small enough. We compare numerical results obtained with the single-ion anisotropy with those from the exchange anisotropy. As the single-ion anisotropy is not appropriate for $S = 1/2$, we show

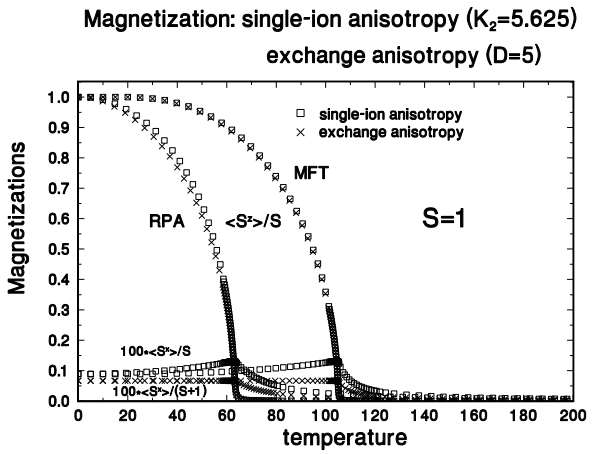

Figure 11: The magnetization $\langle S^z\rangle/S$ of a ferromagnetic spin $S = 1$ Heisenberg monolayer for a square lattice shown as a function of the temperature. Green's function (indicated by RPA) calculations with exchange anisotropy $D = 5$ (crosses) and with single-ion anisotropy ($K_2 = 5.625$), (open squares) in the Anderson-Callen approximation are compared. Also shown are the quantities $100 * \langle S^x\rangle/(S + 1)$ for the exchange anisotropy and $100 * \langle S^x\rangle/S$ for the single-ion anisotropy; the factor 100 is introduced to make the curves visible. The corresponding results for mean field (MFT) calculations are also displayed.

results for $S \geq 1$. In an attempt to obtain universal curves (i.e. independent of the spin quantum number S), we scale the parameters $(B^{x(z)}, J, D)$ in the Hamiltonian as $\tilde{B}^{x(z)}/S = B^{x(z)}$, $\tilde{J}/S(S + 1) = J$ and $\tilde{D}/S(S + 1) = D$ (D being the strength of the exchange anisotropy). We also scale the strength of the single-ion anisotropy according to $\tilde{K_2}/(S - 1/2) = K_2$.

In order to compare results obtained with the single-ion anisotropy with those of the exchange anisotropy, we set the strength of the single-ion anisotropy to $K_2 = 5.625$ for a square lattice monolayer with spin S=1, so that the easy axis magnetization $\langle S^z\rangle/S$ lies as close as possible to the magnetization obtained with the exchange anisotropy ($D = 5$) used in [76]. The exchange interaction parameter is $J = 100$ and there is a small magnetic field in the x-direction, $B^x = 0.01/S$, which stabilizes the calculation. The comparison is shown in Fig. 11. It is surprising that the results for the easy axis magnetization $\langle S^z\rangle$ are very similar over the whole temperature range although the physical origin for the anisotropies is very different. An analogous result was observed for the out-of plane situation discussed in Ref. [37]. For the exchange anisotropy, the hard axis magnetization is a constant below the Curie temperature, whereas for the single-ion anisotropy, it rises slightly up to the Curie temperature. In Ref. [76], it is shown analytically that the hard axis magne-

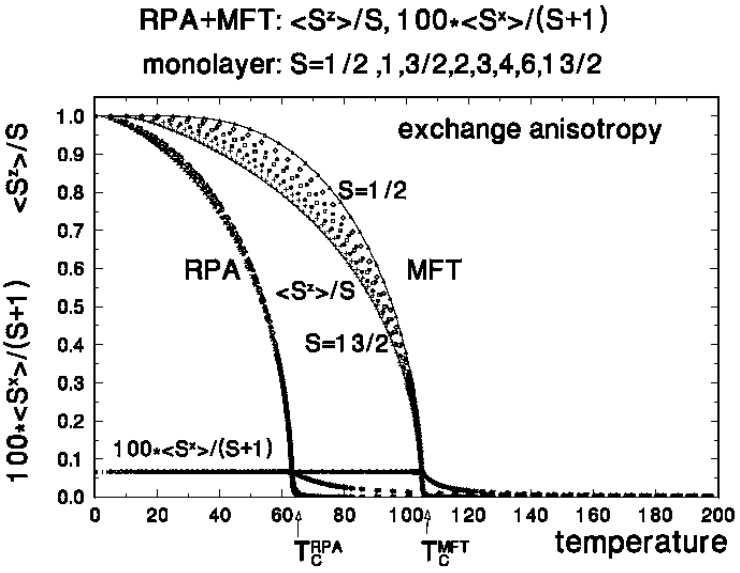

Figure 12: The magnetizations $\langle S^z\rangle/S$ of spin $S = 1/2, 1, 3/2, 2, 3, 4, 6, 13/2$ Heisenberg monolayers for a square lattice as functions of the temperature, from Ref. [76]. Results from Green's function (RPA) calculations are compared with results from mean field theory (MFT) using the exchange anisotropy strength $D = 5$. Also shown is the hard axis magnetization, which scales to a universal curve $100 * \langle S^x\rangle/(S+1)$, where the factor 100 is introduced to make the curves visible.

tization for the exchange anisotropy is universal for a scaling $\langle S^x\rangle/(S+1)$. For the single-ion anisotropy, a scaling $\langle S^x\rangle/S$ is found to be more appropriate. Comparison with the corresponding mean field (MFT) calculations, obtained by neglecting the momentum dependence of the lattice, shows the well-known shift to larger Curie temperatures (by a factor of about two for the monolayer with the present choice of the parameters) owing to the omission of magnon excitations.

In Figs. 12 and 13, we show the easy and hard axes magnetizations for a monolayer with different spins S. Whereas in Fig. 12 one observes a nearly perfect scaling for the RPA calculations with the exchange anisotropy ($S = 1/2, 1, 3/2, 2, 3,$ $4, 6, 13/2$) and a universal Curie temperature $T_C(S)$ for RPA and MFT, this is not the case for the corresponding results with the single-ion anisotropy shown for $S = 1, 3/2, 4, 5$ in Fig. 13, although the violation of scaling is not dramatic.

Turning to the inverse easy and hard axes susceptibilities χ_{zz}^{-1} and χ_{xx}^{-1}, we find very similar results for the exchange anisotropy and the single-ion anisotropy. In particular, in the paramagnetic region ($T > T_{\rm Curie}$), the inverse susceptibilities as a function of temperature are curved owing to the presence of spin waves, whereas the corresponding MFT calculations show a Curie-Weiss (linear in the temperature) behaviour. There is slightly less universal behaviour for the single-ion anisotropy

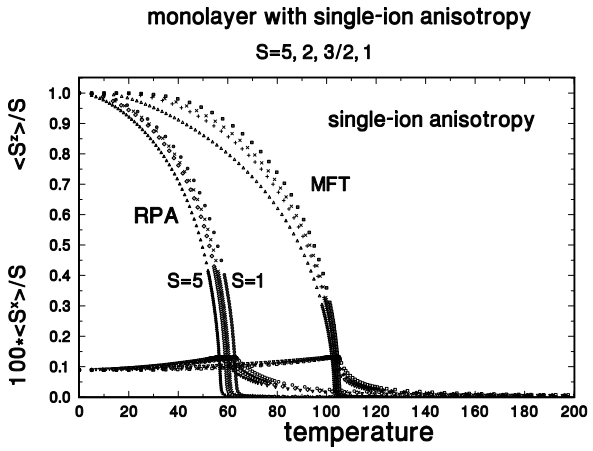

Figure 13: The magnetization $\langle S^z \rangle / S$ of ferromagnetic spin $S = 1, 2, 3/2, 5$ Heisenberg monolayers for a square lattice as a function of the temperature for Green's function (RPA) calculations using the single-ion anisotropy strength of $K_2 = 5.625$ and the corresponding results of mean field theory (MFT). Also shown are the quantities $100 * \langle S^x \rangle / S$; the factor 100 is introduced to make the curves visible.

(Figs. 14 and 15) than for the exchange anisotropy (Figs. 2 and 3 of Ref. [76]). This is connected with the fact that the exchange anisotropy exhibits universal values for the Curie temperatures $T_C^{RPA}(S)$ and $T_C^{MFT}(S)$, which is not strictly the case for the single-ion anisotropy, (Fig. 13). We were also able to show analytically in Ref. [76] that $\chi_{xx}^{-1} * S(S+1)$ is universal for $T < T_C$ for the exchange anisotropy; this is not the case for the single-ion anisotropy. The only difference is in the curves for the imperfectly scaled Green's function results for χ_{zz}^{-1}: for the exchange anisotropy, the curve with the lowest spin value lies to the left of the curves with the higher spin values, whereas the converse is true for the exchange anisotropy. This is not a very pronounced effect and does not lead to a significant difference between the results for the various anisotropies. In treating multilayers with the exchange anisotropy in Ref. [76], we considered only the case $S = 1/2$. The single-ion anisotropy term in the Hamiltonian is a constant for $S = 1/2$; therefore it is not active when calculating the magnetization, so we have to use a larger spin here. In the following, we use spin S=1 as an example but we also have results for $S > 1$ which scale with respect to the spin in the same way as in the monolayer case. The Curie temperatures for the multilayers $N = 2, ..., 19$ (for N=19 one is already close to the bulk limit) are only slightly lower for the single-ion anisotropy than those calculated for the exchange anisotropy.

Some results are shown in Figs. 16 and 17. In order to avoid cluttering the figures, we restrict ourselves to a multilayer with N=9 layers and spin $S = 1$. For

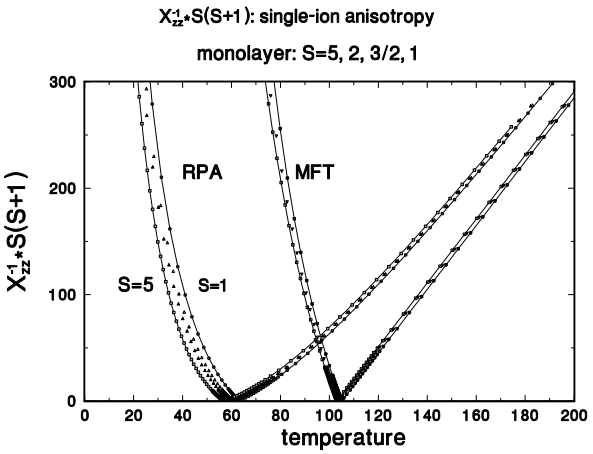

Figure 14: 'Universal' inverse easy axis susceptibilities $\chi_{zz}^{-1} * S(S+1)$ of an in-plane anisotropic ferromagnetic square lattice Heisenberg monolayer as functions of the temperature for single-ion anisotropy and spins $S = 5, 2, 3/2, 1$. Compared are Green's function (RPA) and mean field (MFT) calculations.

$N > 9$ the corresponding curves would shift only slightly in accordance with the saturation of T_C with increasing film thickness. We display only the RPA results for the multilayer (N=9) and compare with the RPA monolayer (N=1) result. Again, there is no significant difference in the results for both anisotropies. We do not plot the corresponding mean field results, which are shifted to higher temperatures and, in the paramagnetic region, show only (a linear in T) Curie-Weiss behaviour, whereas the RPA results have curved shapes owing to the influence of spin waves, which are completely absent in MFT.

Although both kinds of anisotropies are of very different physical origin, it is possible, by fitting the strengths of the anisotropies properly, to obtain nearly identical values for the easy axis magnetizations over the complete temperature range for a spin $S = 1$ monolayer. Using the parameters obtained in this way for monolayers with higher spin values and for multilayers, we looked for differences in the results of calculations with both kinds of anisotropies.

By using scaled variables we find a fairly universal behaviour (independent of the spin quantum number S) of easy and hard axes magnetizations and inverse susceptibilities. Universality holds better for the exchange anisotropy; e.g. we find a universal Curie temperature $T_C(S)$ for RPA and MFT. The scaling is not as perfect for the single-ion anisotropy, but there are *no* dramatic deviations which might enable an experiment to distinguish between the two types of anisotropies. It is sufficient to do a calculation for a particular S and then to apply scaling to obtain the results for other spin values. In principle the measurement of the hard axis

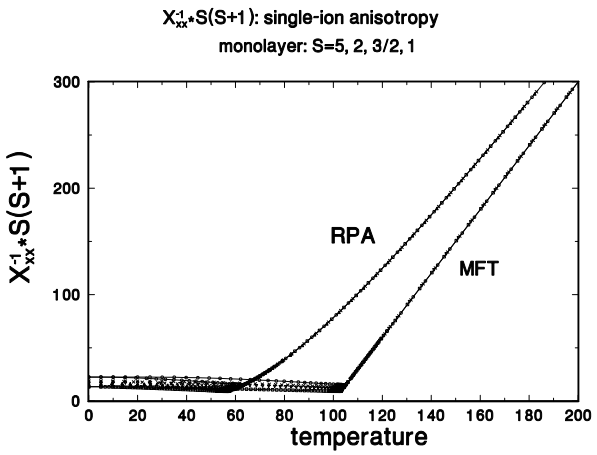

Figure 15: 'Universal' inverse hard axis susceptibilities $\chi_{xx}^{-1} * S(S+1)$ of an in-plane anisotropic ferromagnetic square lattice Heisenberg monolayer as functions of the temperature for single-ion anisotropy and spins $S = 5, 2, 3/2, 1$. Compared are Green's function (RPA) and mean field (MFT) calculations.

susceptibility together with the Curie temperature allows one to obtain information about the parameters of the model, the exchange interaction and the anisotropy strengths. One should, however, keep in mind that the quantitative results of the present calculations correspond to a square lattice. They could change significantly for other lattice types. Further changes could result from the use of layer-dependent exchange interactions and anisotropies. Such calculations are possible, because the numerical program is written in such a way that layer-dependent coupling constants can be used.

A general result is that there are no *qualitative* differences for the calculated observables (easy and hard axes magnetizations and susceptibilities) between the single-ion anisotropy on the one hand and the exchange anisotropy on the other hand. Therefore, it is not possible for us to propose an experiment that could decide which kind of anisotropy is acting in a real ferromagnetic film.

We mention also a paper by Yablonskyi [43], who derives analytical expressions for the static susceptibility and for correlation functions for ferromagnetic and antiferromagnetic Heisenberg monolayers with general spin (no anisotropies) on the basis of the Tyablikov (RPA) decoupling.

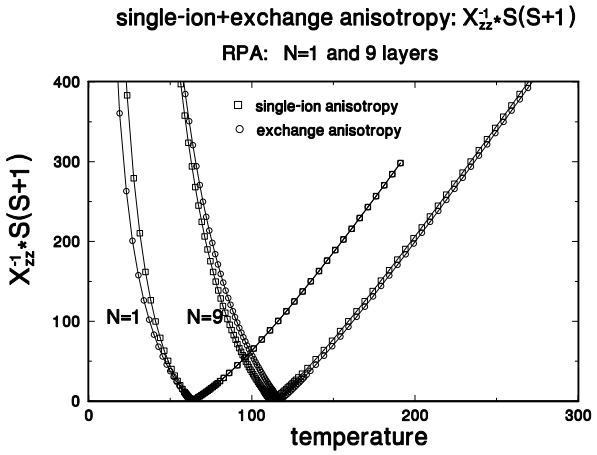

Figure 16: The inverse easy axis susceptibilities χ_{zz}^{-1} of ferromagnetic films in RPA for spin $S = 1$ for a monolayer (N=1) and a multilayer (N=9) as functions of the temperature for single-ion and exchange anisotropies.

.

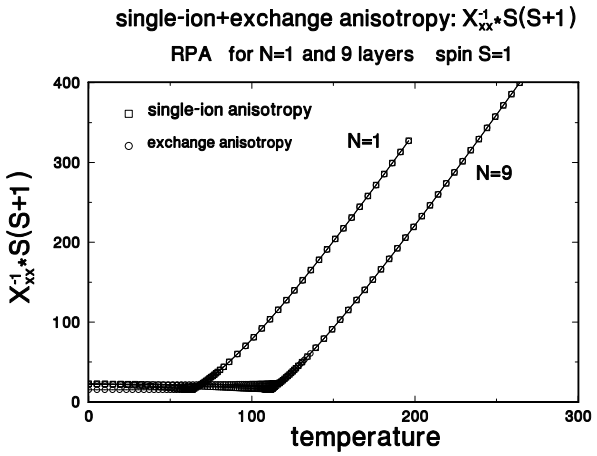

Figure 17: The inverse hard axis susceptibilities χ_{xx}^{-1} of ferromagnetic films in RPA for spin $S = 1$ for a monolayer (N=1) and a multilayer (N=9) as functions of the temperature for single-ion and exchange anisotropies.

4.2.5. Exact treatment of the single-ion anisotropy

Up to now we have worked at the level of the lowest-order GF's, where approximate decoupling schemes lead to closed systems of integral equations which are solved self-consistently. In this subsection, we show that a closed system for the terms stemming from the single-ion anisotropy is attainable without any decoupling by going to higher-order GF's [44], generalizing the work of Devlin [45]. By taking

advantage of relations between products of spin operators [47], one can show that the hierarchy of the equations of motion is automatically closed with respect to the anisotropy terms . In this way, an exact treatment of the single-ion anisotropy results, i.e. anisotropies of arbitrary strength can be treated, whereas e.g. the Anderson-Callen deccoupling of the second-order single-ion anisotropy terms is only reasonable for anisotropies small compared to the exchange interaction. The terms due to the exchange interaction must still be decoupled by a generalized RPA.

We develop the general formulation for a spin-Hamiltonian consisting of an isotropic Heisenberg exchange interaction between nearest neighbour lattice sites, J_{kl}, second-order and fourth-order single-ion lattice anisotropies with strengths $K_{2,k}$ and $K_{4,k}$ respectively, a magnetic dipole coupling with strength g_{kl} and an external magnetic field $\mathbf{B} = (B^x, B^y, B^z)$:

$$\begin{aligned}
\mathcal{H} &= -\frac{1}{2}\sum_{<kl>} J_{kl}(S_k^- S_l^+ + S_k^z S_l^z) \\
&\quad -\sum_k K_{2,k}(S_k^z)^2 - \sum_k K_{4,k}(S_k^z)^4 \\
&\quad -\sum_k \Big(\frac{1}{2}B^- S_k^+ + \frac{1}{2}B^+ S_k^- + B^z S_k^z\Big) \\
&\quad +\frac{1}{2}\sum_{kl}\frac{g_{kl}}{r_{kl}^5}\Big(r_{kl}^2(S_k^- S_l^+ + S_k^z S_l^z) - 3(\mathbf{S}_k\cdot\mathbf{r}_{kl})(\mathbf{S}_l\cdot\mathbf{r}_{kl})\Big)\ , \qquad (201)
\end{aligned}$$

where $S_i^{\pm} = S_i^x \pm iS_i^y$ and $B^{\pm} = B^x \pm iB^y$, k and l being lattice site indices and $\langle kl\rangle$ indicates summation over nearest neighbours only. We have added a fourth-order anisotropy term for which we had no decoupling procedure available when working at the level of the lowest-order GF's.

To allow as general a formulation as possible (with an eye to a future study of the reorientation of the magnetization), we formulate the equations of motion for the Green's functions for all spatial directions:

$$\begin{aligned}
G_{ij}^{+,\mp}(\omega) &= \langle\langle S_i^+; S_j^{\mp}\rangle\rangle_\omega \\
G_{ij}^{-,\mp}(\omega) &= \langle\langle S_i^-; S_j^{\mp}\rangle\rangle_\omega \qquad (202) \\
G_{ij}^{z,\mp}(\omega) &= \langle\langle S_i^z; S_j^{\mp}\rangle\rangle_\omega\ .
\end{aligned}$$

Instead of decoupling the corresponding equations of motion at this stage, as we did in our previous work [28, 9], we add equations for the next higher-order Green's functions:

$$\begin{aligned}
G_{ij}^{z+,\mp}(\omega) &= \langle\langle S_i^z S_i^+ + S_i^+ S_i^z\rangle\rangle = \langle\langle (2S_i^z - 1)S_i^+; S_j^{\mp}\rangle\rangle_\omega \\
G_{ij}^{-z,\mp}(\omega) &= \langle\langle S_i^z S_i^- + S_i^- S_i^z\rangle\rangle = \langle\langle S_i^-(2S_i^z - 1); S_j^{\mp}\rangle\rangle_\omega
\end{aligned}$$

$$
\begin{aligned}
G_{ij}^{++,\mp}(\omega) &= \langle\langle S_i^+ S_i^+; S_j^\mp\rangle\rangle_\omega \\
G_{ij}^{--,\mp}(\omega) &= \langle\langle S_i^- S_i^-; S_j^\mp\rangle\rangle_\omega \\
G_{ij}^{zz,\mp}(\omega) &= \langle\langle (6S_i^z S_i^z - 2S(S+1)); S_j^\mp\rangle\rangle_\omega \ .
\end{aligned} \tag{203}
$$

The particular form for the operators used in the definition of the Green's functions in Eqs. (203) is dictated by expressions coming from the anisotropy terms. Terminating the hierarchy of the equations of motion at this level results in an *exact* treatment of the anisotropy terms for spin $S = 1$, since the hierarchy for these terms breaks off at this stage, as will be shown. The exchange interaction terms, however, still have to be decoupled, which we do with RPA-like decouplings.

For the treatment of arbitrary spin S, it is necessary to use $4S(S+1)$ Green's functions in order to obtain an automatic break-off of the equations-of-motion hierarchy coming from the anisotropy terms. These are functions of the type $G_{ij}^{\alpha,\mp}$ with $\alpha = (z)^n(+)^m$ and $\alpha = (-)^m(z)^n$, where, for a particular spin S, all combinations of m and n satisfying $(n+m) = 2S$ must be taken into account. There are no Green's functions having mixed $+$ and $-$ indices because these can be eliminated by the relation $S^\mp S^\pm = S(S+1) \mp S^z - (S^z)^2$.

Here we treat only the spin $S = 1$ monolayer, for which there are 8 exact equations of motion for the Green's functions defined in (202) and (203).

The crucial point now is that the anisotropy terms in these equations can be simplified by using formulae which reduce products of spin operators by one order. Such relations are derived in Ref. [47]:

$$
\begin{aligned}
(S^-)^m (S^z)^{2S+1-m} &= (S^-)^m \sum_{i=0}^{2S-m} \delta_i^{(S,m)} (S^z)^i, \\
(S^z)^{2S+1-m} (S^+)^m &= \sum_{i=0}^{2S-m} \delta_i^{(S,m)} (S^z)^i (S^+)^m.
\end{aligned} \tag{204}
$$

The coefficients $\delta_i^{(S,m)}$ are tabulated in Ref. [47] for general spin. For spin $S = 1$, only the coefficients with $m = 0, 1, 2$ occur: $\delta_0^{(1,0)} = \delta_2^{(1,0)} = 0; \delta_1^{(1,0)} = 1, \delta_0^{(1,1)} = 0, \delta_1^{(1,1)} = 1, \delta_0^{(1,2)} = 1$.

These relations effect the reduction of the relevant Green's functions coming from the anisotropy terms in the equations of motion

$$
\begin{aligned}
G_{ij}^{(z)^4+,\mp} &= G_{ij}^{(z)^3+,\mp} = G_{ij}^{(z)^2+,\mp} = \frac{1}{2}(G_{ij}^{z+,\mp} + G_{ij}^{+,\mp}), \\
G_{ij}^{-(z)^4,\mp} &= G_{ij}^{-(z)^3,\mp} = G_{ij}^{-(z)^2,\mp} = \frac{1}{2}(G_{ij}^{-z,\mp} + G_{ij}^{-,\mp}), \\
G_{ij}^{(z)^2++,\mp} &= G_{ij}^{z++,\mp} = G_{ij}^{++,\mp}, \\
G_{ij}^{--(z)^2,\mp} &= G_{ij}^{--z,\mp} = G_{ij}^{--,\mp}.
\end{aligned} \tag{205}
$$

The higher Green's functions coming from the anisotropy terms are thus expressed in terms of lower-order functions already present in the hierarchy; i.e. with respect to the anisotropy terms, a closed system of equations of motion results, so that no decoupling of these terms is necessary. In other words, the anisotropy is treated *exactly*. For higher spins, $S > 1$, one can proceed analogously.

No such procedure is available for the exchange interaction terms, which still have to be decoupled. For spin $S = 1$, an RPA-like approximations effects the decoupling:

$$\begin{aligned} \langle\langle S_i^\alpha S_k^\beta; S_j^\mp \rangle\rangle &\simeq \langle S_i^\alpha \rangle G_{kj}^{\beta,\mp} + \langle S_k^\beta \rangle G_{ij}^{\alpha,\mp} \\ \langle\langle S_k^\alpha S_i^\beta S_i^\gamma; S_j^\mp \rangle\rangle &\simeq \langle S_k^\alpha \rangle G_{ij}^{\beta\gamma,\mp} + \langle S_i^\beta S_i^\gamma \rangle G_{kj}^{\alpha,\mp}. \end{aligned} \tag{206}$$

Note that we have constructed the decoupling so as not to break correlations having equal indices, since the corresponding operators form the algebra characterizing the group for a spin $S = 1$ system. For spin $S = 1$, this decoupling model leads to 8 diagonal correlations for each layer i:

$$\langle S_i^+ \rangle, \langle S_i^- \rangle, \langle S_i^z \rangle, \langle S_i^+ S_i^+ \rangle, \langle S_i^- S_i^- \rangle, \langle S_i^z S_i^+ \rangle, \langle S_i^- S_i^z \rangle, \langle S_i^z S_i^z \rangle.$$

These are determined by the 8 decoupled equations. Performing in addition a two-dimensional Fourier transformation to momentum space results in a set of equations of motion which, in compact matrix notation, are

$$(\omega \mathbf{1} - \mathbf{\Gamma}) \mathbf{G}^\mp = \mathbf{A}^\mp, \tag{207}$$

where $\mathbf{G}^\mp$ and $\mathbf{A}^\mp$ are 8-dimensional vectors with components $G^{\alpha,\mp}$ and $A^{\alpha,\mp}$ and $\alpha = +, -, z, z+, -z, ++, --, zz$; $\mathbf{1}$ is the unit matrix. The 8×8 *non-symmetric* matrix $\mathbf{\Gamma}$ is

$$\mathbf{\Gamma} = \begin{pmatrix} H_k^z & 0 & -H_k^+ & \tilde{K_2} & 0 & 0 & 0 & 0 \\ 0 & -H_k^z & H_k^- & 0 & -\tilde{K_2} & 0 & 0 & 0 \\ -\frac{1}{2}H_k^- & \frac{1}{2}H_k^+ & 0 & 0 & 0 & 0 & 0 & 0 \\ \tilde{K_2} - \frac{J_k}{2}\langle 6S^zS^z - 4\rangle & -\langle S^+S^+\rangle J_k & \langle (2S^z-1)S^+\rangle J_k & H^z & 0 & -H^- & 0 & -\frac{1}{2}H^+ \\ \langle S^-S^-\rangle J_k & -\tilde{K_2} + \frac{J_k}{2}\langle 6S^zS^z - 4\rangle & -\langle S^-(2S^z-1)\rangle J_k & 0 & -H^z & 0 & H^+ & \frac{1}{2}H^- \\ -\langle (2S^z-1)S^+\rangle J_k & 0 & 2\langle S^+S^+\rangle J_k & -H^+ & 0 & 2H^z & 0 & 0 \\ 0 & \langle S^-(2S^z-1)\rangle J_k & -2\langle S^-S^-\rangle J_k & 0 & H^- & 0 & -2H^z & 0 \\ 3\langle S^-(2S^z-1)\rangle J_k & -3\langle (2S^z-1)S^+\rangle J_k & 0 & -3H^- & 3H^+ & 0 & 0 & 0 \end{pmatrix}, \tag{208}$$

with the abbreviations

$$\begin{aligned} H_k^\alpha &= B^\alpha + \langle S^\alpha \rangle J(q - \gamma_{\mathbf{k}}), \qquad \alpha = +, -, z \\ H^\alpha &= B^\alpha + \langle S^\alpha \rangle Jq, \qquad \alpha = +, -, z \\ J_k &= J\gamma_{\mathbf{k}}, \\ \tilde{K_2} &= K_2 + K_4. \end{aligned} \tag{209}$$

For a square lattice with a lattice constant taken to be unity, $\gamma_{\mathbf{k}} = 2(\cos k_x + \cos k_y)$, and $q = 4$ is the number of nearest neighbours. For spin $S = 1$ and $S = 3/2$, the K_4 term in the Hamiltonian leads only to a renormalization of the second-order anisotropy coefficient: $\tilde{K_2}(S = 1) = K_2 + K_4$ and $\tilde{K_2}(S = 3/2) = K_2 + \frac{5}{2}K_4$ respectively. Only in the case of higher spins, $S \geq 2$, are there non-trivial corrections due to the fourth- order anisotropy coefficient.

If the theory is formulated only in terms of $\mathbf{G}^-$, there is no equation for determining the $\langle S^+S^+\rangle$ occuring in the $\mathbf{\Gamma}-$matrix. It is for this reason that we introduced G^+ in Eq.(202), for which the $\mathbf{\Gamma}-$matrix is the same, so that, in general, one can take a linear combination of $\mathbf{G}^+$ and $\mathbf{G}^-$ and their corresponding inhomogeneities:

$$\begin{aligned} \mathbf{G} &= (1-a)\mathbf{G}^- + a\mathbf{G}^+, \\ \mathbf{A} &= (1-a)\mathbf{A}^- + a\mathbf{A}^+. \end{aligned} \tag{210}$$

Hence, the equations of motion are

$$(\omega\mathbf{1} - \mathbf{\Gamma})\mathbf{G} = \mathbf{A}, \tag{211}$$

from which the desired correlations $\mathbf{C} = (1-a)\mathbf{C}^- + a\mathbf{C}^+$ can be determined. The parameter a is arbitrary $(0 < a < 1)$.

An examination of the characteristic equation of the $\mathbf{\Gamma}$-matrix reveals that 2 of the eigenvalues are exactly zero, so that the term $\mathbf{R}^0\mathbf{L}^0$ is needed when applying the eigenvector method of Section 3.3. The eigenvector method then yields for the correlations in configuration space $(i = 1, ..., 8)$:

$$C_i = \frac{1}{\pi^2}\int_0^\pi dk_x \int_0^\pi dk_y \sum_{l=1}^{8}\Big(\sum_{j=1}^{6}\sum_{k=1}^{6} R^1_{ij}\mathcal{E}^1_{jk}\delta_{jk}L^1_{kl}A_l + \sum_{j=1}^{2} R^0_{ij}L^0_{jl}C_l\Big). \tag{212}$$

Without loss of generality, the field component B^y can be set to zero, which leads to the symmetry requirements: $\langle S^+\rangle = \langle S^-\rangle$, $\langle S^+S^+\rangle = \langle S^-S^-\rangle$ and $\langle S^zS^+\rangle = \langle S^-S^z\rangle$; i.e. there are only 5 independent variables defining 8 correlations $\mathbf{C}$, i.e. the system of equations is overdetermined. This problem can be overcome with a singular value decomposition: define a vector consisting of the five relevant quantities

$$\mathbf{v} = \begin{pmatrix} \langle S^-\rangle \\ \langle S^z\rangle \\ \langle S^-S^-\rangle \\ \langle S^-S^z\rangle \\ \langle S^zS^z\rangle \end{pmatrix}. \tag{213}$$

Then, the correlations $\mathbf{C}$ can be expressed as

$$\mathbf{C} = \mathbf{u_c^0} + \mathbf{u_c}\mathbf{v} \tag{214}$$

with

$$\mathbf{u_c^0} = \begin{pmatrix} 2-2a \\ 2a \\ 0 \\ 2-2a \\ -2a \\ 0 \\ 0 \\ 0 \end{pmatrix} ; \mathbf{u_c} = \begin{pmatrix} 0 & a-1 & a & 0 & a-1 \\ 0 & a & 1-a & 0 & -a \\ -a & 0 & 0 & 1 & 0 \\ 0 & 1-a & -a & 0 & 3a-3 \\ 0 & a & 1-a & 0 & 3a \\ 2-2a & 0 & 0 & 2a-2 & 0 \\ 0 & 0 & 0 & 2a & 0 \\ 6a-4 & 0 & 0 & 6-12a & 0 \end{pmatrix} . \quad (215)$$

The 8×5 matrix $\mathbf{u_c}$ may be written in terms of its singular value decomposition:

$$\mathbf{u_c} = \mathbf{U}\mathbf{W}\tilde{\mathbf{V}}, \quad (216)$$

where $\mathbf{W}$ is the 5×5 diagonal matrix of singular values which here are all > 0 for $0 < a < 1$. $\mathbf{U}$ is an 8×5 orthogonal matrix and $\mathbf{V}$ is a 5×5 orthogonal matrix. From Eqs. (212) and (214) it follows that

$$\mathbf{u_c v} = \mathbf{R^1}\ \mathcal{E}\ \mathbf{^1L^1}\ \mathbf{A}\ + \mathbf{R^0 L^0}(\mathbf{u_c v} + \mathbf{u_c^0}) - \mathbf{u_c^0}. \quad (217)$$

To get $\mathbf{v}$ from this equation, we need only multiply through by $\mathbf{u_c^{-1}} = \mathbf{V}\mathbf{W^{-1}}\tilde{\mathbf{U}}$, which yields the system of coupled integral equations

$$\mathbf{v} = \mathbf{u_c^{-1}}\Big(\mathbf{R^1}\ \mathcal{E}^{\mathbf{1}}\ \mathbf{L^1}\ \mathbf{A} + \mathbf{R^0 L^0}(\mathbf{u_c v} + \mathbf{u_c^0}) - \mathbf{u_c^0}\Big), \quad (218)$$

or more explicitly with $i = 1, ..., 5$

$$\begin{aligned} v_i \ = \ & \sum_{k=1}^{8} (u_c^{-1})_{ik} \frac{1}{\pi^2} \int_0^\pi dk_x \int_0^\pi dk_y \sum_{j=1}^{8} \Big\{ \sum_{l=1}^{6} R^1_{kl} \mathcal{E}^1_{ll} L^1_{lj} A_j \\ & + \sum_{l=1}^{2} R^0_{kl} L^0_{lj} (\sum_{p=1}^{5} (u_c)_{jp} v_p + (u_c^0)_j \Big\} - \sum_{k=1}^{8} (u_c^{-1})_{ik} (u_c^0)_k. \end{aligned} \quad (219)$$

This set of equations is not overdetermined (5 equations for 5 unknowns in the present example) and is solved by the curve-following method described in Appendix B.

As an example we investigate the magnetization as a function of the second-order anisotropy strength and the temperature for a spin $S = 1$ square monolayer, putting the dipole coupling and the magnetic field equal to zero. In this case the magnetization is in the z-direction only, $\langle S^z \rangle$. The results are shown in Fig. 18 together with those from the Anderson-Callen decoupling. There is rather good agreement for small anisotropies, which, however, worsens as K_2 increases. Another difference concerns the second moments, $\langle S^z S^z \rangle$, which approach the value

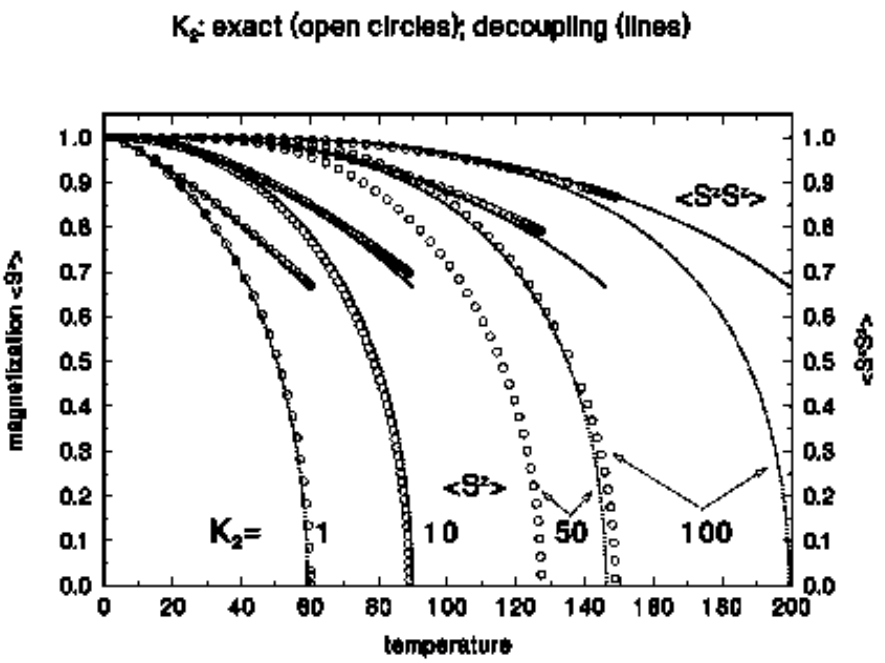

Figure 18: The spin $S = 1$ monolayer with exchange interaction strength $J = 100$. Comparison of GFT calculations for $\langle S^z \rangle$ and $\langle S^z S^z \rangle$ as functions of the temperature for various anisotropies using the exact treatment of the anisotropy (open circles) and the Anderson-Callen decoupling of Section 4.2.1 (small dots).

$\langle S^z S^z \rangle (T \to T_{Curie}) = 2/3$ for the Anderson-Callen decoupling (see Ref. [28]), whereas in the exact treatment, the values of $\langle S^z S^z \rangle (T \to T_{Curie})$ are larger than 2/3. Estimates for the Curie temperature, as e.g. in Refs. [30] or [46], give reasonable values only for small single-ion anisotropies.

To show the difference between the new model and the Anderson-Callen decoupling more clearly, we compare in Fig. 19 the Curie temperatures obtained from MFT, the Green's function theory with the exact treatment of the anisotropy and the Green's function theory with the Anderson-Callen decoupling of Refs. [28, 9]. For small anisotropy, there is only a slight difference between the two GFT results which, in contrast to MFT, obey the Mermin-Wagner theorem. However, for large anisotropy, the GFT results deviate from one another significantly: for $K_2 \to \infty$, the Anderson-Callen result diverges, whereas the exact treatment approaches the MFT limit. This is shown analytically in the appendix of Ref. [44].

Unfortunately, we have not been able to solve the full reorientation problem with the exact treatment of the single-ion anisotropy with the tools developed in Section 3.5, because of numerical difficulties.

When using the Anderson Callen decoupling we obtained rather good results when the external field is in the direction of the anisotropy as long as the anisotropy

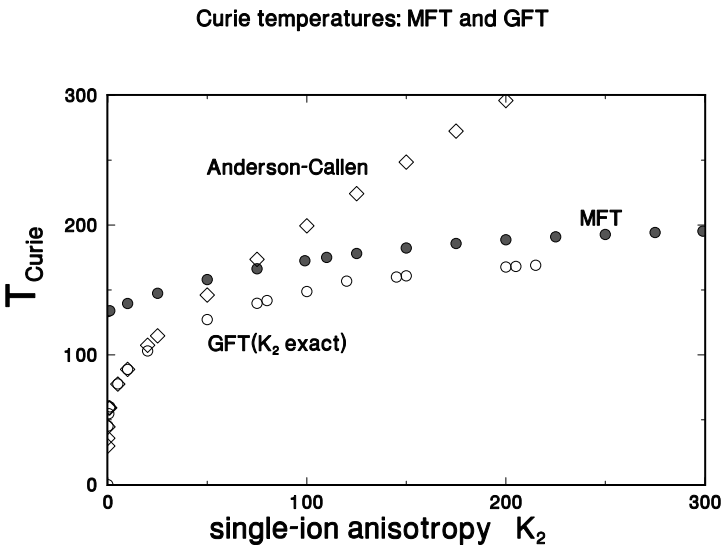

Figure 19: Comparison of the Curie temperatures calculated with the exact treatment of the anisotropy, the Anderson-Callen decoupling and MFT. The first two approaches fulfill the Mermin-Wagner theorem: $T_C \to 0$ for $K_2 \to 0$, whereas MFT does not. For large anisotropies, the exact treatment approaches slowly the MFT result (as also can be shown analytically [44]), whereas the Anderson-Callen decoupling leads to a diverging T_C

is small enough ($K_2 \leq 0.1J$). This is seen by comparing with Quantum Monte Carlo calculations [48]. The approximation is much worse when the field is applied perpendicular to the anisotropy. A considerable simplification and an improvement of the results concerning the reorientation is reported in Ref. [49], where the Anderson-Callen decoupling is made in a frame which is rotated with respect to the original one and in which the magnetization is in the direction of the new z-axis. The reorientation angle is determined from the condition that the magnetization commutes with the Hamiltonian in the rotated frame. In this connection see also Ref. [50], who also apply the approximate Anderson-Callen decoupling in a rotated frame. In Section 4.4.1 we treat the spin reorientation with an exact treatment of the single-ion anisotropy by working also in the rotated frame.

4.2.6. The importance of spin waves in the Co/Cu/Ni trilayer

The importance of spin waves can be demonstrated in Co/Cu/Ni trilayers, where two magnetic layers are separated by a non-magnetic spacer layer. In an experiment, the magnetization of Ni in a Ni/Cu bilayer and a Ni/Cu/Co trilayer is measured as a function of the temperature [53]. Figure 20 shows a shift to higher temperatures of the magnetization curve of Ni for the trilayer system (dots) as compared to the Ni magnetization in the bilayer system (crosses). This shift is largest at the Curie temperature. In the figure, results from Green's function theory are also shown. A Heisenberg exchange interaction and a dipole-dipole interaction can explain the observed shift with realistic strengths [54] for the interlayer coupling $0.5 < J_{inter} < 3.0$ [53], assuming an in-plane magnetization, whereas MFT (owing to the neglect of spin waves) needs unrealistic strong values for J_{inter}. For more recent experimental results concerning Co/Cu/Ni/Cu(100) layers and a comparison with GFT, see Refs. [55, 56] and references therein.

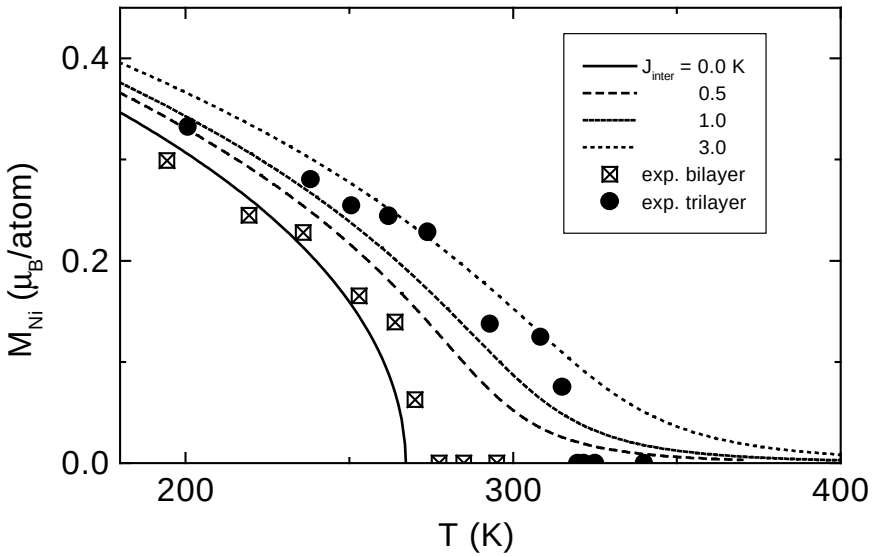

Figure 20: The measured shift of the Ni magnetization curve for the trilayer Co/Cu/Ni system (dots) as compared to the Ni magnetization curve for the bilayer Ni/Cu system (crosses). Green's function theory (lines) can explain this shift with realistic strengths for the interlayer coupling J_{inter} [53], whereas MFT needs unrealistic strong values for J_{inter}.

4.2.7. Temperature dependence of the interlayer coupling

The interlayer coupling between the ferromagnetic layers of Section 4.2.7 is caused by the spin-dependent reflection of spacer electrons at the magnetic/non-magnetic interface leading to a spin-dependent interference and to a renormalisation of the density of states and the free energy within the non-magnetic spacer. The coupling may then be ferromagnetic or antiferromagnetic, oscillating with respect to the spacer thickness with a period depending on the Fermi surface of the spacer. The amplitude and the phase of the coupling is determined mainly by the spacer thickness but may also be influenced by the interface roughness, disorder etc..

The sources of the temperature dependence of the interlayer coupling are discussed in Refs. [57, 58]:

(i) A part of the temperature dependence is induced by the smearing out of the Fermi surface of the spacer, as proposed in [51]. ('spacer effect')

(ii) The temperature dependence also stems from altering the properties of the magnetic layers through spin wave excitations [52]('magnetic layer effect'), which can affect the interlayer coupling.

In Ref. [60], ferromagnetic resonance (FMR) experiments lead to an effective $J_I(T) \sim T^{3/2}$ dependence. Both mechanisms contribute and the dominant mechanism cannot be deduced directly. In Ref.[58], an alternative analysis of FMR measurements is proposed that could distinguish between both mechanisms.

4.3. Antiferromagnetic and coupled ferromagnetic- antiferromagnetic Heisenberg films.

A Green's function theory of antiferromagnetic (AF) and coupled ferro- and antiferromagnetic (AF-AFM)-films relies on periodic structures and therefore requires the introduction of sublattices in which periodicity is guaranteed. We start with a description of an antiferromagnetic monolayer in subsection 4.3.1 and follow this in subsection 4.3.2 with a general formulation in terms of sublattices, which allows a unified treatment of FM , AFM and FM-AFM multilayer-systems.

4.3.1. The antiferromagnetic spin $S = 1/2$ Heisenberg monolayer.

According to the Mermin-Wagner theorem [22] the two-dimensional antiferromagnetic or ferromagnetic Heisenberg monolayers with exchange interaction alone cannot show a finite magnetization. In order to obtain a finite magnetization for the antiferromagnet, one can either introduce an artificial (staggered) field with opposite directions for the up and down spin sublattices [3] or one can introduce anisotropies. We use an exchange anisotropy and demonstrate how the magnetization of an antiferromagnet can be calculated with many-body Green's function theory. The essential step is the introduction of separate sublattices for the up and down spins.

Consider the Hamiltonian

$$\mathcal{H} = -\frac{1}{2}\sum_{<kl>} J_{kl}(S_k^- S_l^+ + S_k^z S_l^z) - \frac{1}{2}\sum_{<kl>} D_{kl}^z S_k^z S_l^z, \tag{220}$$

where the exchange interaction and the exchange anisotropy strengths are negative ($J_{kl} < 0$ and $D_{kl}^z < 0$).

We only consider the magnetization in z-direction. The equation of motion for the relevant Green's function in energy space

$$G_{ij}^{+-} = \langle\langle S_i^+; S_j^- \rangle\rangle \tag{221}$$

is

$$\omega G_{ij}^{+-} = 2\langle S_i^z \rangle \delta_{ij} + \langle\langle [S_i^+, \mathcal{H}]; S_j^- \rangle\rangle. \tag{222}$$

Again, we adopt the Tyablikov (RPA)-decoupling of the higher-order Green's functions occurring on the right-hand side:

$$\langle\langle S_i^z S_l^+; S_j^- \rangle\rangle \approx \langle S_i^z \rangle \langle\langle S_l^+; S_j^- \rangle\rangle \ . \tag{223}$$

This leads to the equation

$$(\omega - \sum_l (J_{il} + D^z_{il})\langle S^z_l\rangle)G^{+-}_{ij} + \langle S^z_i\rangle \sum_l J_{il} G^{+-}_{lj} = 2\langle S^z_i\rangle \delta_{ij}. \tag{224}$$

We now introduce sublattice indices (m, n) for the up (u) and down (d) spins. Four equations of motion corresponding to the pairs $(i_n, j_m) = (u, u), (d, u), (u, d)$ and (d, d) result.

Fourier transforms to momentum space for the sublattices each consisting of $N/2$ lattice sites are

$$\begin{aligned}
G_{mn}(\mathbf{k}) &= \frac{2}{N}\sum_{i_m j_n} G_{i_m j_n} e^{-i\mathbf{k}(\mathbf{R}_{i_m} - \mathbf{R}_{j_n})}, \\
G_{i_m j_n} &= \frac{2}{N}\sum_{\mathbf{k}} G_{mn}(\mathbf{k}) e^{i\mathbf{k}(\mathbf{R}_{i_m} - \mathbf{R}_{j_n})}, \\
\frac{2}{N}\sum_{\mathbf{k}} e^{-i\mathbf{k}(\mathbf{R}_{i_m} - \mathbf{R}_{j_n})} &= \delta_{i_m j_m}, \\
\frac{2}{N}\sum_{i_m} e^{i(\mathbf{k}-\mathbf{k}')\mathbf{R}_{i_m}} &= \delta_{\mathbf{k}\mathbf{k}'},
\end{aligned} \tag{225}$$

where the subscripts of the Green's functions in momentum space $G_{mn}(\mathbf{k})$ now denote sublattice indices and not lattice sites.

Because $\langle S^z\rangle_d = -\langle S^z\rangle_u$ for an antiferromagnet, the 4 equations of motion decouple to two identical pairs of equations which determine $\langle S^z\rangle_u$ or $\langle S^z\rangle_d$ respectively. Before replacing $\langle S^z\rangle_d$ by $-\langle S^z\rangle_u$, the equations for $G^{+-}_{uu}(\mathbf{k})$ and $G^{+-}_{du}(\mathbf{k})$ are

$$\begin{aligned}
\Big(\omega - \langle S^z\rangle_u(J_{uu}(0) - J_{uu}(\mathbf{k}) + D^z_{uu}(0)) \;&-\; \langle S^z\rangle_d(J_{ud}(0) + D^z_{ud}(0)\Big)G^{+-}_{uu}(\mathbf{k}) \\
&+\; \langle S^z\rangle_u J_{ud}(\mathbf{k}) G^{+-}_{du}(\mathbf{k}) = 2\langle S^z\rangle_u \\
\Big(\omega - \langle S^z\rangle_u(J_{du}(0) + D^z_{du}(0)) - \langle S^z\rangle_d(J_{dd}(0) \;&-\; J_{dd}(\mathbf{k}) + D^z_{dd}(0)\Big)G^{+-}_{du}(\mathbf{k}) \\
&+\; \langle S^z\rangle_d J_{du}(\mathbf{k}) G^{+-}_{uu}(\mathbf{k}) = 0\ .
\end{aligned} \tag{226}$$

Restricting the coupling to nearest neighbours only implies that all interaction terms with equal sublattice indices are zero: $J_{uu} = D^z_{uu} = J_{dd} = D^z_{dd} = 0$. After replacing $\langle S^z\rangle_d$ by $-\langle S^z\rangle_u$, the matrix equation is

$$\begin{pmatrix} \omega + \langle S^z\rangle_u(J_{ud}(0) + D^z_{ud}(0)) & \langle S^z\rangle_u J_{ud}(\mathbf{k}) \\ -\langle S^z\rangle_u J_{ud}(\mathbf{k}) & \omega - \langle S^z\rangle_u(J_{ud}(0) + D^z_{ud}(0)) \end{pmatrix} \begin{pmatrix} G^{+-}_{uu}(\mathbf{k}) \\ G^{+-}_{du}(\mathbf{k}) \end{pmatrix} = \begin{pmatrix} 2\langle S^z\rangle_u \\ 0 \end{pmatrix} \tag{227}$$

For a square lattice with lattice constant $a = 1$,

$$\begin{aligned}
J_{ud}(\mathbf{k}) = J_{\mathbf{k}} &= \frac{2}{N}\sum_{i_u l_d} J_{i_u l_d} e^{-i\mathbf{k}(\mathbf{R}_{i_u} - \mathbf{R}_{l_d})} = 2J(\cos k_x + \cos k_y) \\
J_{ud}(0) + D^z_{ud}(0) &= J^z_0 = 4(J + D^z)\ .
\end{aligned} \tag{228}$$

Eliminating $G^{+-}_{du}(\mathbf{k})$ from the two equations yields

$$G^{+-}_{uu}(\mathbf{k}) = \frac{2\langle S^z\rangle_u(\omega - \langle S^z\rangle_u J^z_0)}{(\omega + \langle S^z\rangle_u J^z_0)(\omega - \langle S^z\rangle_u J^z_0) + \langle S^z\rangle^2_u J^2_{\mathbf{k}}} \tag{229}$$

with the poles

$$\omega_{1,2} = \pm\langle S^z\rangle_u \sqrt{((J^z_0)^2 - J^2_{\mathbf{k}})} \tag{230}$$

From the spectral theorem, after integrating over the first Brillouin zone and using the relation $\langle S^- S^+\rangle_u = 1/2 - \langle S^z\rangle_u$ for spin $S = 1/2$, the following equation for the sublattice magnetization $\langle S^z\rangle_u$ for the up-spins results:

$$1/2 + \frac{1}{\pi^2}\int_0^\pi dk_x \int_0^\pi dk_y \frac{\langle S^z\rangle^2_u J^z_0}{\omega_1} \coth(\beta\omega_1/2) = 0\ . \tag{231}$$

This must be iterated to self-consistency in $\langle S^z\rangle_u$. Results for $J = -100$ and $D^z = -0.1, 1.0, -10.0$ are shown in figure 21.

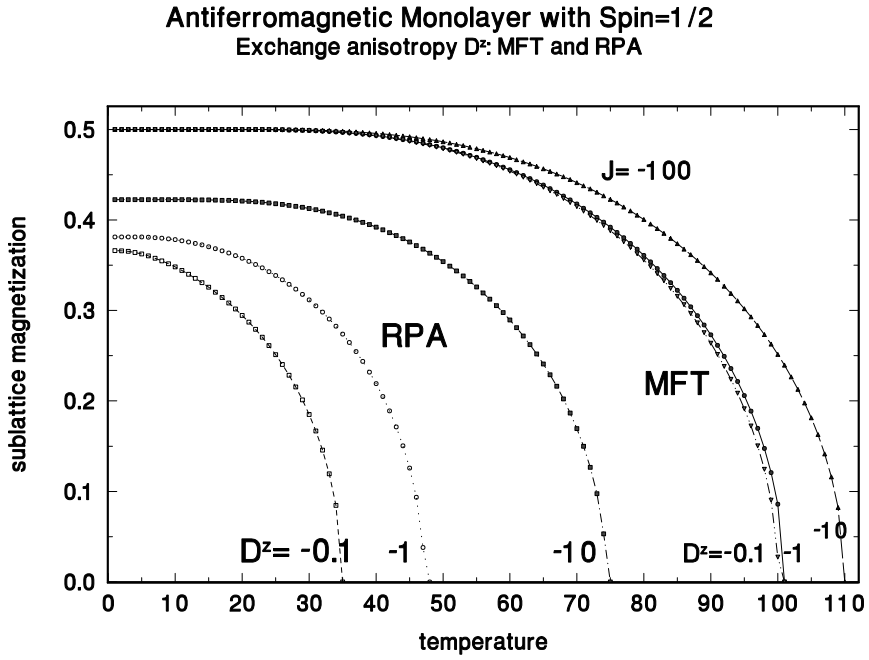

Figure 21: The sublattice magnetization of an antiferromagnetic Heisenberg monolayer with exchange anisotropy as a function of the temperature for RPA and mean field (MFT) calculations for the parameters $J = -100$ and $D^z = -0.1, -1.0, -10.0$.

For the RPA result, the value of the sublattice magnetization at zero temperature is well below its saturation value of $\langle S^z\rangle_u = 1/2$, contrary to the situation for the ferromagnet. This is due to quantum fluctuations. The mean field limit , obtained by setting $J_{\mathbf{k}} = 0$, does not show this suppression and also contradicts the Mermin-Wagner theorem by having a finite Néel temperature for $D^z \to 0$. This theorem ($T_{\text{Néel}} \to 0$ for $D^z \to 0$) is obeyed in the RPA calculation as can be seen by deriving

the Néel temperature from equation (231) by taking first the limit $\langle S^z \rangle \to 0$ and then $D^z \to 0$.

An analytical approximation to the Néel temperature results from a partial fraction decomposition of the expression obtained after expanding the hyperbolic cotangent in eqn (231) for small sublattice magnetization. Then the remaining integrals are expanded around $k_x = k_y = 0$ or around $k_x = k_y = \pi$ repectively with the result

$$T_N \approx \frac{-\pi J}{\ln(1 + \frac{\pi^2}{2D^z/J})}. \tag{232}$$

The values $T_N(D^z = -0.1) = 36.9$, $T_N(D^z = -1.0) = 50.6$ and $T_N(D^z = -10.0) = 80.1$ are only slightly higher (less than 10%) than the results of the exact calculations shown in figure 21.

The extension to AFM multilayers can be found in Refs. [67, 68].

The two-dimensional spin $S = 1/2$ Heisenberg antiferromagnet for a square lattice with nearest neighbour exchange interaction and dipole-dipole coupling (no anisotropy) is treated by Pich and Schwabl in Ref. [61], where they use linear spin wave theory by applying the Holstein-Primakoff transformation [62]. They obtain better results [63] for the Néel temperature (i.e. closer to experimental data) when applying GFT along the lines of Callen [17]. In later papers, they use the same formalism to treat two-dimensional honeycomb antiferromagnets [64] and to study the influence of the dipolar interaction in quasi-one-dimensional antiferromagnets on a hexagonal lattice [65].

4.3.2. A unified formulation for FM, AFM and FM-AFM multilayers

In this section we treat the coupled FM-AFM system in detail [66], introducing sublattices for both the AFM and FM parts. It will then be self-evident that each part by itself can be described as a special case by choosing the signs of the parameters appropriately. This shows that FM, AFM and coupled AFM-FM systems can be handled uniformly within the same formulation.

There is previous work in which Green's function theory treats the coupling of ferromagnetic layers to antiferromagnetic layers: in reference [69], a bilayer is investigated and reference [70] treats an extension to multilayers. In both cases, only a collinear magnetization is considered. In reference [71], a ferromagnetic film is coupled to an antiferromagnetic layer; however, the orientation of the magnetization of the antiferromagnet is frozen. Other work considers an antiferromagnetic coupling between ferromagnetic layers [72, 73, 74].

In our discussion here, we allow a non-collinear magnetization, where the reorientation of the magnetizations of the ferro- and antiferromagnetic layers is determined by the interlayer coupling as in the MFT approach of [78]. We restrict ourselves to Heisenberg systems with spin $S = 1/2$ with an exchange anisotropy. This is not an essential restriction: references [76, 77] show for ferromagnetic layers that through an appropriate choice of anisotropy parameters the exchange- and single-ion anisotropies yield very similar results and that an appropriate scaling leads to universal magnetization curves for different spin quantum numbers. Below, we examine in detail the magnetic arrangement of the simplest system: a perfectly ordered bilayer consisting of a FM monolayer that is coupled to an AFM monolayer.

The starting point is an XXZ-Heisenberg Hamiltonian consisting of an isotropic Heisenberg exchange interaction with strength J_{ij} between nearest neighbour lattice sites, exchange (non-localized) anisotropies in the x- or z-directions having strengths D_{ij}^x and D_{ij}^z respectively and an external magnetic field $\mathbf{B} = (B^x, 0, B^z)$ confined to the film plane, which is the xz-plane:

$$\mathcal{H} = - \frac{1}{2}\sum_{<ij>} J_{ij}(S_i^- S_j^+ + S_i^z S_j^z) - \frac{1}{2}\sum_{<ij>}(D_{ij}^x S_i^x S_j^x + D_{ij}^z S_i^z S_j^z) - \sum_k \Big(B^x S_i^x + B^z S_k^z\Big). \quad (233)$$

Again, $S_i^{\pm} = S_i^x \pm i S_i^y$ and $< ij >$ indicates summation over nearest neighbours only, where i and j are lattice site indices. Because there is no field perpendicular to the film plane ($B^y = 0$), the reorientation of the magnetization can only occur in the xz-plane. For the FM-AFM bilayer we choose the anisotropy of the ferromagnetic layer in the z-direction, D_{ij}^z, and the anisotropy for the antiferromagnetic layer in the x-direction, D_{ij}^x.

For $S = 1/2$, the required commutator Green's functions are

$$G_{ij}^{\alpha-}(\omega) = \langle\langle S_i^{\alpha}; S_j^- \rangle\rangle_{\omega}, \quad (234)$$

where $\alpha = (+, -, z)$ takes care of all directions in space. A generalization to spin quantum numbers $S > 1/2$ is effected in a straight-forward way by introducing $G_{ij}^{\alpha,mn} = \langle\langle S_i^{\alpha}; (S_j^z)^m (S_j^-)^n \rangle\rangle$ with $m + n \leq 2S + 1$ ($m \geq 0;\ n \geq 1;\ m, n$ integer) as in Section 4.2.1.

The equations of motion for the Green's functions in the energy representation are

$$\omega G_{ij}^{\alpha-}(\omega) = A_{ij}^{\alpha-} + \langle\langle [S_i^{\alpha}, \mathcal{H}]; S_j^- \rangle\rangle_{\omega} \quad (235)$$

with the inhomogeneities

$$A_{ij}^{\alpha-} = \langle [S_i^{\alpha}, S_j^-] \rangle = \begin{pmatrix} 2\langle S_i^z \rangle \delta_{ij} \\ 0 \\ -\langle S_i^x \rangle \delta_{ij} \end{pmatrix}, \quad (236)$$

where $\langle ... \rangle = \mathrm{Tr}(... e^{-\beta\mathcal{H}})/\mathrm{Tr}(e^{-\beta\mathcal{H}})$ denotes the thermodynamic expectation value.

In order to obtain a closed system of equations, the higher-order Green's functions on the right hand sides are decoupled as in Section 4.2.1 by a generalized Tyablikov- (RPA) decoupling

$$\langle\langle S_i^{\alpha} S_k^{\beta}; S_j^- \rangle\rangle_{\eta} \simeq \langle S_i^{\alpha} \rangle G_{kj}^{\beta-} + \langle S_k^{\beta} \rangle G_{ij}^{\alpha-}. \quad (237)$$

After introducing two sublattices per layer, the resulting equations are Fourier transformed to momentum space according to eqns. (225), yielding

$$\omega G_{mn}^{\pm-} = \begin{pmatrix} 2\langle S_m^z \rangle \delta_{mn} \\ 0 \end{pmatrix}$$

$$
\begin{aligned}
&\pm\Big(B^z + \sum_p \langle S_p^z\rangle (J_{mp}(\mathbf{0}) + D_{mp}^z(\mathbf{0}))\Big) G_{mn}^{\pm -} \\
&\mp \langle S_m^z\rangle \sum_p (J_{mp}(\mathbf{k}) + \frac{1}{2} D_{mp}^x(\mathbf{k})) G_{pn}^{\pm -} \\
&\mp \frac{1}{2} \langle S_m^z\rangle \sum_p D_{mp}^x(\mathbf{k}) G_{pn}^{\mp -} \\
&\mp \Big(B^x + \sum_p \langle S_p^x\rangle (J_{mp}(\mathbf{0}) + D_{mp}^x(\mathbf{0}))\Big) G_{mn}^{z-} \\
&\pm \langle S_m^x\rangle \sum_p (J_{mp}(\mathbf{k}) + D_{mp}^z(\mathbf{k})) G_{pn}^{z-}, \\
\omega G_{mn}^{z-} \;=\; & -\langle S_m^x\rangle \delta_{mn} \\
&-\frac{1}{2}\Big(B^x + \sum_p \langle S_p^x\rangle (J_{mp}(\mathbf{0}) + D_{mp}^x(\mathbf{0}))\Big) G_{mn}^{+-} \\
&+\frac{1}{2} \langle S_m^x\rangle \sum_p J_{mp}(\mathbf{k}) G_{pn}^{+-} \\
&+\frac{1}{2}\Big(B^x + \sum_p \langle S_p^x\rangle (J_{mp}(\mathbf{0}) + D_{mp}^z(\mathbf{0}))\Big) G_{mn}^{--} \\
&-\frac{1}{2} \langle S_m^x\rangle \sum_p J_{mp}(\mathbf{k}) G_{pn}^{--}.
\end{aligned}
\tag{238}
$$

For a square lattice with lattice constant $a_0 = 1$, one has four nearest-neighbour *intralayer* couplings with sublattice indices n, m from the same layer

$$
\begin{aligned}
J_{mn}(\mathbf{0}) &= q_0\, J_{mn}\ , \qquad J_{mn}(\mathbf{k}) = \gamma_0(\mathbf{k})\, J_{mn}\ , \\
D_{mn}^{x,z}(\mathbf{0}) &= q_0\, D_{mn}^{x,z}\ , \quad D_{mn}^{x,z}(\mathbf{k}) = \gamma_0(\mathbf{k})\, D_{mn}^{x,z}\ ,
\end{aligned}
\tag{239}
$$

with the *intralayer* coordination number $q_0 = 4$ and the momentum-dependent Fourier factor

$$
\gamma_0(\mathbf{k}) = 2(\cos k_x + \cos k_z)\ . \tag{240}
$$

Correspondingly, for the nearest neighbour *interlayer* couplings, m and n now being sublattice indices from different layers, one has

$$
\begin{aligned}
J_{mn}(\mathbf{0}) &= q_{\rm int}\, J_{\rm int}\ , \qquad J_{mn}(\mathbf{k}) = \gamma_{\rm int}(\mathbf{k})\, J_{\rm int}\ , \\
D_{m,n}^{x,z}(\mathbf{0}) &= q_{\rm int}\, D_{\rm int}^{x,z}\ , \quad D_{mn}^{x,z}(\mathbf{k}) = \gamma_{\rm int}(\mathbf{k})\, D_{\rm int}^{x,z}\ .
\end{aligned}
\tag{241}
$$

For sc stacking, the *interlayer* coordination number and the corresponding Fourier factor are given by

$$
q_{\rm int} = \gamma_{\rm int}(\mathbf{k}) = 1\ . \tag{242}
$$

For fcc or bcc stacking,

$$
q_{\rm int} = 4 \quad \text{and} \quad \gamma_{\rm int}(\mathbf{k}) = 4\, \cos(k_x/2)\, \cos(k_z/2). \tag{243}
$$

The mean field approximation is obtained by neglecting the Fourier factors, i.e. $\gamma_0(\mathbf{k}) = \gamma_{\rm int}(\mathbf{k}) = 0$.

By choosing the appropriate signs of the exchange interaction and the exchange anisotropy coupling constants, one can treat ferromagnetic, antiferromagnetic and mixed systems with coupled FM and AFM layers.

The general formalism is valid for any number of layers and sublattices. If Z is the total number of sublattices of the system, the dimension of the set of equations (238) is $3Z^2$. We restrict ourselves here to the investigation of the bilayer, so that there are four sublattices and the system of equations (238) is of dimension 48 with a corresponding Green's function vector. Closer inspection reveals that the system of equations has the following substructure

$$\left(\omega \mathbf{1} - \begin{pmatrix} \mathbf{\Gamma} & 0 & 0 & 0 \\ 0 & \mathbf{\Gamma} & 0 & 0 \\ 0 & 0 & \mathbf{\Gamma} & 0 \\ 0 & 0 & 0 & \mathbf{\Gamma} \end{pmatrix} \right) \begin{pmatrix} \mathbf{G}_1 \\ \mathbf{G}_2 \\ \mathbf{G}_3 \\ \mathbf{G}_4 \end{pmatrix} = \begin{pmatrix} \mathbf{A}_1 \\ \mathbf{A}_2 \\ \mathbf{A}_3 \\ \mathbf{A}_4 \end{pmatrix} \; ; \tag{244}$$

where the diagonal blocks $\mathbf{\Gamma}$ are identical 12×12 matrices, whose explicit form can be read off from equations (238). The sublattice Green's functions $\mathbf{G}_n$ ($n = 1, 2, 3, 4$) are vectors of dimension 12 consisting of 4 subvectors, each of dimension 3:

$$\mathbf{G}_n = \begin{pmatrix} \mathbf{G}_{1n} \\ \mathbf{G}_{2n} \\ \mathbf{G}_{3n} \\ \mathbf{G}_{4n} \end{pmatrix}, \quad n = 1, 2, 3, 4 \; , \tag{245}$$

where the 3-component vectors are

$$\mathbf{G}_{mn} = \begin{pmatrix} \mathbf{G}_{mn}^{+-} \\ \mathbf{G}_{mn}^{--} \\ \mathbf{G}_{mn}^{z-} \end{pmatrix}, \; m = 1, 2, 3, 4 \; . \tag{246}$$

The inhomogeneity vectors have the same structure:

$$\mathbf{A}_n = \begin{pmatrix} \mathbf{A}_{1n}\delta_{1n} \\ \mathbf{A}_{2n}\delta_{2n} \\ \mathbf{A}_{3n}\delta_{3n} \\ \mathbf{A}_{4n}\delta_{4n} \end{pmatrix}, \quad \mathbf{A}_{nm} = \begin{pmatrix} 2\langle S_m^z \rangle \\ 0 \\ -\langle S_m^x \rangle \end{pmatrix}, \qquad m, n = 1, 2, 3, 4 \; . \tag{247}$$

The big equation (244) of dimension 48 for the bilayer can therefore be replaced by 4 smaller equations of dimension 12:

$$(\omega \mathbf{1} - \mathbf{\Gamma}) \mathbf{G}_n = \mathbf{A}_n \quad \text{for } n = 1, 2, 3, 4 \; . \tag{248}$$

It turns out that the 12×12 $\mathbf{\Gamma}$-matrix has 4 zero eigenvalues. In this case we can use the formalism of Section 3.5, where the singular value decomposition of $\mathbf{\Gamma}$ leads

to a system of integral equations for the correlations $\mathbf{C}_n(\mathbf{k})$ corresponding to the GF's $\mathbf{G}_n$ (see eqn (77)):

$$0 = \int d\mathbf{k}\Big(\mathbf{r}\mathcal{E}^{\mathbf{1}}\mathbf{l}\tilde{\mathbf{v}}\mathbf{A}_{-1,n} - \tilde{\mathbf{v}}\mathbf{C}_n(\mathbf{k})\Big) \qquad n = 1, 2, 3, 4. \tag{249}$$

Section 3.5 explains how to find a $\mathbf{k}$-independent vector $\tilde{\mathbf{v}}$ having a layer structure, i.e. $\tilde{\mathbf{v}} = (0, .., 0, \tilde{\mathbf{v}}_n, 0, ., , 0)$. In this way, the non-diagonal correlations disappear from those rows in equation (249) corresponding to $\tilde{\mathbf{v}}_n$ and the $\mathbf{k}$-integration can be performed: $\int d\mathbf{k}\tilde{\mathbf{v}}\mathbf{C}_n(\mathbf{k}) = \tilde{\mathbf{v}} \int d\mathbf{k}\mathbf{C}_n(\mathbf{k}) = \tilde{\mathbf{v}}\mathbf{C}_n$. In the present case $\tilde{\mathbf{v}}_n$ is given by

$$\begin{aligned} \tilde{\mathbf{v}}_n \;\; = \;\; & \Big((\frac{1}{\sqrt{2}}, -\frac{1}{\sqrt{2}}, 1)\delta_{1n}, (\frac{1}{\sqrt{2}}, -\frac{1}{\sqrt{2}}, 1)\delta_{2n}, \\ & (\frac{1}{\sqrt{2}}, -\frac{1}{\sqrt{2}}, 1)\delta_{3n}, (\frac{1}{\sqrt{2}}, -\frac{1}{\sqrt{2}}, 1)\delta_{4n}\Big) \;, \quad n = 1, 2, 3, 4. \end{aligned} \tag{250}$$

Putting equation (250) into equation (249) yields 4 equations which contain the 8 magnetization components implicitly. The necessary additional 4 equations are obtained from the regularity conditions (79)

$$\int d\mathbf{k}\mathbf{L}_0\mathbf{A}_n = \int d\mathbf{k}\tilde{\mathbf{u}}_0\mathbf{A}_n = 0 \;, \qquad n = 1, 2, 3, 4, \tag{251}$$

which are obtained from the regular behaviour of the commutator Green's functions at the origin. The $\tilde{\mathbf{u}}_0$ are the eigenvectors of the singular value decomposition spanning the null-space of the matrix $\mathbf{\Gamma}$. The resulting 8 integral equations are solved self-consistently by the curve-following method described in detail in the Appendix B. Note that the $\tilde{\mathbf{u}}_0$ are determined numerically only up to an orthogonal transformation. To ensure proper behaviour as a function of $\mathbf{k}$, $\tilde{\mathbf{u}}_0$ must be calibrated at each $\mathbf{k}$. A procedure for doing this is indicated in Section 3.5 and presented in detail in an appendix of reference [13].

We now present results for the bilayer ferromagnet, the bilayer antiferromagnet and the coupled ferro- and antiferromagnetic bilayer. All calculations are for an in-plane orientation of the spins of both layers. In each case we compare the results of Green's function theory (GFT) with those of mean field theory (MFT) obtained by putting the momentum-dependent terms equal to zero. In order to see the effects of the interlayer coupling most clearly, we use different exchange interaction strengths for each layer:

(a) FM-FM: $J_{1\mathrm{FM}} = 100, J_{2\mathrm{FM}} = 50$,

(b) AFM-AFM: $J_{1\mathrm{AFM}} = -100, J_{2\mathrm{AFM}} = -50$,

(c) FM-AFM: $J_{\mathrm{FM}} = 100, J_{\mathrm{AFM}} = -50$.

Because of the Mermin-Wagner theorem [22], anisotropies are required in the Green's function description: we take $D^z = +1.0$ for FM layers and $D^x = -1.0$ for AFM

layers. These values are appropriate for 3d transition metal systems. For a compensated interface, the magnetizations of the FM and AFM layers are almost orthogonal to each other even at $T = 0$ because of the interface exchange interaction J_{int}. We choose the FM magnetization to be oriented in the z-direction and the AFM magnetization in the x-direction. Our particular choice of the anisotropies supports this arrangement not only at $T = 0$ but also at finite temperatures. For other choices of anisotropies, the magnetic arrangement could be different. The interlayer coupling is assumed to be positive for the ferromagnetic bilayer and negative for the antiferromagnetic bilayer. For the coupled FM-AFM system, both signs are used. We consider three interlayer coupling constants with strength $J_{int} = 30,\ 75,\ 160$, one smaller than the weakest exchange interaction, one larger than the strongest exchange interaction and one in between.

The ferromagnetic and the antiferromagnetic bilayers

Results for the FM and AFM bilayers are presented in this subsection in order to have a basis for discussing the differences from the coupled FM-AFM bilayer.

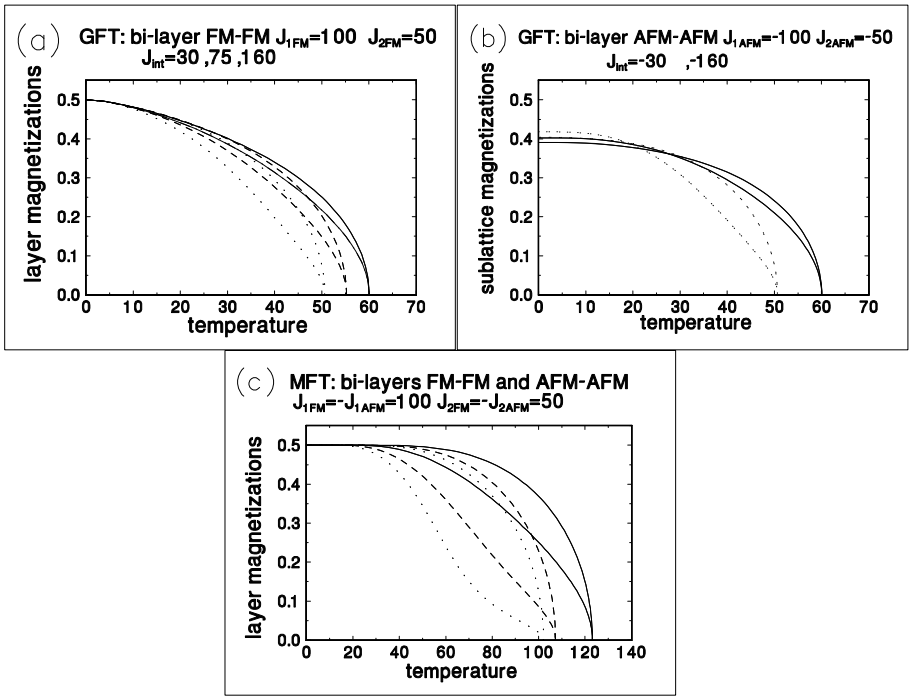

Figure 22: (a) Green's function theory (GFT) for the ferromagnetic bilayer: The sublattice magnetizations are displayed as a function of the temperature for different interlayer couplings $J_{\rm int} = 30$ (dotted), 75 (dashed), 160 (solid). The exchange interaction and anisotropy constants are $J_{\rm 1FM} = 100,\ J_{\rm 2FM} = 50,\ D^z_{\rm 1FM} = 1.0,\ D^z_{\rm 2FM} = 1.0$.
(b) GFT for the antiferromagnetic bilayer: The sublattice magnetizations are displayed as a function of the temperature for two interlayer couplings $J_{\rm int} = -30$ (dotted), -160 (solid). The exchange interaction and anisotropy constants are $J_{\rm 1AFM} = -100,\ J_{\rm 2AFM} = -50,\ D^x_{\rm 1AFM} = -1.0, D^x_{\rm 2AFM} = -1.0$.
(c) Mean field theory (MFT) for the ferromagnetic and antiferromagnetic bilayers with identical parameters: $J_{\rm 1(2)FM} = |J_{\rm 1(2)AFM}|$, $D_{\rm 1(2)FM} = |D_{\rm 1(2)AFM}|$, $J_{\rm intFM} = |J_{\rm intAFM}|$.

In figure 22a, we show the sublattice magnetizations of the ferromagnetic bilayer as a function of the temperature for three interlayer couplings calculated with Green's function theory (GFT). The magnetization profiles are different for the two layers (the magnetization is larger for the layer with the larger exchange interaction) but end in a common Curie temperature, which increases with the strength of the

interlayer coupling: $T_{\text{Curie}} = 50.66,\ 55.24,\ 60.04$.

For the antiferromagnetic bilayer, the parameters are the same as for the ferromagnetic bilayer except for a sign change. In figure 22b we show the sublattice magnetizations of the antiferromagnetic bilayer for two interlayer coupling strengths calculated with Green's function theory. To avoid clutter, we have left out the result for the intermediate interlayer coupling strength. The corresponding magnetization curves lie in between those of the other couplings. At low temperatures one observes clearly the well-known reduction of the magnetization due to quantum fluctuations, which are missing in MFT, see figure 22c. Since $|J_{1\text{AFM}}| > |J_{2\text{AFM}}|$ this reduction is larger for the first layer. With increasing temperature the magnetization curves of the two layers cross each other (a fact which was first observed by Diep [67]) and finally end in a common Néel temperature. A larger interlayer coupling leads to a larger suppression of the magnetization at low temperatures and to a larger Néel temperature. Whereas with the present choice of parameters the magnetization profiles of the FM and AFM bilayers are rather different at low temperatures, the critical temperatures turn out to be identical: $T_{\text{Curie}} = T_{\text{Néel}}$ (cf. figures 22(a) and (b)), a fact already discussed by Lines [83].

For comparison, we show in figure 22(c) the results of mean field theory (MFT) with the same parameters. The magnetization profiles as well as the critical temperatures are identical for the ferromagnetic and antiferromagnetic bilayers. As is well known, the Curie (Néel) temperatures ($T_{\text{Curie(Néel)}} = 102.10,\ 107.25,\ 123.16$) are much larger (with the present choice of parameters by about a factor of 2) in MFT owing to the missing magnon excitations. In MFT the Curie temperature is not very sensitive to the anisotropies as long as they are much smaller than the exchange interaction. In GFT, however, the sensitivity is very much greater because of the Mermin-Wagner theorem [22] ($T_{\text{Curie(Néel)}} \to 0$ for $D^{z(x)} \to 0$). Also, the effect of the interlayer coupling on the magnetization profiles is much stronger in MFT than in GFT.

The coupled ferro-antiferromagnetic bilayer

This is the most interesting case. We consider here two in-plane magnetization com-

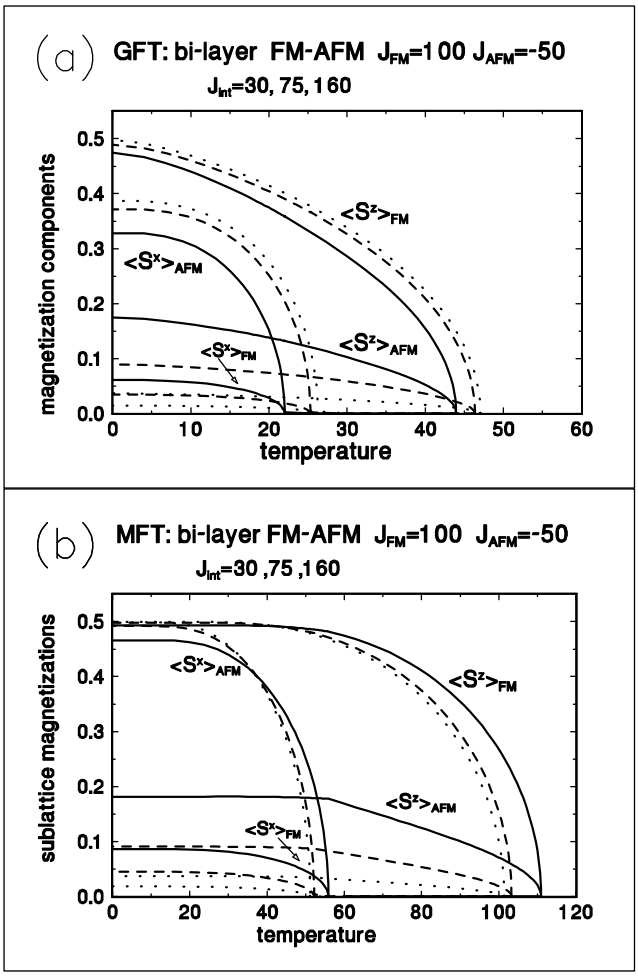

Figure 23: (a) Green's function theory(GFT): the sublattice magnetizations of the ferro- and antiferromagnetic sublattices are displayed as a function of the temperature for different interlayer couplings $J_{\rm int} = 30,\ 75,\ 160$. The exchange interaction and anisotropy constants are $J_{\rm FM} = 100,\ J_{\rm AFM} = -50,\ D^x_{\rm AFM} = -1.0,\ D^z_{\rm FM} = 1.0$. (b) Mean field theory (MFT) with the same parameters.

ponents of each sublattice, thus allowing noncollinear magnetizations in both the FM and AFM layers. Our computer code, when specialized to a single magnetization direction, reproduces the results of reference [69]. Without interlayer coupling, the code also reproduces the results for the monolayer ferromagnet and monolayer antiferromagnet simultaneously. The choice of anisotropies supports the orthogonal arrangement of the magnetizations of the FM and AFM layers favoured by the exchange interaction alone. The interlayer coupling destroys the perpendicular ori-

entation of the ferromagnet (in z-direction) with respect to the antiferromagnet (in x-direction), even at temperature $T = 0$, as can be seen from figure 23. In this figure, we show the sublattice magnetizations calculated with GFT for three interlayer coupling strengths. With a positive interlayer coupling, all sublattice magnetizations develop a positive z-component, whereas the x-components of the two sublattice magnetizations in each layer oppose each other. With increasing temperature, all x-components decrease until they vanish at a common temperature $T^*_{\text{Néel}}$, slightly above the Néel temperature of the uncoupled AFM. For $T > T^*_{\text{Néel}}$ all sublattice magnetizations point in the positive z-direction. The AFM layer assumes a ferromagnetic arrangement and remains so until a common critical temperature T_C is reached, at which the magnetic order vanishes altogether.

Multilayers

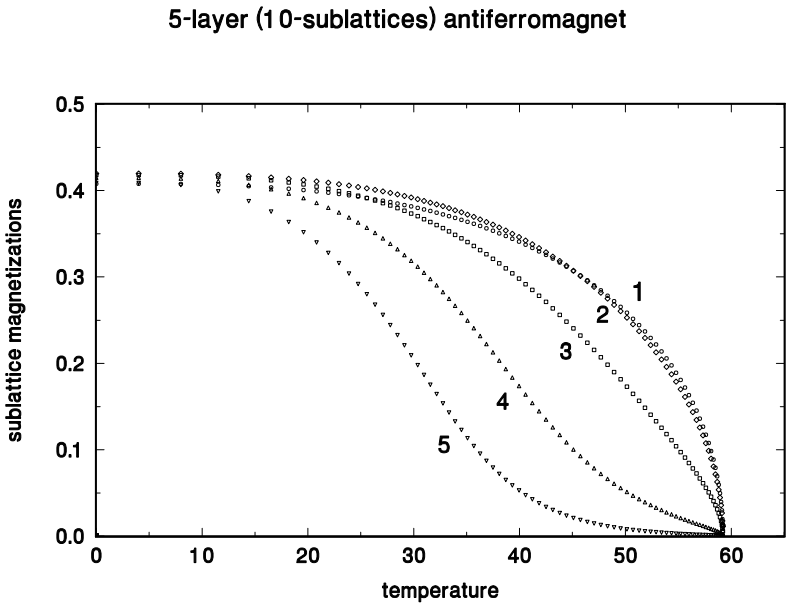

Figure 24: Green's function theory (GFT): Sublattice magnetizations of a 5-layer (10 sublattices) antiferromagnetic as function of the temperature. Parameters: $J_{11} = -100$ $J_{12} = -30$ $J_{22} = -86,66$ $J_{23} = -20$ $J_{33} = -73,33$ $J_{34} = -10$ $J_{44} = -60$ $J_{45} = -8.66$ $J_{55} = -46,66$ $D_{ii}^{x} = -1.0$ $(i = 1, ..., 5)$.

The model is easily extended to ferromagnetic, antiferromagnetic and coupled ferromagnetic-antiferromagnetic multilayers with individual parameters for each layer. It is only a question of computer time. As an example we show in Fig. 24 the results of a 5-layer (10 sublattices) antiferromagnet, where each layer has a different exchange interaction strength so as not to clutter the diagram.

The theory could possibly serve as a basis for studying the exchange bias effect, where it seems, however, to be necessary to include interface disorder [79, 80, 81] in some way, for instance by introducing more sublattices per layer with different magnetic arrangements.

4.4. Working in the rotated frame

In our exposition of GF-theory (e.g. see section 4.2.2), the higher-order Green's functions are all decoupled in a similar way independently of whether they are constructed from S^-, S^+, or S^z operators or from mixed products of these. This might be a general weak point in the decoupling procedure—indeed, there is evidence that this democratic approach ignores essential differences in the roles of these operators. In particular, GF-estimates of the internal energy and specific heat are not as reliable as those for the magnetization and it appears that this might be traceable to an inferior decoupling of the Green's functions transverse to the z-direction, which we normally choose to be in the direction of the anisotropy.

Some recent publications [49, 50] suggest that working in a rotated coordinate system may provide a way to correct this deficiency, especially when considering the field-induced reorientation of the magnetization of a ferromagnetic Heisenberg film. The idea is that since the decoupling procedure for the single-ion anisotropy appears to function better in the direction of the magnetization than in the transverse direction, it ought to be better to change first to a rotated coordinate system where the decoupling can be carried out in the direction of the magnetization only. The angle of the rotation is determined from the condition that the commutator of $S^{z\,\prime}$ with the Hamiltonian vanish in the rotated frame: $[S^{z\,\prime}, H^{\,\prime}] = 0$, where the prime refers to the rotated frame. This procedure is remarkably successful [49] in calculating the magnetic reorientation of a ferromagnetic film as a function of the external magnetic field in the presence of a single-ion anisotropy, as can be shown by comparing with the Quantum Monte Carlo calculations of Ref. [48]. Not only that: the requirement $[S^{z\,\prime}, H^{\,\prime}] = 0$ leads to an equation-of-motion matrix having no null-space—an enormous simplification of the entire calculation!

Because of the apparent advantages of this new approach, we dedicate an entire subsection to it. First, we show how to implement the procedure, applying it to the exact treatment of the single-ion anisotropy; then, we present some of our own results and those of others [49, 82]; finally, we discuss the method, examining the assumptions and pointing out some difficulties.

4.4.1. The ferromagnetic film with an exact treatment of the single-ion anisotropy

In this section, we show how to implement the GF-theory in the rotated frame for a typical case: the field-induced spin reorientation transition for spin $S \geq 1$. We go beyond the treatment in [49, 50] in that we treat the single-ion anisotropy exactly [59].

Consider the Hamiltonian (201) with a field $\mathbf{B} = (B_0^x, 0, B_0^z)$ but without the dipole-dipole interaction and the K_4-term. As the external B_0^x-field is increased from zero, the magnetization vector initially in the z-direction rotates by an angle θ in the xz-plane, so that it points in the z'-direction of a new frame (x', y', z'). As in Ref. [49], we shall do the calculations in the primed system, in which the magnetization vector has the components $(0, 0, \langle S^{z\,\prime}\rangle)$. The transformation between the frames is

$$\begin{pmatrix} \langle S^x\rangle \\ \langle S^y\rangle \\ \langle S^z\rangle \end{pmatrix} = \begin{pmatrix} \cos\theta & 0 & \sin\theta \\ 0 & 1 & 0 \\ -\sin\theta & 0 & \cos\theta \end{pmatrix} \begin{pmatrix} \langle S^{x\,\prime}\rangle \\ \langle S^{y\,\prime}\rangle \\ \langle S^{z\,\prime}\rangle \end{pmatrix}. \tag{252}$$

Because $\langle S^{x\,\prime}\rangle = \langle S^{y\,\prime}\rangle = 0$ in the rotated frame, one need only calculate $\langle S^{z\,\prime}\rangle$ in order to find the components of the magnetization in the original frame, once the angle θ is known.

To get the angle θ, an *approximation* is introduced: we demand that the commutator of $S^{z\,\prime}$ with the Hamiltonian in the rotated system vanish. This implies that the following Green's function is zero:

$$G_{ij}^{z,-} = \langle\langle [S_i^{z\,\prime}, H']; S_j^{-\,\prime}\rangle\rangle = 0. \tag{253}$$

Evaluating the commutator yields a relation between Green's functions $G_{ij}^{+,-} = \langle\langle S_i^{+\,\prime}; S_j^{-\,\prime}\rangle\rangle$ and $G_{ij}^{z+,-} = \langle\langle (2S_i^z - 1)S_i^+; S_j^-\rangle\rangle$,

$$(B_0^x \cos\theta - B_0^z \sin\theta) G_{ij}^{+,-} - K_2 \sin\theta\cos\theta G_{ij}^{z+,-} = 0, \tag{254}$$

which, after applying the spectral theorem, produces the equation defining the reorientation angle in terms of the corresponding diagonal correlations:

$$(B_0^x \cos\theta - B_0^z \sin\theta) C^{-,+} - K_2 \sin\theta\cos\theta C^{-,z+} = 0\ . \tag{255}$$

This is a generalization of the angle condition given in Refs [49, 50] that can be used for the exact treatment of the single-ion anisotropy instead of applying the Anderson-Callen decoupling. Note that, as used here, the condition on the commutator must be considered an *approximation*. In Refs [49, 50] the condition is fulfilled automatically because of the use of the Andersen-Callen decoupling. In general, the condition *does not hold*, as will be shown later.

Following Ref. [49], we introduce another approximation that in general also does not hold: we neglect all GF's not containing an equal number of $S^{-\,\prime}$ and $S^{+\,\prime}$ operators.

After transforming the Hamiltonian to the primed system and making the above approximations, the following Green's functions are needed:

$$\begin{aligned} G_{ij}^{+,-} &= \langle\langle S_i^{+\,\prime}; S_j^{-\,\prime}\rangle\rangle\ , \\ G_{ij}^{(z)^n+,-} &= \langle\langle (S_i^{z\,\prime})^{n-1}(2S_i^{z\,\prime} - 1)S_i^{+\,\prime}; S_j^{-\,\prime}\rangle\rangle\ . \end{aligned} \tag{256}$$

The single-ion anisotropy requires that spin $S \geq 1$. Thus, in order to treat films with $S = 1, 3/2, 2, ...$, one needs the first Green's function and those for $n = 1, 2, 3, ...$ To get the equations of motion, the exchange interaction terms are treated by a generalized Tyablikov (RPA)-decoupling in which products of spin operators with equal indices are retained

$$\langle\langle (S_i^z\ ')^n S_k^+\ '; S_j^-\ '\rangle\rangle \simeq \langle (S_i^z\ ')^n\rangle \langle\langle S_k^+\ '; S_j^-\ '\rangle\rangle + \langle S_k^+\ '\rangle \langle\langle (S_i^z\ ')^n; S_j^-\ '\rangle\rangle\ . \qquad (257)$$

Now in the rotated system, $\langle S_k^+\ '\rangle = 0$; i.e. the second term vanishes. After applying the decoupling procedure and performing a Fourier transform to momentum space, one obtains the following set of equations of motion.

$$\begin{aligned}
\omega G^{+,-} &= 2\langle S^z\ '\rangle + \langle S^z\ '\rangle J(q-\gamma_{\mathbf{k}}) G^{+,-} \\
&\quad + (B_0^x \sin\theta + B_0^z \cos\theta) G^{+,-} + K_2(1 - \tfrac{3}{2}\sin^2\theta) G^{z+,-}, \\
\omega G^{z+,-} &= (6\langle (S^z\ ')^2\rangle - 2S(S+1)) - \tfrac{1}{2} J\gamma_{\mathbf{k}} \Big(6\langle (S^z\ ')^2\rangle - 2S(S+1)\Big) G^{+,-} \\
&\quad + Jq\langle S^z\ '\rangle G^{z+,-} + (B_0^x \sin\theta + B_0^z \cos\theta) G^{z+,-} \\
&\quad + K_2(1 - \tfrac{3}{2}\sin^2\theta)\Big(2G^{(z)^2+,-} - G^{z+,-}\Big)\ , \\
\omega G^{(z)^2+,-} &= 8\langle (S^z\ ')^3\rangle + 3\langle (S^z\ ')^2\rangle - (4S(S+1)-1)\langle S^z\ '\rangle - S(S+1) \\
&\quad + J\gamma_{\mathbf{k}}\Big(\tfrac{1}{2}S(S+1) + (2S(S+1)-1)\langle S^z\ '\rangle - \tfrac{3}{2}\langle (S^z\ ')^2\rangle - 4\langle (S^z\ ')^3\rangle\Big) G^{+,-} \\
&\quad + Jq\langle S^z\ '\rangle G^{(z)^2+,-} + (B_0^x \sin\theta + B_0^z \cos\theta) G^{(z)^2+,-} \\
&\quad + K_2(1 - \tfrac{3}{2}\sin^2\theta)\Big(2G^{(z)^3+,-} - G^{(z)^2+,-}\Big)\ ; \\
\omega G^{(z)^3+,-} &= 10\langle (S^z\ ')^4\rangle + 8\langle (S^z\ ')^3\rangle - (6S(S+1)-5)\langle (S^z\ ')^2\rangle \\
&\quad - (4S(S+1)-1)\langle S^z\ '\rangle - S(S+1) \\
&\quad + J\gamma_{\mathbf{k}}\Big(\tfrac{1}{2}S(S+1) + (2S(S+1) - \tfrac{1}{2})\langle S^z\ '\rangle + (3S(S+1) - \tfrac{5}{2})\langle (S^z\ ')^2\rangle \\
&\quad - 4\langle (S^z\ ')^3\rangle - 5\langle (S^z\ ')^4\rangle\Big) G^{+,-} \\
&\quad + Jq\langle S^z\ '\rangle G^{(z)^3+,-} + (B_0^x \sin\theta + B_0^z \cos\theta) G^{(z)^3+,-} \\
&\quad + K_2(1 - \tfrac{3}{2}\sin^2\theta)\Big(2G^{(z)^4+,-} - G^{(z)^3+,-}\Big)\ . \qquad (258)
\end{aligned}$$

Here $a = 1$ is the lattice constant for a square lattice, $q = 4$ the number of nearest neighbours, and $\gamma_{\mathbf{k}} = 2(\cos k_x + \cos k_y)$.

As they stand, the equations (258) do not form a closed system. This, however, can be achieved by using formulas derived in Ref. [47] that reduce products of spin operators by one order (!), allowing the expression of some higher-order Green's functions in terms of lower order ones:

$$\begin{aligned}
\text{for S} = 1: &\qquad G^{(z)^2+,-} = \tfrac{1}{2}(G^{z+,-} + G^{+,-})\ , \\
\text{for S} = 3/2: &\qquad G^{(z)^3+,-} = G^{(z)^2+,-} + \tfrac{3}{4}G^{z+,-}\ , \\
\text{for S} = 2: &\qquad G^{(z)^4+,-} = \tfrac{3}{2}G^{(z)^3+,-} + \tfrac{7}{4}G^{(z)^2+,-} \\
&\qquad - \tfrac{9}{8}G^{z+,-} - \tfrac{9}{8}G^{+,-}\ . \qquad (259)
\end{aligned}$$

Inserting these relations into the system of equations (258) produces a closed system of equations.

The equations of motion can be written in compact matrix notation

$$(\omega \mathbf{1} - \mathbf{\Gamma})\mathbf{G} = \mathbf{A}. \tag{260}$$

The quantities $\mathbf{\Gamma},\ \mathbf{G},$ and $\mathbf{A}$ can be read off from equation (258), where the *non-symmetric* matrix $\mathbf{\Gamma}$ is a $(2 \times 2),\ (3 \times 3),\ (4 \times 4)$ -matrix for spins $S = 1,\ 3/2,\ 2,$ respectively. The desired correlation vector corresponding to the Green's functions (256),

$$\mathbf{C} = \begin{pmatrix} \langle S^- \, 'S^+ \, ' \rangle \\ \langle S^- \, 'S^{(z')^{n-1}} (2S^z \, ' - 1) S^+ \, ' \rangle \end{pmatrix}, \tag{261}$$

is obtained via the spectral theorem. With the eigenvector method of Section 3.3, the components of the correlation vector $\mathbf{C}$ in configuration space are found to be

$$\begin{aligned} C_i \ &= \ \int d\mathbf{k} C_i(\mathbf{k}) = \frac{1}{\pi^2} \int_0^\pi dk_x \int_0^\pi dk_y \sum_{j,k,l=1}^{2S} R_{ij} \epsilon_{jk} L_{kl} A_l \\ &\quad (i = 1, 2, .., 2S), \end{aligned} \tag{262}$$

where the integration is over the first Brillouin zone and $\mathbf{R}(\mathbf{L})$ are matrices comprising the columns (rows) of the right (left) eigenvectors of the matrix $\mathbf{\Gamma}$ and $\epsilon_{jk} = \delta_{jk}/(e^{\beta\omega_j} - 1)$ is a diagonal matrix, in which ω_j are the eigenvalues $(j = 1, .., 2S)$ of the $\mathbf{\Gamma}$-matrix. In sharp contrast to section 4.2.5, there are no zero eigenvalues of $\mathbf{\Gamma}$!

Equation (255) and the set of integral equations (262) have to be iterated simultaneously to self-consistency in order to obtain the magnetization $\langle S^z \, ' \rangle$ and its moments in the rotated system together with the reorientation angle θ. The curve-following method described in appendix B accomplishes this with alacrity as before. The components of the magnetizations in the coordinate system in which the magnetic reorientation is measured follow from the relations (252). With the formulas from Ref. [47] it would be possible to treat the fourth-order anisotropy term $-\sum_i K_{4,i} (S_i^z)^4$ exactly. A generalization to multilayers is also possible.

4.4.2. Results of calculations in the rotated frame

Here we describe results of calculations in the rotated frame, including results from the method described above.

The paper [49] deals with the Heisenberg ferromagnet with weak single-ion anisotropy in a varying transverse field. The Anderson-Callen decoupling is used in the rotated frame. The small anisotropies (e.g. for $S = 2,\ K_2 = 0.01J$) are

appropriate to 3d transition metals. For the reorientation as a function of the transverse field, there is excellent agreement with QMC calculations[48], see Fig. 25. In particular, the correlation $\langle S^x \rangle / S$ is a linear function of B^x, which is an improvement over calculations in the original coordinate system [28], where the decoupling is performed for GF's corresponding to the components of the magnetization in the non-rotated frame.

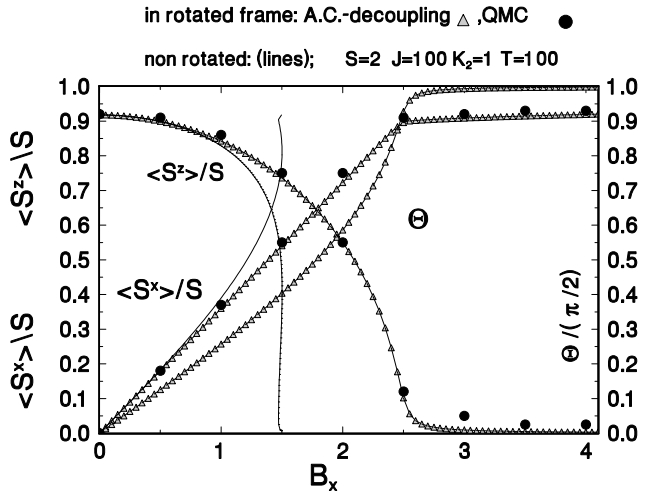

Figure 25: Normalized magnetizations $\langle S^z \rangle / S$ and $\langle S^x \rangle / S$ and the reorientation angle Θ for a spin S=2 Heisenberg monolayer for a weak anisotropy as a function of the external field: QMC [48](solid circles), Anderson-Callen decoupling in the rotated frame [49](triangles) and in the non-rotated frame [28](lines).

If the anisotropy is treated exactly (see the previous subsection), the same thing is found, there being no difference from the results of Ref. [49] for weak anisotropies within the line thickness. This astonishingly good result is perhaps the main point in favour of working in the rotated system.

For the lanthanides, where values of the anisotropy can be of the order of the exchange interaction, the Andersen-Callen decoupling should break down and one would expect the exact treatment of the anisotropy to be superior. Surprisingly, the Anderson-Callen decoupling in the rotated frame still yields excellent results when compared with the exact treatment of K_2 and with QMC results [48] for anisotropies up to $K_2 \leq 0.2J$. This is seen in Fig. 26 for the magnetic reorientation induced by the transverse B^x-field for $K_2 = 0.2J$ and $T = J = 100$. The results of both Green's function theories (Anderson-Callen decoupled and exact treatment of the single-ion anisotropy) are nearly identical and deviate only slightly from the Quantum Monte Carlo results, which can be considered exact to within the statistical error. The reason for this is that at $T = 100$, the magnetizations from the two theories still lie very close to each other; at higher temperatures, this is no longer the case and the

results diverge beyond a certain value of B^x.

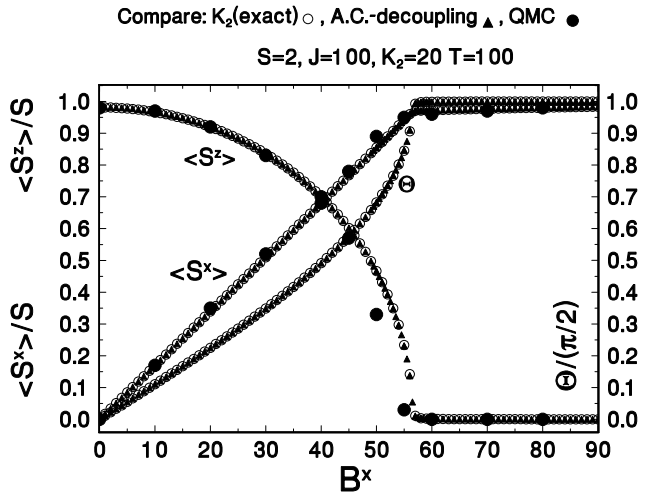

Figure 26: Normalized magnetizations $\langle S^z\rangle/S$ and $\langle S^x\rangle/S$ and the reorientation angle Θ for a spin S=2 Heisenberg monolayer as a function of the external field: QMC [48](solid circles), Anderson-Callen decoupling [49](triangles), present theory [59] (open circles).

Large differences must also appear as the anisotropy strength is increased, since it is known that the results from the Andersen-Callen decoupling do not approach the correct limit. This is evident from Fig. 27, where the field-induced reorientation for a Heisenberg monolayer with $S = 2$ from each GF theory is compared for a temperature somewhat below the reorientation temperature and for a large anisotropy $K_2 = 0.5J$ ($T/J = 4.9$). In this case, implementation of the Anderson-Callen decoupling along the lines of [49] leads to a discontinuous transition from an angle ($\theta/(\pi/2) \approx 0.6$) to full reorientation ($\theta/(\pi/2) = 1$), whereas exact treatment of the anisotropy K_2 produces a continuous reorientation transition. Such discontinuous transitions are also reported in Ref. [50] for a treatment which is very similar to that of Ref. [49]. The reason why discontinuities are not observed in Ref. [49] is that only very small anisotropies are considered there. We attribute the discontinuous transition to the approximate Anderson-Callen decoupling, which is not justified for large anisotropy. The difference between the corresponding reorientation fields, B_R, increases with anisotropy. For the present case it is: $B_R^{\mathrm{K}_2^{\mathrm{exact}}} - B_R^{\mathrm{A.C.}} \simeq 11$ (for $\mathrm{K}_2 = 0.5\mathrm{J}$).

Unfortunately, we cannot say anything about the accuracy of the model treating the anisotropy exactly because there are no QMC calculations available for large anisotropies. The least understood approximation in this model is the generalised RPA decoupling of the exchange interaction terms of the higher-order GF, eqn.(257) . Previous calculations [14] have shown (by comparing with QMC) that RPA is a good

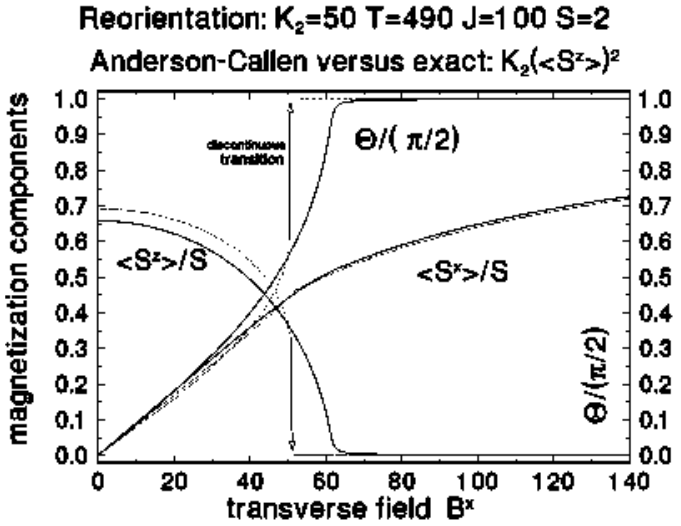

Figure 27: Normalized magnetizations $\langle S^z\rangle/S$ and $\langle S^x\rangle/S$ and the reorientation angle $\Theta/(\pi/2)$ for a spin S=2 Heisenberg monolayer as function of a transverse field B^x: Anderson-Callen decoupling [49](dotted lines) and the present theory [59](solid lines) for $K_2 = 0.5J$ $(T/J = 4.9)$.

approximation for a Heisenberg model (no anisotropy) with a field perpendicular to the film plane. To improve the present approach for a field in the transverse direction, one could resort to the procedure of [85] which goes beyond the RPA with respect to the exchange interaction terms.

We now consider a Heisenberg *antiferromagnet* monolayer with *exchange* anisotropy in a transverse field for $S = 1/2$. The Tyablikov decoupling is used. A recent paper [82] reports results from an approximate GF treatment where the sublattices are rotated in such a way as to make the transverse component of the magnetization in each sublattice vanish. As in the ferromagnetic case, it is assumed that $[S_i^z{}', H'] = 0$ at this angle, with the consequence that there are no zero eigenvalues of the resulting equation-of-motion matrix. The authors describe their results as unexpected: the staggered magnetization of the easy axis shows a non-monotonic behaviour as a function of the transverse field and there is a nonvanishing easy-axis magnetization above the Néel temperature below a critical transverse field.

To check the above results, we have computed the components of magnetization in the *non-rotated frame* directly from equations (238) of Section 4.3.2. Because we have developed [13] a procedure to deal with zero eigenvalues of the equation-of-motion matrix, we do not need, contrary to Ref. [82], any further approximation apart from the Tyablicov decoupling. In complete contrast to Ref. [82], our results behave as one would expect: the easy axis magnetization decreases monotonically and vanishes as a function of the transverse field for temperatures above the Néel

temperature. Our results are shown in Fig. 28. We should welcome Quantum Monte Carlo calculations that could resolve the crass differences between these two sets of results.

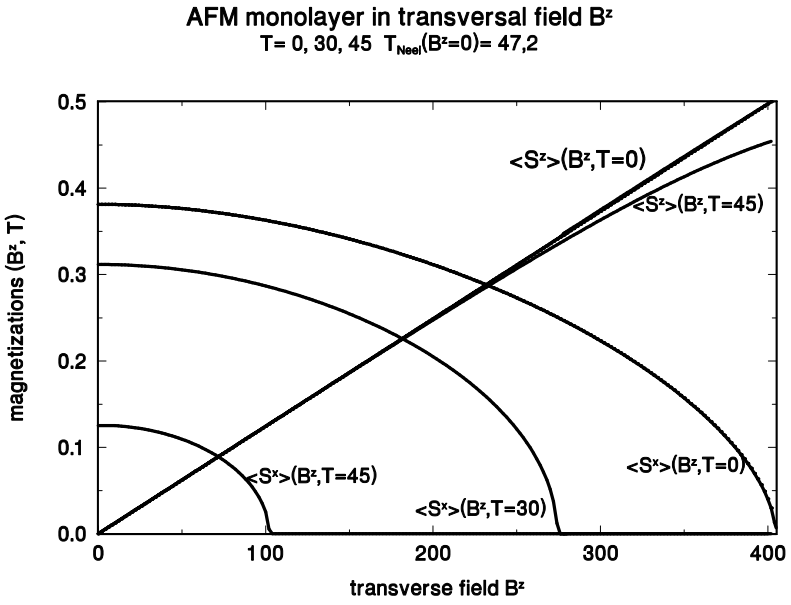

Figure 28: The magnetization components of a spin $S = 1/2$ antiferromagnetic monolayer (with the easy axis in x-direction) in a transverse field B^z shown as a function of B^z for different temperatures ($T = 0, 30, 45$). The Néel temperature $T_{\text{Néel}}(B^z = 0) = 47,2$ for J=-100 and the exchange-anisotropy strength $D^x = -0.1$.

4.4.3. Discussion

The most appealing aspect of decoupling in the rotated frame is not the excellent result for the field reorientation of the Heisenberg ferromagnet with single-ion anisotropy but rather the fact that the condition $[S_i^z\,', H\,'] = 0$ leads to an equation-of-motion matrix devoid of zero eigenvalues. Ref. [49] may convey the impression that this condition is exact; if that were correct, decoupling in the rotated frame would undoubtedly be the method of choice because of the great simplification it offers.

But "if" stands stiff. We offer a counter-example as a warning that the approximations used in Refs. [49, 50, 82] should be taken with a grain of salt: an exactly solvable model demonstrates that $[S_i^z\,', H\,'] = 0$ is not in general valid!

Consider a Hamiltonian having only an external field and a single-ion anisotropy:

$$H = -\sum_k K_{2,k}(S_k^z)^2 - \sum_k (B_0^x S_k^x + B_0^z S_k^z). \tag{263}$$

If it were true that a rotation angle could be found for which the commutator in the rotated system $[S_i^z\,', H\,']$ vanishes, then the singular values of the matrix $\langle SM'|[S^z\,', H\,']|SM\rangle$ in the $|SM\rangle$ representation would also vanish. A numerical calculation for $S = 1$ shows that this is *not* the case for a finite K_2. Furthermore, the numerical calculation also shows that the correlations $\langle S^-\,' S^-\,'\rangle$ and $\langle S^-\,' S^z\,'\rangle$ do not vanish simultaneously with $\langle S^+\,'\rangle = \langle S^-\,'\rangle = 0$. This shows that arguing with the Lehmann representation of the corresponding Green's functions as in Ref. [49] is not correct because it is erroneously assumed that the intermediate energy states $|m\rangle$ are eigenstates of the z-component of the angular momentum. They are in fact, however, given by the superposition $|m\rangle = \sum_M c_{mM}|SM\rangle$, such that e.g. the relevant matrix element $\sum_{nm}\langle n|S^-|m\rangle\langle m|S^-|n\rangle$ does not vanish in general. In Refs. [50, 82] the Green's function $G_{ij}^{-,-}$ is taken into account correctly.

Alternatively, consider finding a rotation that diagonalizes the model Hamiltonian (263). If this were possible, then the commutator would be zero at the corresponding rotation angle, since two diagonal matrices commute. For this model, it is possible to show algebraically that no such angle can be found unless K_2 itself vanishes.

At first sight it may seem strange that there is no angle at which the projection of the spin onto the z' axis is a good quantum number, for the non-commutativity of $S^z\,'$ with H' implies that $S^z\,'$ is not a constant of the motion but varies in time. But there is nothing wrong with this! One cannot argue that $S^z\,'$ be time-invariant: the intrinsic anisotropy and the applied external field favour different directions and they do so according to completely different mechanisms. It would be wrong to think that there should be a "resultant" direction along which $S^z\,'$ is quantized. Rather, the time-dependence of the opertor $S^z\,'$ is simply a property of the Hamiltonian that must be respected.

In conclusion, we regard the procedure of working in the rotated frame as not yet settled. It may in fact be advantageous if it succeeds in providing a more uniform way of treating the decoupling. The practice of employing $[H, S^z] = 0$ is very likely much too severe in general. The method seems to work for the spin reorientation problem for the ferromagnet but is questionable for the antiferromagnet in a transverse field. The embedded null-space arising from a non-vanishing commutator is more likely an essential ingredient intimately bound up with the properties of spin. As such, it could be dangerous to ignore it.

5. Beyond RPA

Up till now, with the exception of Section 4.2.5, we did not go beyond the Tyablikov (RPA) decoupling. In this section, we develop a formalism for treating the field induced reorientation of the magnetization for a spin 1/2 Heisenberg monolayer with an exchange anisotropy and, specializing to the magnetization in one direction, we show how higher-order GF theories discussed in the literature [85, 87, 89] follow quite naturally as limiting cases of our formalism.

5.1. Field-induced reorientation of the magnetization of a Heisenberg monolayer

We consider here a spin $S = 1/2$ Heisenberg monolayer with exchange anisotropy in an external field. We go beyond the Tyablikov (RPA) treatment by decoupling terms due to higher-order GF's. In the limit of the magnetization in one direction, we recover the results of Ref. [85] for a vanishing anisotropy and of Ref. [87] for the one-dimensional chain in the limit of a vanishing magnetic field. Without field and anisotropy one recovers the theory of Ref. [89]. The Hamiltonian under investigation is

$$H = -\frac{1}{2}\sum_{lm} J_{lm}(S_m^- S_l^+ + S_m^z S_l^z) - \frac{1}{2}\sum_{lm} D_{lm} S_m^z S_l^z - \sum_m (\frac{1}{2}B^- S_m^+ + \frac{1}{2}B^+ S_m^- + B^z S_m^z) \ . \tag{264}$$

The exchange interaction strength is J_{lm}, the strength of the exchange anisotropy is D_{lm} and $B^\pm = B^x \pm iB^y$ with the external magnetic field $\mathbf{B} = (B^x, B^y, B^z)$.

To get the equations of motion for the spin reorientation problem, the following first and second-order Green's functions are needed:

$$\begin{aligned} G_{ij}^{\alpha-(1)} &= \langle\langle S_i^\alpha; S_j^- \rangle\rangle, \\ G_{ij}^{\alpha-(2)} &= \langle\langle [S_i^\alpha, H]; S_j^- \rangle\rangle, \qquad (\alpha = +, -, z) \\ G_{ij}^{zz(1)} &= \langle\langle S_i^z; S_j^- \rangle\rangle, \\ G_{ij}^{zz(2)} &= \langle\langle [S_i^z, H]; S_j \rangle\rangle. \end{aligned} \tag{265}$$

The corresponding 8 equations of motion are

$$\begin{aligned} \omega G_{ij}^{\alpha-(1)} &= I_{ij}^{\alpha-(1)} + G_{ij}^{\alpha-(2)} \\ \omega G_{ij}^{\alpha-(2)} &= I_{ij}^{\alpha-(2)} + \langle\langle [[S_i^\alpha, H], H]; S_j^- \rangle\rangle, \qquad (\alpha = +, -, z) \\ \omega G_{ij}^{zz(1)} &= I_{ij}^{zz(1)} + G_{ij}^{zz(2)}, \\ \omega G_{ij}^{zz(2)} &= I_{ij}^{zz(2)} + \langle\langle [[S_i^z, H], H]; S_j \rangle\rangle. \end{aligned} \tag{266}$$

The double-commutator Green's functions must be decoupled in order to obtain a closed system of equations. After Fourier transformation to momentum space these are

$$(\omega - \mathbf{\Gamma})\mathbf{G}_{\mathbf{q}} = \mathbf{I}_{\mathbf{q}}, \tag{267}$$

a form that is amenable to the eigenvector method of Section 3.3.

Generalizing the procedure of Ref. [84] to the case where one has components of the magnetization in all directions of space, products of three spin operators are decoupled in the following way:

$$\begin{aligned}
S_k^z S_l^z S_i^+ &\approx \alpha^{+-} c_{kl}^{zz} S_i^+ + \alpha^{z-} c_{ki}^{z+} S_l^z + \alpha^{z-} c_{li}^{z+} S_k^z \ , \\
S_l^- S_k^+ S_i^+ &\approx \alpha^{--} c_{lk}^{++} S_l^- + \alpha^{+-} c_{li}^{-+} S_k^+ + \alpha^{+-} c_{lk}^{-+} S_i^+ \ , \\
S_i^z S_j^+ S_l^- &\approx \alpha^{zz} c_{jl}^{+-} S_i^z + \alpha^{+z} c_{jl}^{z-} S_j^+ + \alpha^{-z} c_{ij}^{z+} S_l^- \ ,
\end{aligned} \tag{268}$$

where the correlation functions are defined as $c_{ij}^{\alpha\beta} = \langle S_i^\alpha S_j^\beta \rangle$. Here we have introduced the vertex parameters α^{+-}, α^{--}, α^{z-} and $\alpha^{zz}, \alpha^{+z}, \alpha^{-z}$, where the indices refer to the indices of their associated Green's functions after the decoupling. In the limiting cases discussed later, we deal only with the magnetization in one direction, where only the vertex parameters α^{+-} and α^{zz} play a role. We show later how they may be determined by additional constraints. For the reorientation problem all 6 vertex parameters could play a role; however, for simplicity we assume that $\alpha^{+-} \approx \alpha^{--} \approx \alpha^{z-}$ and $\alpha^{zz} \approx \alpha^{-z} \approx \alpha^{+z}$, in order not to have too many additional parameters.

The inhomogeneities in eqn (267) are defined as the Fourier transformed thermodynamic expectation values of the following commutators

$$I_{\mathbf{q}} = FT \begin{pmatrix} \langle [S_i^+, S_j^-] \rangle \\ \langle [S_i^z, S_j^z] \rangle \\ \langle [S_i^-, S_j^-] \rangle \\ \langle [S_i^z, S_j^-] \rangle \\ \langle [[S_i^+, H], S_j^-] \rangle \\ \langle [[S_i^z, H], S_j^z] \rangle \\ \langle [[S_i^-, H], S_j^-] \rangle \\ \langle [[S_i^z, H], S_j^-] \rangle \end{pmatrix} = \begin{pmatrix} I_{\mathbf{q}}^{+-(1)} \\ I_{\mathbf{q}}^{zz(1)} \\ I_{\mathbf{q}}^{--(1)} \\ I_{\mathbf{q}}^{z-(1)} \\ I_{\mathbf{q}}^{+-(2)} \\ I_{\mathbf{q}}^{zz(2)} \\ I_{\mathbf{q}}^{--(2)} \\ I_{\mathbf{q}}^{z-(2)} \end{pmatrix} =$$

$$\begin{pmatrix} 2\langle S^z\rangle \\ 0 \\ 0 \\ -\langle S^-\rangle \\ zJ(1-\gamma_{\mathbf{q}})(c_{10}^{+-}+2c_{10}^{zz})+zD(2c_{10}^{zz}-\gamma_{\mathbf{q}}c_{10}^{+-})+2B^z\langle S^z\rangle+B^+\langle S^-\rangle \\ zJc_{10}^{+-}(1-\gamma_{\mathbf{q}})+\frac{1}{2}B^+\langle S^-\rangle+\frac{1}{2}B^-\langle S^+\rangle \\ -zJ(1-\gamma_{\mathbf{q}})c_{10}^{--}+zD\gamma_{\mathbf{q}}c_{10}^{--}-B^-\langle S^-\rangle \\ -zJ(1-\gamma_q)c_{10}^{z-}-B^-\langle S^z\rangle \end{pmatrix} \tag{269}$$

Here,

$$\gamma_{\mathbf{q}}=\begin{cases}\cos q & \text{for the linear chain with nearest neighbours} \quad z=2\\ \frac{1}{2}(\cos q_x+\cos q_y) & \text{for the square lattice with} \quad z=4.\end{cases} \tag{270}$$

The $\mathbf{\Gamma}$-matrix has the following form

$$\mathbf{\Gamma}=\begin{pmatrix} 0 & 0 & 0 & 0 & 1 & 0 & 0 & 0\\ 0 & 0 & 0 & 0 & 0 & 1 & 0 & 0\\ 0 & 0 & 0 & 0 & 0 & 0 & 1 & 0\\ 0 & 0 & 0 & 0 & 0 & 0 & 0 & 1\\ \Gamma_{51} & 0 & \Gamma_{53} & \Gamma_{54} & \Gamma_{55} & 0 & 0 & \Gamma_{58}\\ 0 & \Gamma_{62} & 0 & \Gamma_{64} & 0 & 0 & 0 & 0\\ \Gamma_{71} & 0 & \Gamma_{73} & \Gamma_{74} & 0 & 0 & \Gamma_{77} & \Gamma_{78}\\ \Gamma_{81} & 0 & \Gamma_{83} & \Gamma_{84} & \Gamma_{85} & 0 & \Gamma_{87} & 0 \end{pmatrix}. \tag{271}$$

Without loss of generality, the external field may be chosen such that the reorientation of the magnetization takes place in the xz-plane: $\mathbf{B}=(B^x,0,B^z)$. Then, $\langle S^y\rangle=0$ and $B^+=B^-=B^x$, implying a number of symmetry relations for the correlation functions, such as $\langle S^+\rangle=\langle S^-\rangle=\langle S^x\rangle$, $c_{lm}^{++}=c_{lm}^{--}$, $c_{ij}^{+z}=c_{ji}^{z-}$, etc. The non-zero matrix elements are then

$$\begin{aligned}
\Gamma_{15}=\quad & \Gamma_{26}=\Gamma_{37}=\Gamma_{48}=1\\
\Gamma_{51}=\quad & -\tfrac{1}{2}B^xB^x-B^zB^z-\tfrac{1}{2}DB^xz\gamma_{\mathbf{q}}\langle S^x\rangle\\
& +zD^2\Big(\tfrac{1}{4}+\alpha^{+-}(c_{20}^{zz}+(z-2)c_{11}^{zz})\Big)\\
& +zJD\Big(\tfrac{1}{2}(1-\gamma_{\mathbf{q}})+\alpha^{+-}[(2-\gamma_{\mathbf{q}})(c_{20}^{zz}+(z-2)c_{11}^{zz})-\tfrac{1}{2}(c_{20}^{+-}+(z-2)c_{11}^{+-})\gamma_{\mathbf{q}}]\\
& -\alpha^{+-}[(z-1)\gamma_qc_{10}^{zz}-\tfrac{1}{2}(z\gamma_{\mathbf{q}}^2-1)c_{10}^{+-}]\Big)\\
& +\tfrac{z}{2}(1-\gamma_{\mathbf{q}})J^2\Big(1+\alpha^{+-}[2c_{20}^{zz}+c_{20}^{+-}\\
& +(z-2)(2c_{11}^{zz}+c_{11}^{+-})-(1+z\gamma_{\mathbf{q}})(2c_{10}^{zz}+c_{10}^{+-})]\Big)\\
\Gamma_{53}=\quad & \tfrac{1}{2}B^xB^x+\tfrac{1}{2}DB^xz\gamma_{\mathbf{q}}\langle S^x\rangle\\
& +\tfrac{z}{2}\alpha^{+-}DJ\Big((c_{20}^{--}+(z-2)c_{11}^{--})\gamma_{\mathbf{q}}-(z\gamma_{\mathbf{q}}^2-1)c_{10}^{--}\Big)
\end{aligned}$$

$$
\begin{aligned}
& -\tfrac{z}{2}(1-\gamma_{\mathbf{q}})J^2\alpha^{+-}\Big(c_{20}^{--}+(z-2)c_{11}^{--}-c_{10}^{--}(1+z\gamma_{\mathbf{q}})\Big)\\
\Gamma_{54} = \quad & B^zB^x - DB^xz(1+\gamma_{\mathbf{q}})\langle S^z\rangle + zD^2\alpha^{+-}2(z-1)c_{10}^{z-}\gamma_{\mathbf{q}}\\
& +z\alpha^{+-}JD\Big([2-z(1+\gamma_{\mathbf{q}}^2)+3\gamma_{\mathbf{q}}(z-1)]c_{10}^{z-}-c_{20}^{z-}-(z-2)c_{11}^{z-}\Big)\\
& -z(1-\gamma_{\mathbf{q}})J^2\alpha^{+-}\Big(c_{20}^{z-}+(z-2)c_{11}^{z-}-c_{10}^{z-}(1+z\gamma_{\mathbf{q}})\Big)\\
\Gamma_{55} = \quad & 2B^z\\
\Gamma_{58} = \quad & -2B^x\\
\Gamma_{62} = \quad & B^xB^x + zB^xD\langle S^x\rangle\gamma_{\mathbf{q}} - zJD\alpha^{zz}c_{10}^{+-}(1-\gamma_{\mathbf{q}})(z\gamma_{\mathbf{q}}+1)\\
& +\tfrac{z}{2}J^2(1-\gamma_{\mathbf{q}})\Big(1+2\alpha^{zz}(c_{20}^{+-}+(z-2)c_{11}^{+-}-(1+z\gamma_{\mathbf{q}})c_{10}^{+-})\Big)\\
\Gamma_{64} = \quad & B^xB^z + zDB^x\langle S^z\rangle + zJD\alpha^{zz}(1-\gamma_{\mathbf{q}})\Big((z-1)c_{10}^{z-}-(c_{20}^{z-}+(z-2)c_{11}^{z-})\Big)\\
& -zJ^2(1-\gamma_{\mathbf{q}})\alpha^{zz}\Big(c_{20}^{z-}+(z-2)c_{11}^{z-}-(1+z\gamma_{\mathbf{q}})c_{10}^{z-}\Big)\\
\Gamma_{71} = \quad & \tfrac{1}{2}B^xB^x + \tfrac{z}{2}DB^x\langle S^x\rangle\gamma_{\mathbf{q}}\\
& +\tfrac{z}{2}DJ\alpha^{+-}\Big((c_{20}^{--}+(z-2)c_{11}^{--})\gamma_{\mathbf{q}}-(z\gamma_{\mathbf{q}}^2-1)c_{10}^{--}\Big)\\
& -\tfrac{z}{2}(1-\gamma_{\mathbf{q}})J^2\alpha^{+-}\Big(c_{20}^{--}+(z-2)c_{11}^{--}-(z\gamma_{\mathbf{q}}+1)c_{10}^{--}\Big)\\
\Gamma_{73} = \quad & -\tfrac{1}{2}B^xB^x - B^zB^z - \tfrac{z}{2}DB^x\langle s^x\rangle\gamma_{\mathbf{q}} + zD^2\Big(\tfrac{1}{4}+\alpha^{+-}(c_{20}^{zz}+(z-2)c_{11}^{zz})\Big)\\
& +zJD\Big(\tfrac{1}{2}(1-\gamma_{\mathbf{q}})+\alpha^{+-}[(2-\gamma_{\mathbf{q}})(c_{20}^{zz}+(z-2)c_{11}^{zz})-(z-1)\gamma_q c_{10}^{zz}\\
& +\tfrac{1}{2}(z\gamma_{\mathbf{q}}^2-1)c_{10}^{+-}-\tfrac{1}{2}(c_{20}^{+-}+(z-2)c_{11}^{+-})\gamma_{\mathbf{q}}]\Big)\\
& +\tfrac{z}{2}(1-\gamma_{\mathbf{q}})J^2\Big(1+\alpha^{+-}[2c_{20}^{zz}+c_{20}^{+-}\\
& +(z-2)(2c_{11}^{zz}+c_{11}^{+-})-(1+z\gamma_{\mathbf{q}})(2c_{20}^{zz}+c_{20}^{+-})]\Big)\\
\Gamma_{74} = \quad & B^zB^x - zDB^x\langle S^z\rangle(1+\gamma_{\mathbf{q}}) + zD^2\alpha^{+-}2(z-1)\gamma_{\mathbf{q}}c_{10}^{z-}\\
& zJD\alpha^{+-}\Big([2-z(1+\gamma_{\mathbf{q}}^2)+3\gamma_{\mathbf{q}}(z-1)]c_{10}^{z-}-(c_{20}^{z-}+(z-2)c_{11}^{z-})\Big)\\
& -z(1-\gamma_{\mathbf{q}})J^2\alpha^{+-}\Big(c_{20}^{z-}+(z-2)c_{11}^{z-}-(z\gamma_{\mathbf{q}}+1)c_{10}^{z-}\Big)\\
\Gamma_{77} = \quad & -2B^z\\
\Gamma_{78} = \quad & 2B^x\\
\Gamma_{81} = \quad & \tfrac{1}{2}B^xB^z + \tfrac{z}{2}DB^x\langle S^z\rangle\\
& +\tfrac{z}{2}JD\alpha^{+-}(1-\gamma_{\mathbf{q}})\Big((z-1)c_{10}^{z-}-c_{20}^{z-}-(z-2)c_{11}^{z-}\Big)\\
& -\tfrac{z}{2}J^2(1-\gamma_{\mathbf{q}})\alpha^{+-}\Big(c_{20}^{z-}+(z-2)c_{11}^{z-}-(1+z\gamma_{\mathbf{q}})c_{10}^{z-}\Big)\\
\Gamma_{83} = \quad & \Gamma_{81}\\
\Gamma_{84} = \quad & B^xB^x + zB^xD\langle S^x\rangle\gamma_{\mathbf{q}} - zJD\alpha^{+-}c_{10}^{+-}(1-\gamma_{\mathbf{q}})(z\gamma_{\mathbf{q}}+1)\\
& +\tfrac{z}{2}J^2(1-\gamma_{\mathbf{q}})\Big(1+2\alpha^{+-}(c_{20}^{+-}+(z-2)c_{11}^{+-}-(1+z\gamma_{\mathbf{q}})c_{10}^{+-})\Big)\\
\Gamma_{85} = \quad & -B^x\\
\Gamma_{87} = \quad & B^x\ . \qquad (272)
\end{aligned}
$$

We have no explicit calculations with the eigenvector method for the spin reorientation problem but we show now that, when specialized to one magnetization direction

only, limiting cases of the above equations lead to results found in the literature.

5.2. Limiting cases

For a magnetization in only one direction (the z-direction), the equations of motion reduce to a four-dimensional problem in energy-momentum space:

$$(\omega - \mathbf{\Gamma})\mathbf{G_q} = \mathbf{I_q} \tag{273}$$

with

$$\mathbf{G_q} = \begin{pmatrix} G_{\mathbf{q}}^{+-(1)} \\ G_{\mathbf{q}}^{zz(1)} \\ G_{\mathbf{q}}^{+-(2)} \\ G_{\mathbf{q}}^{zz(2)} \end{pmatrix} \tag{274}$$

and

$$\mathbf{I_q} = \begin{pmatrix} I_{\mathbf{q}}^{+-(1)} \\ I_{\mathbf{q}}^{zz(1)} \\ I_{\mathbf{q}}^{+-(2)} \\ I_{\mathbf{q}}^{zz(2)} \end{pmatrix} = \begin{pmatrix} 2\langle S^z\rangle \\ 0 \\ 2B^z\langle S^z\rangle + zJ(c_{10}^{+-} + 2c_{10}^{zz})(1-\gamma_{\mathbf{q}}) + zD(2c_{10}^{zz} - \gamma_{\mathbf{q}}c_{10}^{+-}) \\ zJc_{10}^{+-}(1-\gamma_{\mathbf{q}}) \end{pmatrix}. \tag{275}$$

5.2.1. Ferromagnet in a magnetic field, no anisotropy

In this case, $D = 0, B^+ = B^- = 0, B^z \neq 0$, leading to the theory of reference [85] with the 4×4 Γ-matrix which is, in the notation corresponding to eqn. (271),

$$\mathbf{\Gamma} = \begin{pmatrix} 0 & 0 & 1 & 0 \\ 0 & 0 & 0 & 1 \\ \Gamma_{51} & 0 & \Gamma_{55} & 0 \\ 0 & \Gamma_{62} & 0 & 0 \end{pmatrix}, \tag{276}$$

where now

$$\begin{aligned} \Gamma_{62} &= (\omega_{\mathbf{q}}^{zz})^2 = \frac{z}{2}(1-\gamma_{\mathbf{q}})J^2\Big(1 + 2\alpha^{zz}[(z-2)c_{11}^{+-} + c_{20}^{+-} - (1+z\gamma_{\mathbf{q}})c_{10}^{+-}]\Big), \\ \Gamma_{51} &= -B^zB^z + (\omega_{\mathbf{q}}^{+-})^2, \text{ with} \\ (\omega_{\mathbf{q}}^{+-})^2 &= \frac{z}{2}(1-\gamma_{\mathbf{q}})J^2\Big(1 + 2\alpha^{+-}[(z-2)(\frac{1}{2}c_{11}^{+-} + c_{11}^{zz}) \\ &\quad + (\frac{1}{2}c_{20}^{+-} + c_{20}^{zz}) - (1+z\gamma_{\mathbf{q}})(\frac{1}{2}c_{10}^{+-} + c_{10}^{zz})]\Big), \\ \Gamma_{55} &= 2B^z, \end{aligned} \tag{277}$$

where z and $\gamma_{\mathbf{q}}$ are defined in equation (270) for the linear chain and the square lattice respectively. For the linear chain (z=2), there are 7 unknowns ($\langle S^z\rangle, c_{10}^{+-}$, $c_{20}^{+-}, c_{10}^{zz}, c_{20}^{zz}, \alpha^{+-}, \alpha^{zz}$) and, for the square lattice (z=4), two additional unknowns (c_{11}^{+-}, c_{11}^{zz}).

In both cases, the relations

$$\begin{aligned} c_{00}^{+-} &= 1/2 - \langle S^z \rangle \\ c_{00}^{zz} &= 1/4 \end{aligned} \tag{278}$$

are valid.

The eigenvector method of Section 3.3 yields 6 equations for the chain

$$\begin{aligned} c_{j0}^{+-} &= \tfrac{1}{\pi} \int_0^\pi dq \cos(jq) (\mathbf{R}\mathcal{E}\mathbf{LI})_1 \ , \\ c_{j0}^{zz} &= \tfrac{1}{\pi} \int_0^\pi dq \cos(jq) (\mathbf{R}\mathcal{E}\mathbf{LI})_2 \end{aligned} \tag{279}$$

with $j = 0, 1, 2$.

For the square lattice, 8 equations are obtained ($j = 0, 1, 2$):

$$\begin{aligned} c_{j0}^{+-} &= \tfrac{1}{\pi^2} \int_0^\pi dq_x \int_0^\pi dq_y \cos(q_x j) (\mathbf{R}\mathcal{E}\mathbf{LI})_1 \ , \\ c_{j0}^{zz} &= \tfrac{1}{\pi^2} \int_0^\pi dq_x \int_0^\pi dq_y \cos(q_x j) (\mathbf{R}\mathcal{E}\mathbf{LI})_2 \ , \\ c_{11}^{+-(zz)} &= \tfrac{1}{\pi^2} \int_0^\pi dq_x \int_0^\pi dq_y \cos(q_x + q_y) (\mathbf{R}\mathcal{E}\mathbf{LI})_{1(2)} \ . \end{aligned} \tag{280}$$

These equations do not yet suffice to determine the unknowns because the vertex parameters enter implicitly. In both cases, the missing condition is supplied by an expression for the intrinsic energy:

$$E_i = \frac{\langle H \rangle}{N} = -\tfrac{z}{2} J (c_{10}^{+-} + c_{10}^{zz}) \ . \tag{281}$$

In order to evaluate $\langle H \rangle$, eqn (115) for $\langle S_i^- [S_i^+, H] \rangle$ is compared with the explicit evaluation of $\langle S_i^- [S_i^+, H] \rangle$ to yield

$$\begin{aligned} E_i &= -\frac{zJ}{8} - \frac{B^z}{2} + \frac{1}{2} \frac{1}{N} \sum_{\mathbf{q}} \frac{i}{2\pi} \times \\ &\lim_{\delta \to 0+} \int_{-\infty}^{\infty} d\omega \frac{\omega + B^z + \frac{1}{2} J (1 - \gamma_{\mathbf{q}})}{e^{\beta\omega} - 1} \Big(G_{\mathbf{q}}^{+-(1)}(\omega + i\delta) - G_{\mathbf{q}}^{+-(1)}(\omega - i\delta) \Big) \ . \end{aligned} \tag{282}$$

The Green's function $G_{\mathbf{q}}^{+-} = G_1$ is the first component of the Greens function vector, given by

$$G_1 = \sum_i R_{1i} \frac{(\mathbf{LI})_i}{\omega - \omega_i} \ . \tag{283}$$

Using

$$G_1(\omega + i\delta) - G_1(\omega - i\delta) = -2\pi i \sum_i R_{1i} \delta(\omega - \omega_i) (\mathbf{LI})_i \tag{284}$$

in eqn (283), performing the ω-integration and comparing with eqn (281) yields the additional equation needed to determine all unknowns:

$$\begin{aligned} &-B^z \langle S^z \rangle - \tfrac{z}{2} J (c_{10}^{+-} + c_{10}^{22}) \\ &= -\frac{zJ}{8} - \frac{B^z}{2} + \frac{1}{2} \begin{pmatrix} \frac{1}{\pi} \int_0^\pi dq \\ \frac{1}{\pi^2} \int_0^\pi dq_x \int_0^\pi dq_y \end{pmatrix} \sum_i R_{1i} \frac{\omega_i + B^z + \frac{z}{2} J (1 - \gamma_{\mathbf{q}})}{e^{\beta\omega_i - 1}} (\mathbf{LI})_i \ . \end{aligned} \tag{285}$$

The equations (278) together with (279,280) and (285) determine the unknowns, from which one obtains the magnetization $\langle S^z\rangle$, the intrinsic energy E_i, the susceptibility $\chi = d\langle S^z\rangle/dB^z$ and the specific heat $c_V = dE_i/dT$.

The numerical results in Ref. [85] (obtained not with the present method but with the standard spectral theorem) demonstrate that RPA is a rather good approximation for the magnetization and the susceptibility but that it is inadequate when transverse correlations play a role, as is the case for the intrinsic energy and the specific heat. In this case, it is very important to go beyond RPA.

5.2.2. Ferromagnet with no magnetic field and no exchange anisotropy

In this case, D=0 and $\mathbf{B} = \mathbf{0}$ and, for a linear chain ($z = 2, \gamma_{\mathbf{q}} = \cos q$), one obtains the model discussed by Kondo and Yamaji [89]. Because of the Mermin-Wagner theorem, the magnetization is $\langle S^z\rangle = 0$, and, for $S = 1/2$, isotropy demands that

$$c^{zz}_{n0} = \tfrac{1}{2}c^{+-}_{n0}. \tag{286}$$

Therefore, one needs either the GF's $\langle\langle S^z_i; S^z_j\rangle\rangle$ and $\langle\langle [S^z_i, H]; S^z_j\rangle\rangle$ or $\langle\langle S^+_i; S_j\rangle\rangle$ and $\langle\langle [S^+_i, H]; S^-_j\rangle\rangle$. The first choice reduces the problem to two dimensions:

$$\begin{pmatrix} \omega & 0 \\ 0 & \omega \end{pmatrix} - \begin{pmatrix} 0 & 1 \\ (\omega^{zz}_q)^2 & 0 \end{pmatrix} \begin{pmatrix} G^{zz(1)}_q \\ G^{zz(2)}_q \end{pmatrix} = \begin{pmatrix} I^{zz(1)}_q \\ I^{zz(2)}_q \end{pmatrix} \tag{287}$$

with

$$\begin{aligned} I^{zz(1)}_q = 0\ , \quad I^{zz(2)}_q = 4c^{+-}_{10}(1-\cos q)\ , \\ (\omega^{zz}_q)^2 = (1-\cos q)J^2\Big(1 + 2\alpha^{zz}(c^{+-}_{20} - (1+2\cos q)c^{+-}_{10})\Big). \end{aligned} \tag{288}$$

These equations yield

$$G^{zz(1)}_q = \frac{I^{zz(2)}_q}{\omega^2 - (\omega^{zz(2)}_q)^2} = \frac{I^{zz(2)}_q}{2|\omega^{zz}_q|}\Big(\frac{1}{\omega - \omega^{zz}_q} - \frac{1}{\omega + \omega^{zz}_q}\Big)\ . \tag{289}$$

The standard spectral theorem produces 3 equations for determining the 3 unknowns $\alpha^{zz}, c^{+-}_{10,}, c^{+-}_{20}$. For spin 1/2, $c^{zz}_{00} = \langle S^z_0 S^z_0\rangle = \frac{1}{4}$. This, together with

$$c^{zz}_{n0} = \tfrac{1}{2}c^{+-}_{n0} = \tfrac{1}{\pi}\int_0^\pi dq\cos(nq)\frac{I^{zz(2)}_q}{|\omega^{zz}_q|}\coth(\frac{\beta}{2}|\omega^{zz}_q|); \quad n = 0, 1, 2\ , \tag{290}$$

determines the unknowns.

It is instructive to apply the eigenvector method of Section 3 and to obtain the same expression from

$$c^{zz}_{n0} = \tfrac{2}{\pi}\int_0^\pi dq\cos(nq)\Big(\mathbf{R}\mathcal{E}\mathbf{L}\mathbf{I}\Big)_1; \quad n = 0, 1, 2. \tag{291}$$

Here the matrix $\mathbf{R}$ consists of the right eigenvectors as columns of the nonsymmetric matrix in eqn (287) and $\mathbf{L} = \mathbf{R^{-1}}$ consists of the left eigenvectors as rows and can be

calculated as the inverse of $\mathbf{R}$. Note that $\mathbf{R}$ and $\mathbf{L}$ are not separately orthonormal. It is only necessary that $\mathbf{RL} = \mathbf{1}$. One finds

$$\mathbf{R} = \begin{pmatrix} 1 & 1 \\ \omega_q^{zz} & -\omega_q^{zz} \end{pmatrix}, \quad \mathbf{L} = \frac{1}{2\omega_q^{zz}} \begin{pmatrix} \omega_q^{zz} & 1 \\ \omega_q^{zz} & -1 \end{pmatrix}, \quad \mathcal{E} = \begin{pmatrix} \frac{1}{e^{\beta\omega_q^{zz}}-1} & 0 \\ 0 & \frac{1}{e^{-\beta\omega_q^{zz}}-1} \end{pmatrix}. \tag{292}$$

Evaluation of eqn (291) with these expressions produces eqn (290).

Solution of these equations yields the intrinsic energy per particle

$$E = -\tfrac{1}{2N} \sum_{nm} J_{nm}(c_{nm}^{+-} + c_{nm}^{zz}) = -\tfrac{3}{2} J c_{10}^{+-}, \tag{293}$$

the specific heat per particle,

$$c_V = \frac{dE}{dT} = \tfrac{3}{2} J\beta^2 \frac{d}{d\beta} c_{10}^{+-}, \tag{294}$$

and the susceptibility

$$\chi = \beta \sum_n c_n^{zz} = \tfrac{1}{2} \sum_{n=0}^{2} c_{n0}^{+-}. \tag{295}$$

The results of Kondo and Yamaji [89], here reproduced numerically by the eigenvector method, are largely in agreement with the exact calculations of Bonner and Fisher [92] for a finite number of spins .

The Kondo-Yamaji decoupling is generalized in Refs. [90, 91] in order to treat the spin S=1 antiferromagnetic Heisenberg chain. It is also used in Ref. [93] for the spin S=1 low-dimensional quantum XY ferromagnet and in Refs. [94, 95] for a kagomé antiferromagnet.

5.2.3. Ferromagnet with exchange anisotropy but no magnetic field

This case ($D \neq 0, B = 0$) is discussed in Ref. [87] for the easy-plane XXZ chain, where 4 vertex parameters are used: $\alpha_1^{+-}, \alpha_2^{+-}, \alpha_1^{zz}, \alpha_2^{zz}$. These are fixed by the exact expression for the ground state energy and by assuming that the ratios of corresponding parameters do not vary with the temperature.

A 2×2-problem results with the equations of motion

$$\left\{ \begin{pmatrix} \omega & 0 \\ 0 & \omega \end{pmatrix} - \begin{pmatrix} \Gamma_{51} & 0 \\ 0 & \Gamma_{62} \end{pmatrix} \right\} \begin{pmatrix} G_q^{+-(1)} \\ G_q^{zz(1)} \end{pmatrix} = \begin{pmatrix} I_q^{+-(2)} \\ I_q^{zz(2)} \end{pmatrix}, \tag{296}$$

where

$$\begin{aligned} I_{\mathbf{q}}^{+-(2)} &= 2J(c_{10}^{+-} + 2c_{10}^{zz})(1-\gamma_q) + 2D(2c_{10}^{zz} - \gamma_q c_{10}^{+-}), \\ I_{\mathbf{q}}^{zz(2)} &= 2Jc_{10}^{+-}(1-\gamma_q), \end{aligned} \tag{297}$$

and

$$\Gamma_{51} = 2D^2(\tfrac{1}{4} + \alpha_2^{+-} c_{20}^{zz}) + 2JD\Big(\tfrac{1}{2}(1-\gamma_q)$$

$$
\begin{aligned}
&+\alpha_2^{+-}[(2-\gamma_q)c_{20}^{zz} - \tfrac{1}{2}c_{20}^{+-}\gamma_q] + \alpha_1^{+-}[-\gamma_q c_{10}^{zz} + \tfrac{1}{2}(2\gamma_q^2-1)c_{10}^{+-}]\Big) \\
&+(1-\gamma_q)J^2\Big(1+\alpha_2^{+-}(2c_{20}^{zz}+c_{20}^{+-}) - \alpha_1^{+-}(1+2\gamma_q)(2c_{10}^{zz}+c_{10}^{+-})\Big)\ , \\
\Gamma_{62} \;=\; & -2JDc_{10}^{+-}\alpha_1^{zz}(1-\gamma_q)(2\gamma_q+1) \\
&+J^2(1-\gamma_q)\Big(1+2\alpha_2^{zz}c_{20}^{+-} - 2\alpha_1^{zz}(1+2\gamma_q)c_{10}^{+-}\Big)\ . \qquad (298)
\end{aligned}
$$

The thermodynamics of the $S \geq 1$ ferromagnetic Heisenberg chain with uniaxial single-ion anisotropy using second-order GF's is treated in Ref. [86]. The antiferromagnetic easy-plane XXZ-model for $S = 1/2$ is treated in Ref. [88].

5.3. The Tserkovnikov formulation of the GF theory

Until now we have not considered the damping of spin waves. This is because we have neglected the influence of the self-energy, the imaginary part of which leads to damping effects. In this Section, we present a formalism which allows the treatment of damping. In the first subsection we develop the general formalism and, in the second subsection, we specialize it to a Heisenberg monolayer in an external field, evaluating the self-energy approximately. The formalism follows Tserkovnikov [96], who derives a closed expression for the self-energy without making decoupling assumptions. For a review of the formalism, see e.g. Ref. [97]; a compact derivation can be found in the appendix of Ref. [98]. The formal derivation of a Dyson equation for a Heisenberg ferromagnet is given in Ref. [99].

5.3.1. The general formalism

The equation of motion for the single-particle Green's function $G_1 = \langle\langle A^+; A\rangle\rangle_\omega$ is

$$\omega G_1 = I_1 + G_2, \quad \text{with} \quad I_1 = \langle [A^+, A]\rangle \ \text{ and } \ G_2 = \langle\langle [A^+, H]; A\rangle\rangle \ . \tag{299}$$

Analogously, the equation for the two-particle Green's function G_2 may be written

$$\omega G_2 = I_2 + G_3, \tag{300}$$

with $I_2 = \langle [[A^+, H], A]\rangle$. G_3 is the three-particle GF, which Tserkovnikov obtains by a time derivation with respect to the second operator of G_2 as $G_3 = \langle\langle [A^+, H]; [A, H]\rangle\rangle$.

On the way to deriving an equation for the self-energy, Tserkovnikov introduces the ansatz

$$\langle\langle [A^+, H]; A\rangle\rangle = C\langle\langle A^+; A\rangle + \langle\langle B; A\rangle\rangle. \tag{301}$$

If one determines B such that $\langle [B, A]\rangle = 0$ the quantity C is determined by

$$C = I_2 I_1^{-1}, \tag{302}$$

which can be proved by looking at $\langle [[A^+, H], A]\rangle = C\langle [A^+, A]\rangle + \langle [B, A]\rangle$. Introduction of the zero-order Green's function G_0 generates a generalized mean field expression:

$$\omega G_0 = I_1 + I_2 I_1^{-1} G_0 \quad \text{ or } \quad G_0 = \frac{I_1}{\omega - I_2 I_1^{-1}} \ . \tag{303}$$

A Dyson equation is now defined for G_1:

$$G_1 = G_0 + G_0 M G_1, \tag{304}$$

where the mass operator M is defined by

$$M = I_1^{-1}\langle\langle B; A\rangle\rangle G_1^{-1}. \tag{305}$$

The exact single-particle GF may then be written as

$$G_1 = \frac{I_1}{\omega - I_2 I_1^{-1} - I_1 M} = \frac{I_1}{\omega - I_2 I_1^{-1} - \Sigma}\ , \tag{306}$$

where the self-energy is defined as $\Sigma = I_1 M$.

The self-energy can now be expressed by

$$\Sigma = (G_3 - G_2 G_1^{-1} G_2) I_1^{-1}. \tag{307}$$

The proof of this expression follows from eqns (306,299,300):

$$\begin{aligned}
\Sigma &= \omega - I_1 G_1^{-1} - I_2 I_1^{-1} \\
&= (G_2 G_1^{-1} I_1 - I_2) I_1^{-1} \\
&= \Big(G_2 G_1^{-1}(G_1\omega - G_2) + G_3 - \omega G_2\Big) I_1^{-1} \\
&= (G_3 - G_2 G_1^{-1} G_2) I_1^{-1}.
\end{aligned} \tag{308}$$

5.3.2. The Heisenberg monolayer in an external field

The Green's function G_0 of eqn (303) leading to the generalized mean field expression for the Heisenberg monolayer in an external field (see the Hamiltonian of (116)) is obtained from a Fourier transform to momentum space of

$$\begin{aligned}
I_1 &= \langle [S_i^+, S_g^-]\rangle = 2\langle S^z\rangle \delta_{ig} \\
I_2 &= \langle [[S_i^+, H], S_g^-]\rangle = \delta_{ig} B 2\langle S^z\rangle + \\
&\quad + \delta_{ig} \sum_l J_{il}\Big(2\langle S_i^z S_l^z\rangle + \langle S_l^+ S_i^-\rangle\Big) - \sum_l J_{il}\delta_{gl}\Big(2\langle S_i^z S_l^z\rangle + \langle S_i^+ S_g^-\rangle\Big),
\end{aligned} \tag{309}$$

and reads

$$G_{\mathbf{k},0} = \frac{2\langle S^z\rangle}{\omega - E_{\mathbf{k}}^0}, \tag{310}$$

with

$$E_{\mathbf{k}}^0 = B + \frac{1}{2\langle S^z\rangle}\frac{1}{N}\sum_{\mathbf{q}}(J_{\mathbf{q}} - J_{\mathbf{k}-\mathbf{q}})(2\psi_{\mathbf{q}}^{zz} + \psi_{\mathbf{q}}^{+-}), \tag{311}$$

where

$$\psi_{\mathbf{q}}^{-+} = \frac{1}{N}\sum_{ij}\langle S_i^- S_j^+\rangle e^{i\mathbf{q}(\mathbf{R}_i - \mathbf{R}_j)}, \tag{312}$$

and

$$\begin{aligned}
\psi_{\mathbf{q}}^{zz} &= \frac{1}{N}\sum_{ij}\langle S_i^z S_j^z\rangle e^{i\mathbf{q}(\mathbf{R}_i - \mathbf{R}_j)} \\
&= \frac{1}{N}\sum_{ij}\Big(\langle S_i^z\rangle\langle S_j^z\rangle + \langle (S_i^z - \langle S_i^z\rangle)\rangle\langle (S_j^z - \langle S_j\rangle)\rangle\Big) e^{i\mathbf{q}(\mathbf{R}_i - \mathbf{R}_j)} \\
&= 2\langle S_i^z\rangle\langle S_j^z\rangle\delta_{\mathbf{q},\mathbf{0}} + \frac{1}{N}\sum_{ij} K_{ij}^{zz} e^{i\mathbf{q}(\mathbf{R}_i - \mathbf{R}_j)}.
\end{aligned} \tag{313}$$

With this expression, the dispersion relation is evaluated as

$$E^0_{\mathbf{k}} = B + \langle S^z\rangle(J_{\mathbf{0}} - J_{\mathbf{k}}) + \frac{1}{2\langle S^z\rangle}\frac{1}{N}\sum_{\mathbf{q}}(J_{\mathbf{q}} - J_{\mathbf{k}-\mathbf{q}})(2K^{zz}_{\mathbf{q}} + \psi^{+-}_{\mathbf{q}}) \ . \tag{314}$$

The first term corresponds to the Tyablikov (RPA) decoupling (see eqn(126)), the term proportional to $K^{zz}_{\mathbf{q}}$ corresponds to the fluctuations of the z-component of the spin, and the term proportional to the transverse component $\psi^{-+}_{\mathbf{q}}$ is similar to the result of the Callen decoupling but with a different prefactor (see eqn (141)).

In order to describe the damping of magnons, one must go beyond this generalized mean field approach, approximating the self-energy of eqn. (308). The relevant term, which is the proper part in a diagram expansion [97] (leading to the name irreducible GF theory), is

$$\Sigma(t) = G_3 I_1^{-1} = \langle\langle [S^+_i, H]; [S^-_i, H]\rangle\rangle \frac{1}{2\langle S^z\rangle}. \tag{315}$$

Evaluating the commutators yields

$$\Sigma_{ij}(t) = \frac{1}{2\langle S^z\rangle}\sum_{lg} J_{il}J_{gj}\langle\langle (S^+_i S^z_l - S^+_l S^z_i); (S^-_g S^z_j - S^-_j S^z_g)\rangle\rangle. \tag{316}$$

A Fourier transformation to momentum space, together with the formulas of Section 3.4 needed to derive the spectral theorem, allows one to express the self-energy in terms of the corresponding correlation function

$$\begin{aligned}\Sigma(\omega) &= \frac{1}{2\pi}\int_{-\infty}^{\infty}\frac{d\omega'}{\omega-\omega'}(e^{\beta\omega'}-1)\int_{-\infty}^{\infty}dt e^{i\omega' t} \\ &\times \frac{1}{2\langle S^z\rangle}\frac{1}{N}\sum_{ijgl} J_{il}J_{gj}e^{i\mathbf{k}(\mathbf{R}_i-\mathbf{R}_j)}\langle (S^-_g S^z_j - S^-_j S^z_g)(S^+_i S^z_l - S^+_l S^z_i)\rangle. \end{aligned}\tag{317}$$

In order to proceed, the correlation function in this expression must be decoupled:

$$\begin{aligned}&\langle (S^-_g S^z_j - S^-_j S^z_g)(S^+_i S^z_l - S^+_l S^z_i)\rangle \\ \simeq\ &\langle S^z_j S^z_l\rangle\langle S^-_g S^+_i\rangle - \langle S^z_j S^z_i\rangle\langle S^-_g S^+_l\rangle - \langle S^z_g S^z_l\rangle\langle S^-_j S^+_i\rangle + \langle S^z_g S^z_i\rangle\langle S^-_i S^+_l\rangle \\ =\ &\psi^{zz}_{jl}\psi^{-+}_{gi} - \psi^{zz}_{ji}\psi^{-+}_{gl} - \psi^{zz}_{gl}\psi^{-+}_{ji} + \psi^{zz}_{gi}\psi^{-+}_{il}. \end{aligned}\tag{318}$$

The longitudinal correlation function is approximated by its static value:

$$\langle S^z_j S^z_l\rangle(t) = \psi^{zz}_{jl}(t) = \psi^{zz}_{jl}(0). \tag{319}$$

The transverse correlation function is given via the spectral theorem by the single-particle Green's function G_1

$$\begin{aligned}\psi^{-+}_{gi} &= \frac{i}{2\pi}\int_{-\infty}^{\infty}d\omega\frac{e^{-i\omega t}}{e^{\beta\omega}-1}\Big(G_{ig,1}(\omega+i\delta) - G_{ig,1}(\omega-i\delta)\Big) \\ &\simeq \frac{1}{N}\sum_{\mathbf{q}}\frac{2\langle S^z\rangle e^{-iE^0_{\mathbf{q}}t}}{e^{\beta E^0_{\mathbf{q}}}-1}e^{-i\mathbf{q}(\mathbf{R}_i-\mathbf{R}_j)}. \end{aligned}\tag{320}$$

Here, the full Green's functions G_1 in the brackets have been approximated by the zero-order GF G_0 (a procedure which can be iterated to self-consistency) as

$$2i\mathrm{Im}\frac{1}{N}\sum_{\mathbf{q}} G_{\mathbf{q},\mathbf{0}} e^{-i\mathbf{q}(\mathbf{R}_i-\mathbf{R}_j)} = \frac{1}{N}\sum_{\mathbf{q}} 2\langle S^z\rangle 2\pi\delta(\omega - E^0_{\mathbf{q}}) e^{-i\mathbf{q}(\mathbf{R}_i-\mathbf{R}_j)}. \tag{321}$$

Now the t- and ω'-integrations in the expression for the self-energy (317) can be performed and, after a Fourier transform to momentum space, one obtains

$$\Sigma_{\mathbf{k}}(\omega) = \frac{1}{N}\sum_{\mathbf{q}} \frac{1}{\omega - E^0_{\mathbf{k}-\mathbf{q}}} (J_{\mathbf{q}} - J_{\mathbf{q}-\mathbf{k}})^2 \psi^{zz}_{\mathbf{q}}. \tag{322}$$

The single-particle GF is now specified and the magnetization can be calculated via the spectral theorem. The imaginary part of the self-energy describes the damping of magnons. This is the result obtained by Plakida in Ref. [99].

We are not aware of a numerical evaluation of the formulas above. The damping of magnons with the present formalism is, however, treated by analytical estimates for a two-dimensional $S = 1/2$ Heisenberg antiferromagnet in Ref. [101] and numerically in Ref. [100] and is also treated numerically in Ref. [98] for a doped antiferromagnet within the t-J model.

6. Conclusions

In this review we have given an overview of the formalism of many-body Green's function theory (GFT) and have applied it mainly to ferromagnetic, antiferromagnetic and coupled ferromagnetic-antiferromagnetic Heisenberg films.

A prerequisite is that the systems to be examined have periodic structures in order to be amenable to the resulting two-dimensional Fourier transform from momentum to configuration space. Any attempt to deal with local magnetic impurities would require calculations on a grid in real space, where one is limited technically by the number of lattice sites which can be taken into account. In this regard, the situation is the same as for Quantum Monte Carlo (QMC) calculations. A Green's function calculation including local magnetic impurities and a comparison with QMC results is reported in Ref. [105].

The crucial approximation in GFT is the decoupling of the higher-order GF's in the equation-of-motion hierarchy. The Tyablikov (RPA) decoupling yields reasonable results for the magnetization and susceptibility in one direction. This is seen by comparison of GFT with 'exact' QMC calculations for simple cases (see Sections 4.1.5 and 4.2.5). If transverse correlations play a role, e.g. in calculations of the intrinsic energy or the specific heat, one has to go beyond RPA (see Section 5). In this case, third-order GF's have to be decoupled, requiring vertex parameters that have to be determined by additional constraints. For GF's of even higher order there is still no systematic procedure for the decoupling. Therefore, it is very difficult to make progress in this direction. In rare cases, e.g. for the single-ion anisotropy terms, it is possible to treat the corresponding terms exactly by using spin relations that close the hierarchy of equations automatically with respect to these terms (Section 4.2.5). The exchange interaction and exchange anisotropy terms, however, have to be decoupled by generalised RPA procedures at the level of the higher-order GF's.

A particular problem is the occurrence of exact zero eigenvalues of the equation-of-motion matrix. After application of the the spectral theorem, an adjunct term taking into account the corresponding null-space must be retained. If this term is momentum-independent, one can apply the standard spectral theorem in which the commutator and anticommutator GF's have to be used (Section 3.3). If, on the other hand, this term turns out to be momentum-dependent, the standard spectral theorem fails, and one must perform a singular value decomposition of the equation-of-motion matrix in order to eliminate the null-space from the matrix. This not only reduces the number of integral equations which have to be solved self-consistently but also makes the use of the anticommutator GF superfluous (Section 3.3). This

procedure is successful in a number of cases (see Sections 4.2.3 and 4.3.2). We were not, however, able to prove that this procedure works in general. For instance, we could not solve the spin reorientation problem of Section 4.2.5 in full because of numerical difficulties which we think are related to our inability to eliminate fully the momentum dependence of the terms connected with the null-space. We were able, however, to find an approximate solution for the spin reorientation problem with an exact treatment of the single-ion anisotropy by working in a rotated frame (see Section 4.4.2). The rotation angle is determined from the condition that $S^{z\,\prime}$ commutes with the Hamiltonian in the rotated frame. This treatment simplifies the calculations because the null-space vanishes. However, we can show by a counter example that the condition above cannot be fulfilled in general. For the antiferromagnet in a transverse field we can successfully deal with the null-space working in the non-rotated frame (see Section 4.4.2).

The result of this full GF treatment deviates drastically from a GF calculation [82] in the rotated frame that employs the additional approximation that, as in the ferromagnet, the reorientation angle is determined by the condition $[S^{z\,\prime}, H^{\,\prime}] \simeq 0$. To resolve the discrepancy between these results, QMC calculations would be welcome.

In most of the applications, we have considered only a simple square lattice because the double integrals in the Fourier transform from momentum space to real space can be transformed into a one-dimensional integral (Appendix C). This reduces the computer time considerably (by a factor of a few hundreds) because the Fourier transform must be calculated many times in the self-consistency procedure. There is, however, nothing preventing the use of double integrals directly for other lattice types if enough computer time is available.

We are not aware of detailed numerical work which applies the Tserkovnikov formulation of GFT of Section 6.2 to Heisenberg films. This would allow a calculation of the damping of spin waves.

We hope that we have succeeded in giving an overview of the present status of the application of many-body GFT to Heisenberg films that will stimulate the use of the reviewed techniques to related problems.

7.1. Appendix A: Calculating the intrinsic energy with GFT

The following Heisenberg Hamiltonian for a monolayer is taken as an example:

$$H = -B\sum_i S_i^z - \frac{1}{2}\sum_{il} J_{il}(S_i^- S_l^+ + S_i^z S_l^z) - \sum_i K_{2,i}(S_i^z)^2. \tag{323}$$

The intrinsic energy per lattice site is given by

$$E_i = -B\langle S_i^z\rangle - \frac{1}{2}\sum_l J_{il}(\langle S_i^- S_l^+\rangle + \langle S_i^z S_l^z\rangle) - K_{2,i}\langle (S_i^z)^2\rangle. \tag{324}$$

In the following, we take $S = 1/2$ and $S = 1$ as examples.

1. S = 1/2

In this case, the the single-ion anisotropy term is a constant because $\langle S^z S^z\rangle = 1/4$. In order to determine the intrinsic energy within GFT, one has to calculate the quantities entering eqn (115) of Section 3.7. Because $(S_i^z)^2 = 1/4$ and $S_i^- S_i^+ = 1/2 - S_i^z$, the direct commutator yields

$$B_i^{+,-} = \langle S_i^-[S_i^+, H]_-\rangle = B(\tfrac{1}{2} - \langle S_i^z\rangle) + \tfrac{z}{2}J\langle S_i^z\rangle - \sum_l J_{il}(\langle S_i^z S_l^z\rangle + \langle S_i^- S_l^+\rangle + \langle S_i^z S_i^- S_l^+\rangle). \tag{325}$$

A different expression for $B_i^{+,-}$ can be obtained from

$$B_i^{+,-} = \lim_{\delta\to 0}\frac{1}{N}\sum_{\mathbf{k}}\frac{i}{2\pi}\int\frac{\omega d\omega}{e^{\beta\omega}-1}\Big(G_{\mathbf{k}}^{+,-}(\omega + i\delta) - G_{\mathbf{k}}^{+,-}(\omega - i\delta)\Big). \tag{326}$$

where $G_{\mathbf{k}}^{+,-}$ is the Fourier transform of the Green's function

$$G_{ij}^{+,-} = \langle\langle S_i^+; S_j^-\rangle\rangle. \tag{327}$$

Equating the expressions (325) and (326) yields an expression for the intrinsic energy if relation (324),

$$-\sum_l J_{il}\langle S_i^z S_l^z\rangle = 2E_i + 2B\langle S_i^z\rangle + \sum_l J_{il}\langle S_i^- S_l^+\rangle + 2K_2\tfrac{1}{4}, \tag{328}$$

is inserted into eqn (325):

$$\begin{aligned} E_i = \; & -\frac{1}{4}B - \langle S_i^z\rangle(\frac{1}{2}B + \frac{1}{4}zJ) + \frac{1}{2}\sum_l J_{il}\langle S_i^z S_i^- S_l^+\rangle - K_2\tfrac{1}{4} \\ & + \frac{1}{2}\lim_{\delta\to 0}\frac{1}{N}\sum_{\mathbf{k}}\frac{i}{2\pi}\int\frac{\omega d\omega}{e^{\beta\omega}-1}(G_{\mathbf{k}}^{+,-}(\omega + i\delta) - G_{\mathbf{k}}^{+,-}(\omega - i\delta)). \end{aligned} \tag{329}$$

One now needs an approximation for calculating the Green's function and the expectation values occuring in equation (329). We have done this in Section 4.1.1

in the Tyablikov (RPA) approximation. The resulting Green's function is (see eqn (125))

$$G_{\mathbf{k}}(\omega) = \frac{\langle [S_i^+, S_i^-] \rangle}{\omega - \omega_{\mathbf{k}}^{RPA}} = \frac{2\langle S_i^z \rangle}{\omega - \omega_{\mathbf{k}}^{RPA}} \ , \tag{330}$$

with the dispersion relation

$$\omega_{\mathbf{k}}^{RPA} = B + \langle S_i^z \rangle (J_0 - J_{\mathbf{k}}). \tag{331}$$

Now from eqn (326),

$$B_i^{+,-} = \frac{1}{N} \sum_{\mathbf{k}} \int \frac{2\langle S_i^z \rangle \omega d\omega}{e^{\beta\omega} - 1} \delta(\omega - \omega_{\mathbf{k}}^{RPA}) = \frac{1}{N} \sum_{\mathbf{k}} \frac{2\langle S_i^z \rangle \omega_{\mathbf{k}}^{RPA}}{e^{\beta\omega_{\mathbf{k}}^{RPA}} - 1} \ . \tag{332}$$

The quantity $\sum_l J_{il} \langle S_i^z S_i^- S_l^+ \rangle$ in equation (329) is obtained from the Green's function

$$\langle\langle S_i^+ ; S_j^z S_j^- \rangle\rangle, \tag{333}$$

which has same dispersion relation (331) but a different inhomogeneity $\langle [S_i^+, S_i^z S_i^-] \rangle$; i.e.

$$\langle\langle S^+ ; S^z S^- \rangle\rangle_{\mathbf{k}}(\omega) = \frac{\langle [S_i^+, S_i^z S_i^-] \rangle}{\omega - \omega_{\mathbf{k}}^{RPA}}. \tag{334}$$

Applying the spectral theorem and a Fourier transform one obtains

$$\sum_l J_{il} \langle S_i^z S_i^- S_l^z \rangle = \frac{1}{N} \sum_{\mathbf{k}} J_{\mathbf{k}} \frac{\langle [S_i^+, S_i^z S_i^-] \rangle}{e^{\beta\omega_{\mathbf{k}}^{RPA}} - 1} = -\frac{1}{N} \sum_{\mathbf{k}} J_{\mathbf{k}} \frac{\langle S_i^z \rangle}{e^{\beta\omega_{\mathbf{k}}^{RPA}} - 1}. \tag{335}$$

We can now evaluate eqn (329) to obtain the following expression for the internal energy:

$$E_i = -\tfrac{1}{4}B - \langle S_i^z \rangle (\tfrac{1}{2}B + \tfrac{1}{4}zJ) + \frac{1}{N} \sum_{\mathbf{k}} (\omega_{\mathbf{k}}^{RPA} - \tfrac{1}{2}J_{\mathbf{k}}) \frac{\langle S_i^z \rangle}{e^{\beta\omega_{\mathbf{k}}^{RPA}} - 1} - \tfrac{1}{4}K_2 \ , \tag{336}$$

which can be calculated after the magnetization has been determined self-consistently from equation (130) resulting from the spectral theorem in Section 4.1.1:

$$\langle S_i^z \rangle = \frac{1}{2} - \langle S_i^- S_i^+ \rangle = \frac{1}{2} - \frac{1}{N} \sum_{\mathbf{k}} \frac{2\langle S_i^z \rangle}{e^{\beta\omega_{\mathbf{k}}^{RPA}} - 1} \ . \tag{337}$$

Knowledge of the intrinsic energy allows a determination of the specific heat and the free energy via eqns (111) and (112).

2. S=1

For $S = 1$ the single-ion anisotropy of eqn (323) is active. If the magnetization is in the z-direction only, the exact treatment of the anisotropy of Section 4.2.5 requires the Green's functions:

$$\begin{aligned} G_{ij}^{+,-} &= \langle\langle S_i^+ ; S_j^- \rangle\rangle, \\ G_{ij}^{z+,-} &= \langle\langle (2S_i^z - 1) S_i^+ ; S_j^- \rangle\rangle \ . \end{aligned} \tag{338}$$

with the exact equations of motion

$$\begin{aligned}
\omega G_{ij}^{+,-} &= 2\delta_{ij}\langle S_i^z\rangle - \sum_k J_{ik}\langle\langle (S_i^z S_k^+ - S_k^z S_i^+); S_j^-\rangle\rangle + K_{2,i} G_{ij}^{z+,-} + B G_{ij}^{+,-}, \\
\omega G_{ij}^{z+,-} &= \delta_{ij}\langle 6S_i^z S_i^z - 4\rangle + K_{2,i} G_{ij}^{+,-} - \frac{1}{2}\sum_k J_{ik}\Big(\langle\langle (6S_i^z S_i^z - 4) S_k^+; S_j^-\rangle\rangle \\
&+ 2\langle\langle S_k^- S_i^+ S_i^+; S_j^-\rangle\rangle - 2\langle\langle S_k^z (S_i^z S_i^+ + S_i^+ S_i^z); S_j^-\rangle\rangle\Big) + B G_{ij}^{z+,-}. \quad (339)
\end{aligned}$$

We treat the single-ion anisotropy terms exactly, whereas we introduce RPA-like decouplings for the exchange interaction terms, taking care not to break terms with equal indices

$$\begin{aligned}
\langle\langle S_i^z S_k^+ - S_k^z S_i^+; S_j^-\rangle\rangle &\simeq \langle S_i^z\rangle G_{kj}^{+,-} - \langle S_k^z\rangle G_{ij}^{+,-} \ , \\
\langle\langle (6S_i^z S_i^z - 4) S_k^+; S_j^-\rangle\rangle &\simeq \langle 6S_i^z S_i^z - 4\rangle G_{kj}^{+,-} \ , \\
\langle\langle S_k^z (S_i^z S_i^+ + S_i^+ S_i^z); S_j^-\rangle\rangle &\simeq \langle S_k^z\rangle G_{ij}^{z+,-} \ , \\
\langle\langle S_k^- S_i^+ S_i^+; S_j^-\rangle\rangle &\simeq 0 \text{ (neglect of transverse correlations)} \ . \quad (340)
\end{aligned}$$

A Fourier transform to momentum space yields

$$\begin{pmatrix} \omega - a & -b \\ -c & \omega - d \end{pmatrix} \begin{pmatrix} G_{\mathbf{k}}^{+,-} \\ G_{\mathbf{k}}^{z+,-} \end{pmatrix} = \begin{pmatrix} A^{+,-} \\ A^{z+,-} \end{pmatrix}. \quad (341)$$

Here

$$\begin{aligned}
A^{+,-} &= 2\langle S^z\rangle \\
A^{z+,-} &= \langle 6S^z S^z - 4\rangle \\
a &= B + \langle S^z\rangle (J_0 - J_{\mathbf{k}}) \\
b &= K_2 \\
c &= K_2 - \frac{1}{2}(\langle 6S^z S^z - 4\rangle) J_{\mathbf{k}} \\
d &= B + \langle S^z\rangle J_0. \quad (342)
\end{aligned}$$

For a linear chain, $J_0 = 2J, \quad J_{\mathbf{k}} = 2\cos k$; for a square lattice, $J_0 = 4J, \quad J_{\mathbf{k}} = 2(\cos k_x + \cos k_y)$.

The eigenvalues of the matrix equations are

$$\omega^{\pm} = B + \langle S^z\rangle (J_0 - \tfrac{1}{2} J_{\mathbf{k}}) \pm \sqrt{K_2^2 - \frac{1}{2}(6\langle S^z S^z\rangle - 4) K_2 J_{\mathbf{k}} + (\frac{1}{2}\langle S^z\rangle J_{\mathbf{k}})^2}. \quad (343)$$

The Green's functions are then given by solving eqn (341).

$$\begin{aligned}
G_{\mathbf{k}}^{+,-} &= \frac{A^{+,-}(\omega - d) + b A^{z+,-}}{(\omega - \omega^+)(\omega - \omega^-)} \ , \\
G_{\mathbf{k}}^{z+,-} &= \frac{A^{z+,-}(\omega - a) + c A^{+,-}}{(\omega - \omega^+)(\omega - \omega^-)} \ . \quad (344)
\end{aligned}$$

The spectral theorem then yields two equations determining $\langle S_i^z\rangle$ and $\langle S_i^z S_i^z\rangle$:

$$\langle S_i^- S_i^+\rangle = 2 - \langle S_i^z\rangle - \langle S_i^z S_i^z\rangle = \frac{1}{N}\sum_{\mathbf{k}}\langle S^- S^+\rangle_{\mathbf{k}} = \frac{1}{N}\sum_{\mathbf{k}}\frac{1}{(\omega^+ - \omega^-)} \times$$
$$\Big\{(A^{+,-}(\omega^+ - d) + bA^{z+,-})\frac{1}{e^{\beta\omega^+}-1} - (A^{+,-}(\omega^- - d) + bA^{z+,-})\frac{1}{e^{\beta\omega^-}-1}\Big\},$$
$$\langle S_i^-(2S_i^z - 1)S_i^+\rangle = \langle S_i^z\rangle - \frac{1}{2}(6\langle S_i^z S_i^z\rangle - 4) = \frac{1}{N}\sum_{\mathbf{k}}\frac{1}{(\omega^+ - \omega^-)} \times$$
$$\Big\{(A^{z+,-}(\omega^+ - a) + cA^{+,-})\frac{1}{e^{\beta\omega^+}-1} - (A^{z+,-}(\omega^- - a) + cA^{+,-})\frac{1}{e^{\beta\omega^-}-1}\Big\}. \tag{345}$$

Now, substitution of a) $A_i = S_i^-$, $C_i = S_i^+$ and b) $A_i = S_i^-$, $C_i = (2S_i^z - 1)S_i^+$ into eqn (115) of Section 3.7 and insertion of the GF's (344) yields

$$\begin{aligned} B^{+,-} &= \langle S_i^-[S_i^+, H]\rangle = \frac{1}{N}\sum_{\mathbf{k}}\frac{1}{(\omega^+ - \omega^-)} \times \\ &\quad \Big\{(A^{+,-}(\omega^+ - d) + bA^{z+,-})\frac{\omega^+}{e^{\beta\omega^+}-1} - (A^{+,-}(\omega^- - d) + bA^{z+,-})\frac{\omega^-}{e^{\beta\omega^-}-1}\Big\}, \\ B^{z+,-} &= \langle S_i^-[(2S_i^z - 1)S_i^+, H]\rangle = \frac{1}{N}\sum_{\mathbf{k}}\frac{1}{(\omega^+ - \omega^-)} \times \\ &\quad \Big\{(A^{z+,-}(\omega^+ - a) + cA^{+,-})\frac{\omega^+}{e^{\beta\omega^+}-1} - (A^{z+,-}(\omega^- - a) + cA^{+,-})\frac{\omega^-}{e^{\beta\omega^-}-1}\Big\}. \end{aligned} \tag{346}$$

Calculating the commutators directly, inserting eqn (324) and eliminating $\sum_k J_{ik}\langle (S_i^z)^2 S_k^z\rangle$ by forming the difference $3B^{+,-} - B^{z+,-}$ and solving for E_i yields

$$\begin{aligned} E_i = {} & \tfrac{1}{8}(3B^{+,-} - B^{z+,-}) - \tfrac{1}{2}(B + K_2) - \tfrac{1}{2}(B + K_2 + zJ)\langle S_i^z\rangle) \\ & + \frac{1}{8}\sum_k J_{ik}\Big(- \langle S_k^- S_i^+\rangle - 2\langle S_i^- S_k^+\rangle + \langle S_k^-(2S_i^z - 1)S_i^+\rangle\Big). \end{aligned} \tag{347}$$

The first term comes from eqn (346). Performing a Fourier transform on the last term gives

$$\tfrac{1}{8}\tfrac{1}{N}\sum_{\mathbf{k}} J_{\mathbf{k}}(-3\langle S^- S^+\rangle_{\mathbf{k}} + \langle S^-(2S^z - 1)S^+\rangle_{\mathbf{k}}). \tag{348}$$

This together with eqns (345) and (342) yields the final result for the intrinsic energy

$$\begin{aligned} E_i = {} & -\tfrac{1}{2}(B + K_2) - \tfrac{1}{2}(B + K_2 + zJ)\langle S_i^z\rangle \\ & + \tfrac{1}{8}\sum_{\mathbf{k}}\frac{1}{\omega^+ - \omega^-}\Big\{\Big[\Big(2\langle S_i^z\rangle(3(\omega^+ - B - \langle S_i^z\rangle J_0) - K_2 + \tfrac{1}{2}\langle 6S_i^z S_i^z - 4\rangle J_{\mathbf{k}}\Big) \\ & + \langle 6S_i^z S_i^z - 4\rangle\Big(3K_2 - (\omega^+ - B - \langle S_i^z\rangle(J_0 - J_{\mathbf{k}})\Big)\frac{\omega^+ - J_{\mathbf{k}}}{e^{\beta\omega^+}-1}\Big] + \Big[\omega^+ \to \omega^-\Big]\Big\}\ . \end{aligned} \tag{349}$$

For larger values of spin higher-order GF's are needed, but one can proceed analogously. The procedure applies of course to other Hamiltonians as well.

7.2. Appendix B: The curve-following procedure

Consider a set of n coupled equations characterised by m parameters $\{P_i; i = 1, 2 \ldots, m\}$ and n variables $\{V_i; i = 1, 2, \ldots, n\}$:

$$S_i(\mathbf{P}[m]; \mathbf{V}[n]) = 0, \text{ for } \; i = 1, \ldots, n. \tag{350}$$

In our case, the parameters are the temperature, the magnetic field components, the dipole coupling strengths, the anisotropy strengths, etc; the variables are the spin-correlations. The coupled equations S_i are obtained from the spectral theorem expressions for the correlations supplemented by the regularity conditions if necessary.

For fixed parameters $\mathbf{P}$, we look for solutions $S_i = 0$ at localised points, $\mathbf{V}[n]$, in the n-dimensional space. If now one of the parameters P_k is considered to be an additional variable $V_\circ$ (e.g. the temperature), then the solutions to the coupled equations define curves in the $(n+1)$-dimensional space $\mathbf{V}[n+1]$. From here on, we denote the points in this space by $\{V_i; i = 0, 1, 2, \ldots \ldots, n\}$. The curve-following method is a procedure for generating these solution-curves point by point from a few closely-spaced points already on a curve; i.e. the method generates a new solution-point from the *approximate* direction of the curve in the vicinity of a new *approximate* point. This is done by an iterative procedure described below. If no points on the curve are known, then an approximate solution point and an approximate direction must be estimated before applying the iterative procedure to obtain the first point on the curve. A second point can then be obtained in the same fashion. If at least two solution-points are available, then the new approximate point can be extrapolated from them and the approximate direction can be taken as the tangent to the curve at the last point.

The iterative procedure for finding a better point, $\mathbf{V}$, from an approximate point, $\mathbf{V}^\circ$, is now described. One searches for the isolated solution-point in the n-dimensional subspace perpendicular to the approximate direction, which we characterise by a unit vector, $\widehat{\mathbf{u}}$. The functions S_i are expanded up to first order in the corrections about the approximate point, $\mathbf{V}^\circ$:

$$S_i(\mathbf{V}) = S_i(\mathbf{V}^\circ) + \sum_{j=0}^{n} \frac{\partial S_i^\circ}{\partial V_j} \Delta V_j, \tag{351}$$

where $\Delta V_j = V_j - V_j^\circ$. At the solution, the S_i are all zero, whereas at the approximate point $\mathbf{V}^\circ$ the functions have non-zero values, S_i°; hence, one must solve for the corrections ΔV_j for which the left-hand side in the above equation is zero:

$$\sum_{j=0}^{n} \frac{\partial S_i^\circ}{\partial V_j} \Delta V_j = -S_i^\circ; \{i = 1, 2, \ldots, n\}. \tag{352}$$

These n equations are supplemented by the constraint requiring the correction to be perpendicular to the unit direction vector:

$$\sum_{j=0}^{n} \widehat{u_j} \Delta V_j = 0. \tag{353}$$

This improvement algorithm in the subspace is repeated until each of the S_i° is sufficiently small. In practice we required that $\sum_i (S_i^\circ)^2 \leq \epsilon$, where we took $\epsilon = 10^{-16}$. If there is no convergence, the extrapolation step-size used to obtain the original $\mathbf{V}^\circ$ is halved, a new extrapolated point obtained and the improvement algorithm repeated.

The curve-following method is quite general and can be applied to any coupled equations characterised by differentiable functions. By utilizing the information about the solution at neighbouring points, the method is able to find new solutions very efficiently, routinely converging after a few iterations once two starting points have been found. In addition, no single parameter or variable is singled out as "the" independent variable; instead, the $(n+1)$-dimensional curve can be viewed as being described parametrically in terms of the distance along the curve. This vantage point has great practical consequence: solutions in the neighbourhood of turning points (e.g. hysteresis for $\langle S^z \rangle$ as a function of field $\mathbf{B}$) are just as easily determined as in any other region because the solution is always sought in a subspace nearly orthogonal to the solution curve.

7.3. Appendix C: Reducing a 2-dimensionsl to a 1-dimensional integral for a square lattice

In the following we show how the double integral occuring from a two-dimensional Fourier transform when dealing with a square lattice (see e.g. eqn (130)) can be transformed into a 1-dimensional integral. This transformation saves a lot of computer time in many of the applications discussed in the present review.

Consider the evaluation of a double integral with the structure

$$I = \frac{1}{\pi^2} \int_0^\pi \int_0^\pi f(\cos k_x + \cos k_y)\, dk_x\, dk_y. \tag{354}$$

By substituting $x = k_x/\pi$ and $y = k_y/\pi$, this can be written as

$$\int_0^1 \int_0^1 f(\cos \pi x + \cos \pi y)\, dx\, dy. \tag{355}$$

By making use of the fact that the integrand has the same value for all values of x and y satisfying the relation

$$\cos \pi x + \cos \pi y = 2\gamma, \tag{356}$$

where γ lies in the range $(-1, 1)$, it is possible to reduce the double integral to a single integral over some suitable variable. The contours of constant γ are shown in Fig. 29. Each contour is given by an equation

$$\pi y(x) = \arccos(2\gamma - \cos \pi x). \tag{357}$$

Define now a function, $A(\gamma)$, which is the area in the unit square in the $xy-$plane

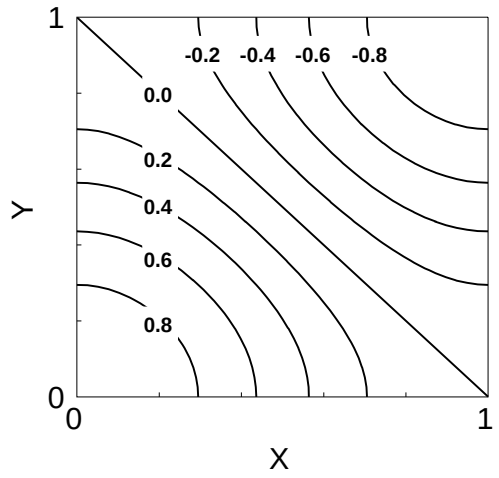

Figure 29: Contours of constant γ

lying to the left of the line $y(x)$ defined by Eq. 357 for each value of γ. From the diagram, it is evident that the function $A(\gamma)$ is given by

$$A(\gamma) = \frac{1}{\pi}\int_0^{x_0} \arccos(2\gamma - \cos \pi x)\, dx \tag{358}$$

for $\gamma > 0$ and

$$A(\gamma) = x_1 + \frac{1}{\pi}\int_{x_1}^{1} \arccos(2\gamma - \cos \pi x)\, dx \tag{359}$$

for $\gamma \leq 0$, where $x_0 = \frac{1}{\pi}\arccos(2\gamma - 1)$ and $x_1 = \frac{1}{\pi}\arccos(2\gamma + 1)$. These areas are shown in Fig. 30 and Fig. 31

The double integral may now be written as a single integral over the variable A over the interval $(0, 1)$:

$$I = \int_0^1 f(2\gamma(A))\, dA. \tag{360}$$

In order to evaluate the integral numerically, it is only necessary to have an efficient representation of the function $\gamma(A)$, so that a quadrature can be used to estimate the integral. A good strategy is to compute the function $\gamma(A)$ at a sufficiently large number of points so that it can be accurately fitted to a cubic spline function. Thus, the labour involved in evaluating the integral I is enormously reduced, since the numerical representation of $\gamma(A)$ need only be computed once.

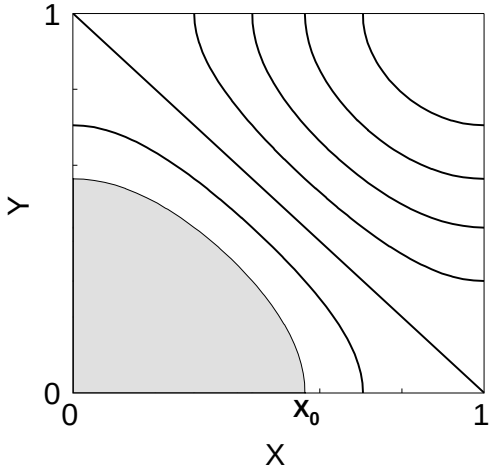

Figure 30: Area of the unit square to the left of a γ-contour for $\gamma > 0$

The numerical evaluation of $\gamma(A)$ is not without its problems, since the first derivative of the inverse function $A(\gamma)$ has a singularity in its first derivative at $\gamma = 0$. Even though we need the inverse function, $\gamma(A)$, whose derivatives go to zero at $\gamma = 0$, there are still numerical difficulties in representing $\gamma(A)$ by a spline function in the neighbourhood of $A = 0.5$; hence, it is better use a spline function to represent the function $g(A)$, defined as $(0.5 - A)\gamma(A)$, and to get $\gamma(A)$ from

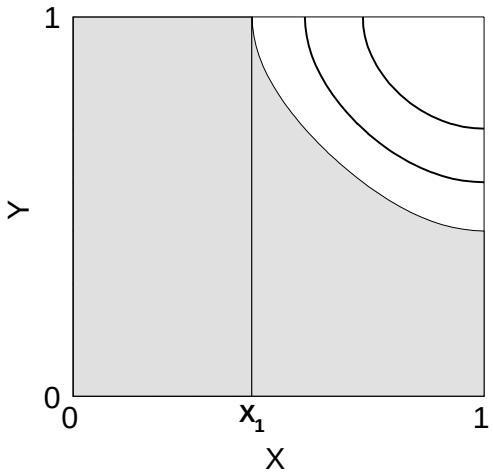

Figure 31: Area of the unit square to the left of a γ-contour for $\gamma < 0$

$g(A)/(0.5 - A)$ in the neighbourhood of the singularity, using the value $\gamma(0.5) = 0$ at the singularity itself. The function $g(A)$, fitted to a cubic spline function, yields numerically stable values of the function and its first two derivatives. The spline fit to $g(A)$ is obtained from values of the function tabulated at a set of knots equally spaced in the range $(0, 0.5)$ plus values of the derivative of the function at $A = 0$, (derivative $= -1/(2\pi)$) and $A = 0.5$, (derivative=0). The second derivative of $g(A)$ actually goes smoothly to zero at $A = 0.5$. Values of $\gamma(A)$ in the range $(0.5, 1)$ are obtained from the fitted values using the symmetry relation $\gamma(0.5+u) = -\gamma(0.5-u)$. The function $\gamma(A)$ is shown in Fig. 32.

While the above procedure allows one to obtain accurate values of $\gamma(A)$ over the whole range of area, it does nothing to suppress the effects of the singularity in the first derivative of $A(\gamma)$ at $\gamma = 0$. These effects are not serious but they demand more effort from the integrator near $A = 0.5$. They can, however, be minimized by integrating out the constant part of the function $f(2\gamma)$, which is just $f(0)$ itself:

$$I = f(0) + \int_0^1 (f(2\gamma(A) - f(0))\, dA. \tag{361}$$

We mention that in Ref. [40] the double integral is transformed into an elliptic integral of the first kind with a transformation found in Ref. [102].

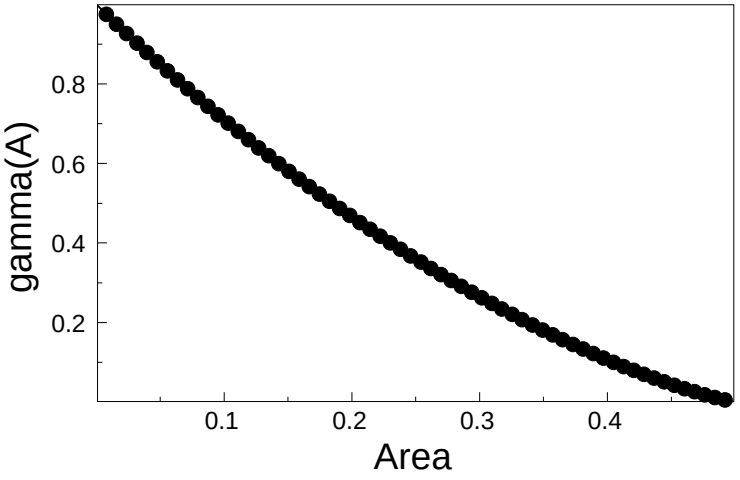

Figure 32: γ as a function of area A.

7.4. Appendix D: Treatment of the magnetic dipole-dipole interaction

In this appendix, we apply the generalized Tyablikov (165)decoupling to the magnetic dipole-dipole interaction. From this result the mean field approximation, as it is used e.g. in eqn (172), is obtained by neglecting the momentum dependence due to the lattice. After the decoupling procedure, the resulting term $\langle\langle[S_i^\alpha, H^{dipole}]; (S_j^z)^m (S_j^-)^n\rangle\rangle$ is added to the equations of motion (164), where H^{dipole} is the last term in eqn (160). After a Fourier transform to momentum space, one has the following additional terms in the equation of motion:

$$\begin{pmatrix} -T_{\mathbf{k}}^{+} & -T_{\mathbf{k}}^{-} & -T_{\mathbf{k}}^{z} \\ (T_{\mathbf{k}}^{-})^* & T_{\mathbf{k}}^{+} & (T_{\mathbf{k}}^{z})^* \\ T_{\mathbf{k}}^{z\pm} & -(T_{\mathbf{k}}^{z\pm})^* & 0 \end{pmatrix} \begin{pmatrix} G_\eta^{+,mn} \\ G_\eta^{-,mn} \\ G_\eta^{z,mn} \end{pmatrix} , \tag{362}$$

where

$$\begin{aligned} T_{\mathbf{k}}^{+} &= g\langle S^z\rangle\Big(T_{20}^0 + T_{02}^0 + \tfrac{1}{2}T_{20}^{\mathbf{k}} + \tfrac{1}{2}T_{02}^{\mathbf{k}}\Big) , \\ T_{\mathbf{k}}^{-} &= \tfrac{3}{2}g\langle S^z\rangle\Big(T_{20}^{\mathbf{k}} - T_{02}^{\mathbf{k}} + 2iT_{11}^{\mathbf{k}}\Big) , \\ T_{\mathbf{k}}^{z} &= g\langle S^+\rangle\Big(T_{20}^{\mathbf{k}} + T_{02}^{\mathbf{k}} + \tfrac{1}{2}T_{20}^0 + \tfrac{1}{2}T_{02}^0\Big) , \\ T_{\mathbf{k}}^{z\pm} &= \tfrac{1}{4}g\Big(\langle S^-\rangle(T_{20}^{\mathbf{k}} + T_{02}^{\mathbf{k}} - T_{20}^0 - T_{02}^0) \\ &\quad -3\langle S^+\rangle(T_{20}^{\mathbf{k}} - T_{02}^{\mathbf{k}} - 2iT_{11}^{\mathbf{k}})\Big) , \end{aligned} \tag{363}$$

and

$$T_{\mu\nu}^{\mathbf{k}} = \sum_{lm} \frac{x_l^\mu y_m^\nu}{(x_l^2 + y_m^2)^{5/2}} \exp(ik_x x_l) \exp(ik_y y_m) \tag{364}$$

are oscillating lattice sums, which can be evaluated with Ewald summation techniques as outlined e.g. in Ref. [103].

This RPA treatment of the magnetic dipole coupling complicates the calculation of the magnetization considerably because of the presence of complex and dispersive (**k**-dependent) terms; therefore, we have neglected these terms in the applications and retained the non-dispersive terms only. This corresponds to a mean field treatment of the dipole coupling. In this approximation, eqns (363) reduce to

$$\begin{aligned} T^{+}_{\mathbf{k}} &= g\langle S^z\rangle(T^0_{20}+T^0_{02}) \ , \\ T^{-}_{\mathbf{k}} &= 0 \ , \\ T^{z}_{\mathbf{k}} &= \frac{g}{2}\langle S^+\rangle(T^0_{20}+T^0_{02}) \ , \\ T^{z\pm}_{\mathbf{k}} &= -\frac{g}{4}\langle S^-\rangle(T^0_{20}+T^0_{02}). \end{aligned} \tag{365}$$

This simplification takes the dipole coupling into account by an effective renormalization of the external magnetic field and leads to eqns (172) of Section 4.2.1.

In order to justify this procedure we have done RPA calculations for the dipole interaction for two limiting cases: a perpendicular and an in-plane magnetization. In the appendix of Ref. [9], it is shown that, for these cases, a mean field calculation is a rather good approximation to the RPA result if the dipole coupling strength is much smaller than the strength of the exchange interaction, which is the case for many systems. We are not aware of a numerical treatment of the dipole coupling for the spin reorientation problem in GFT taking the dispersive and complex terms of eqn (363) into account.

In the present review, we have applied the dipole-dipole interaction only in cases where the dipole coupling strength is small as compared to the strength of the exchange interaction, $g/J << 1$. Ref. [104] reviews dipolar effects in quasi-two-dimensional magnetic films, treating also cases $g \simeq J$, $g >> J$ and $J = 0$ with classical Monte Carlo simulations.

References

[1] D.M. Zubarev, Sov. Phys. Usp. **3**, 320 (1960).

[2] V.L. Bonch-Brevich, S.V. Tyablicov, The Green Function Method in Statistical Mechanics, North-Holland, Amsterdam, 1962.

[3] W. Gasser, E. Heiner, K. Elk, Greensche Funktionen in der Festkörper- und Vielteilchenphysik, Wiley-VHC, Berlin, 2001.

[4] S.V. Tyablicov, Methods in the Quantum Theory of Magnetism, Plenum Press, New York, 1967.

[5] W.Nolting, Quantentheorie des Magnetismus, vol.2, Teubner, Stuttgart, 1986.

[6] K. Held, Electronic Structure Calculations using Dynamical Mean Field Theory, cond-mat/0511293, based on the Habilitation thesis/ Stuttgart University, 2004.

[7] P.J. Jensen, K.H. Bennemann, Surface Science Reports **61**, 129 (2006).

[8] P. Fazekas, Lecture Notes on Electron Correlations and Magnetism, World Scientific, Singapore, 1999.

[9] P. Fröbrich, P.J. Jensen, P.J. Kuntz, A. Ecker, Eur. Phys. J. B **18**, 579 (2000).

[10] K.W.H. Stevens, G.A. Tombs, Proc. Phys. Soc. **85**, 1307 (1965).

[11] J.G. Ramos, A.A. Gomes, Il Nuovo Cimento **3**, 441 (1971).

[12] W.H. Press, B.P. Flannery, S.A. Teukolsky, W.T. Vetterling, Numerical Recipes, Cambridge University Press, 1989.

[13] P. Fröbrich, P.J. Kuntz, J. Phys.: Condens. Matter **17**, 1167 (2005).

[14] A. Ecker, P. Fröbrich, P.J. Jensen, P.J. Kuntz, J. Phys.: Condens. Matter **11**, 1557 (1999).

[15] C. Timm, S.M. Girvin, P. Henelius, A.W. Sandvik, Phys. Rev. B **58** (1998) 1464.

[16] S.V. Tyablikov, Ukr. Mat. Zh. **11**, 289 (1959).

[17] H.B. Callen, Phys. Rev. **130**, 890 (1963).

[18] E. Pravecki, Phys. Lett. **6**, 147 (1963).

[19] R. A. Tahir-Kheli, D. ter Haar, Phys. Rev. **127**, 88 and 95 (1962).

[20] P.J. Jensen, K.H. Bennemann, in Magnetism and Electronic Correlations in Local-Moment Systems: Rare-Earth Elements and Compounds, ed. M. Donath, P.A. Dowben, W. Nolting, World Scientific, Singapore, 1998, p.131-141.

[21] A. Hucht, K.D. Usadel, Phil. Mag. B **80**, 275 (2000).

[22] N.M. Mermin, H. Wagner, Phys. Rev. Lett. **17**, 1133 (1966).

[23] I. Turek, J. Kudrnovsky, V. Drchal, P. Bruno, S. Blügel, phys. stat. sol. (b) **236**, 318 (2003).

[24] S.V. Vonsovskii, in Magnetism, vol. 2, Chapter 23 (J. Wiley and Sons, 1974).

[25] Diep-The-Hung, J.C.S. Levy, O.Nagai, phys. stat. sol. (b) **93**, 351 (1979).

[26] R. Schiller, W. Nolting, Solid State Commun. **110**, 121 (1999).

[27] C. Cucci, M.G. Pini, P. Politi, A.Rettori, J. Mag. Mag. Mat. **231**, 98 (2001).

[28] P. Fröbrich, P.J. Jensen, P.J. Kuntz, Eur. Phys. J. B **13**, 477 (2000).

[29] M.E. Lines, Phys. Rev. **156**, 534 (1967).

[30] R.P. Erickson, D.L. Mills, Phys. Rev. B **43**, 11527 (1991).

[31] R.P. Erickson, D.L. Mills, Phys. Rev. B **44**, 11825 (1991).

[32] F.B. Anderson, H.B. Callen, Phys. Rev. **136**, A1068 (1964).

[33] H.Y. Wang, Z.H. Dai, P. Fröbrich, P.J. Jensen, P.J. Kuntz, Phys. Rev. B **70**, 134424 (2004).

[34] L. Hu, H. Li, R. Tao, Phys. Rev. B **60**, 10222 (1999).

[35] W. Guo, L.P. Shi, D.L. Lin, Phys. Rev. B **62**, 14259 (2001).

[36] W. Guo, D.L. Lin, Phys. Rev. B **67**, 224402 (2003).

[37] P. Fröbrich, P.J. Kuntz, Eur. Phys. J. B **32**, 445 (2003).

[38] P. Fröbrich, P.J. Kuntz, Phys. Rev. B **68**, 014410 (2003).

[39] H.Y. Wang, C.Y. Wang, E.G. Wang, Phys. Rev. B **69**, 174431 (2004).

[40] V. Ilkovic, phys. stat. sol. (b) **241**, 420 (2004).

[41] S. Tuleja, J. Kecer, V. Ilkovic, phys. stat. sol. (b) **243**, 1352 (2006).

[42] D.K. Morr, P.J. Jensen, K.H. Bennemann, Surface Science **307-309**, 1109 (1994).

[43] D.A. Yablonskyi, Phys. Rev. B **44**, 4467 (1991).

[44] P. Fröbrich, P.J. Kuntz, M. Saber, Ann. Phys. (Leipzig) **11**, 387 (2002).

[45] J.F. Devlin, Phys. Rev. B **4**, 136 (1971).

[46] M. Bander, D.L. Mills, Phys. Rev. B **38**, R12015 (1988).

[47] P.J. Jensen, F. Aguilera-Granja, Phys. Lett. A **269**, 158 (2000).

[48] P. Henelius, P. Fröbrich, P.J. Kuntz, C. Timm, P.J. Jensen, Phys. Rev. B **66**, 094407 (2002).

[49] S. Schwieger, J. Kienert, W. Nolting, Phys. Rev. B **71**, 024428 (2005).

[50] M.G. Pini, P. Politi, R.L. Stamps, Phys. Rev. B **72**, 014454 (2005).

[51] P. Bruno, C. Chappert, Phys. Rev. Lett. **67**, 1602 (1991).

[52] N.S. Almeida, D.L. Mills, M. Teitelman, Phys. Rev. Lett. **75**, 733 (1995).

[53] P.J. Jensen, K.H. Bennemann, P. Poulopoulos, M. Farle, F. Wilhelm, K. Baberschke , Phys. Rev. B **60**, R14994 (1999).

[54] P. Bruno, Phys. Rev. B **52**, 411 (1995).

[55] P.J. Jensen, C. Sorg, A. Scherz, M. Bernien, K. Baberschke, H. Wende, Phys. Rev. Lett. **93**, 039703 (2005).

[56] A. Scherz, C. Sorg, M. Bernien, N. Ponpandian, K. Baberschke, H. Wende, J. Jensen, Phys. Rev. B **72**, 054447 (2005).

[57] S. Schwieger, W. Nolting, Phys. Rev. B **69**, 224413 (2004)

[58] S. Schwieger, J. Kienert, W. Nolting, Phys. Rev. B **71**, 174441 (2005).

[59] P. Fröbrich, P.J. Kuntz, in Progress in Nonequilibrium Green's Functions III, J. Phys.: Conf. Series **35**, 157 (2006).

[60] J. Lindner, C. Rüdt, E. Kosubek, P. Poulopoulos, K. Baberschke, P. Blomquist, R. Wäppling, D.L. Mills, Phys. Rev. Lett. **88**, 167206 (2002).

[61] C. Pich, F. Schwabl, Phys. Rev. B **47**, 7957 (1993).

[62] T. Holstein, H. Primakoff, Phys. Rev. **58**, 1098 (1940).

[63] C. Pich, F. Schwabl, Phys. Rev. B **49**, 413 (1994).

[64] C. Pich, F. Schwabl, J. Mag. Mag. Mat. **148**, 30 (1995).

[65] M. Hummel, C. Pich, F. Schwabl, Phys. Rev. B **63**, 094425 (2001).

[66] P. Fröbrich, P.J. Kuntz, P.J. Jensen, J. Phys.: Condens. Matter **17**, 5059 (2005).

[67] H.T. Diep, Phys. Rev. B **40**, 4818 (1989) ; ibid. **43**, 8509 (1991).

[68] H.Y. Wang, M. Qian, E.G. Wang, J. Appl. Phys. **95**, 7551 (2004).

[69] A. Moschel, K.D. Usadel, A. Hucht, Phys. Rev. B **47**, 8676 (1993).

[70] A. Moschel, K.D. Usadel, Phys. Rev. B **48**, 13991 (1993).

[71] H.Y. Wang, Z.H. Dai, Commun. Theor. Phys. (Beijing, China) **42**, 141 (2004).

[72] A. Moschel, K.D. Usadel, J. Mag. Mag. Mat. **136**, 99 (1994).

[73] Li Qing'an, Phys. Rev. B **70**, 014406 (2004).

[74] V. Than Ngo, H. Viet Nguyen, H.T. Diep, V. Lien Nguyen, Phys. Rev. B **69**, 134429 (2004).

[75] P.J. Jensen, S. Knappmann, W. Wulfhekel, H.P, Oepen, Phys. Rev. B **67** 184417 (2003).

[76] P. Fröbrich, P.J. Kuntz, phys. stat. sol. (b) **241**, 925 (2004).

[77] P. Fröbrich, P.J. Kuntz, J. Phys. Condens. Matter **16**, 3453 (2004).

[78] P.J. Jensen, M. Kiwi, H. Dreyssé, Eur. Phys. J. B **46**, 541 (2005).

[79] T.J. Moran, J. Nogués, D. Lederman, I.K. Schuller, Appl. Phys. Lett. **72**, 617 (1998).

[80] T.C. Schulthess, W.H. Butler, Phys. Rev. Lett. **81**, 4516 (1998).

[81] U. Nowak, R.W. Chantrell, E.C. Kennedy, Phys. Rev. Lett. **84**, 163 (2000).

[82] P.J. Jensen, K.H. Bennemann, D.K. Morr, H. Dreyssé, Phys. Rev. B **73**, 144405 (2006).

[83] M. E. Lines, Phys. Rev. **133**, A841 (1964).

[84] H. Shimahara, S. Takada, J. Phys. Soc. Jpn. **60**, 2394 (1991); ibidem **61**, 989 (1992).

[85] I.Junger, D. Ihle, J. Richter, A. Klümper, Phys. Rev. B **70**, 104419 (2004).

[86] I.J. Junger, D. Ihle, J. Richter, Phys. Rev. B **72**, 064454 (2005).

[87] C. Schindelin, H. Fehske, H. Büttner, D. Ihle, Phys. Rev. B **62**, 12141 (2000).

[88] D. Ihle, C. Schindelin, H. Fehske, Phys. Rev. B **64**, 054419 (2001).

[89] J. Kondo, K. Yamaji, Progr. Theor. Phys. **47**, 807 (1972).

[90] S.Q. Bao, H. Zhao, J.L. Shen, G.Z. Yang, Phys. Rev. B **53**, 735 (1996).

[91] S.Q. Bao, Solid State Communication **10**, 193 (1997).

[92] J.C. Bonner, M. E. Fisher, Phys. Rev. **135**, A640 (1964).

[93] M.E. Gouvea, A.S.T. Pires, Phys. Rev. B **63**, 134408 (2001).

[94] W.Yu, S. Feng, Eur. Phys. J. B **13**, 265 (2000).

[95] B.H. Bernhard, B. Canals, C. Lacroix, Phys. Rev. B **66**, 104424 (2002).

[96] Yu. A. Tserkovnikov, Teor. Mat. Fiz. **7**, 147 (1970); ibid. **12**, 135 (1972).

[97] A.L. Kuzemsky, Rivista Nuovo Cimento **25**, 1 (2002).

[98] A. Belkasri, J.L. Richard, Phys. Rev. B **50**, 12896 (1994).

[99] N.M. Plakida, Phys. Lett. **43A**, 481 (1973).

[100] S. Winterfeldt, D. Ihle, Phys. Rev. B **59**, 6010 (1999).

[101] A.F. Barabanov, L.A. Maksimov, Phys. Lett. A **207**, 390 (1995).

[102] J.H.P. Colpa, Physica **57**, 347 (1972).

[103] P.J. Jensen, Ann. Physik **6**, 317 (1997).

[104] K. De'Bell, A.B. MacIsaac, J.P. Whitehead, Rev. Mod. Phys. **72**, 225 (2000).

[105] Y. Song, H.Q. Lin, A.W. Sandvik, J. Phys. Condens. Matter **12**, 5285 (2000).